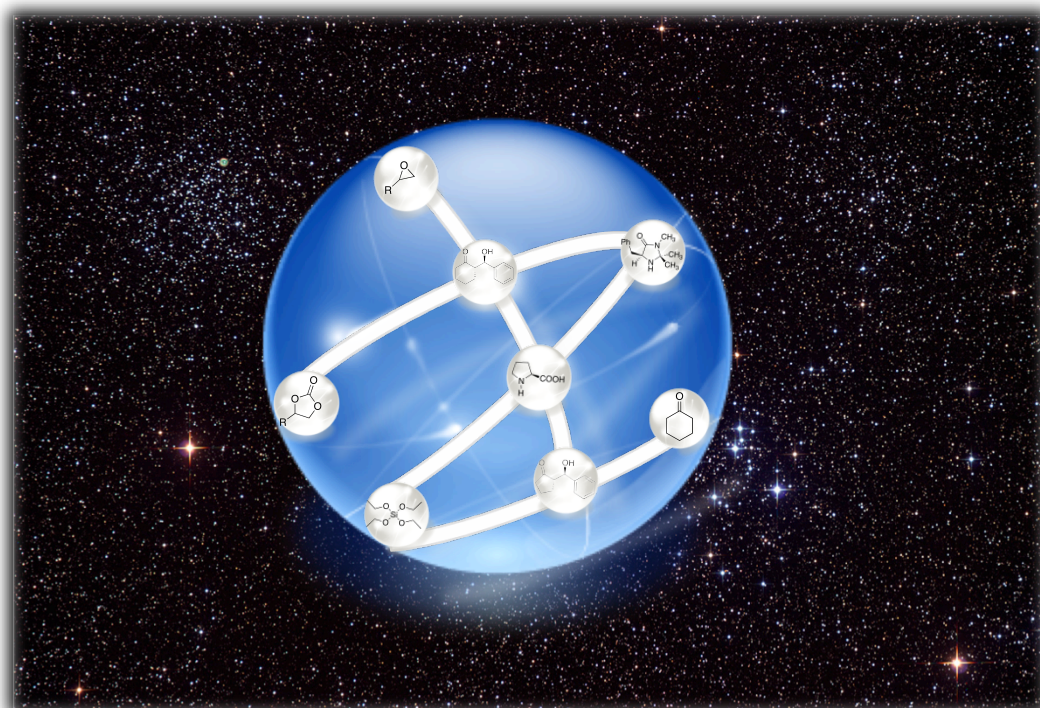# Organocatalysis:
Catalysts and New Recyclable Materials
for Organic Synthesis

Tutor e Coordinatore
Prof. Michelangelo Gruttadauria

Tesi di Dottorato di:
Paola Agrigento

UNIVERSITÀ DEGLI STUDI DI PALERMO
DIPARTIMENTO DI BENI CULTURALI, STORICO-ARCHEOLOGICI,

TUTOR
MARIO ROSSI

MAGISTRALE

Table of Contents

Acknowledgments

I wish to express my gratitude to Prof. Michelangelo Gruttadauria and Prof. Renato Noto for giving me the opportunity to carry out my doctoral study in their research group. I would like to thank them for the opportunity to explore myself by working in the fascinating field of organocatalysis. They have always generously supported me and their wise guidance and strong passion for science helped me to grow personally and professionally.

Many thanks to Dr. Francesco Giacalone for his excellent mentoring, his enthusiasm, and encouragement throughout my entire PhD. I profited a lot from our countless scientific discussions that helped to improve my chemical knowledge and led to many essential advances of our projects.

I thank Prof. Alfons Baiker and Dr. Angelo Vargas for allowing me to work at ETH, Zürich (Switzerland), in the synthesis and characterization of magnetic nanoparticles. I thank Prof. Sotiris E. Pratsinis of the Particle Technology Laboratory, Institute of Process Engineering, (Switzerland) for the flame synthesis of magnetic nanoparticles.

Furthermore, I would like to thank Prof. Paolo P. Pescarmona of Centre for Surface and Catalysis, Katholieke Universiteit Leuven (Belgium), and Prof. Carmela Aprile, Facultés Universitaires Notre-Dame de la Paix , University Namur (Belgium). They allow me to carry out a high-throughput study, by means of the use of unique high throughput experimentation unit for the study of catalytic system under supercritical conditions. I want to thank them for the freedom they gave me in conducting my research work as well as for helpful discussions.

Finally, I am grateful to all the people who have helped and supported me during the past years and during the completion of this thesis.

Preface

The work presented in this PhD thesis has been mainly carried out at the Department of Organic Chemistry "E. Paternò", Università degli Studi di Palermo, Italy, under the supervision of Prof. Michelangelo Gruttadauria.

The whole PhD was devoted to organocatalysis, a relatively new and popular field, and particular attention was given at the development of new recyclable materials for organic synthesis.

The thesis is organized in 4 chapters. The introduction presents the general concept of organocatalysis, followed by an overview on the main approaches for the immobilization of organocatalysis.

Chapter 1 focuses on asymmetric organocatalysis, simple hydrophobic proline-derivatives are employed in only very low loading at room temperature without additives for the aldol reaction between cyclohexanone or cyclopentanone and substituted benzaldehydes.

During the period from January 2010 to July 2010 the PhD research was performed at ETH Hönggerberg, Zürich (Switzerland), in the *Institut für Chemie-und Bioingenieurwissenshaften*, as an exchange student in the Baiker research group, under the supervision of Prof. A. Baiker and Dr. A. Vargas.

During the first period it was carried out the wet synthesis of magnetic nanoparticles possessing an iron oxide core, and an outer silica shell. The outer shell of the obtained material was grafted with n-propyl thiol functional group. The thus obtained functional material was characterized in term of available functional group by means of ATR infrared and UV-vis spectroscopy.

Then it was investigated the coupling reaction between the prepared functionalized material and an organocatalyst that was used to perform an asymmetric aldol reaction. The results of this work are presented in the chapter 2.

Chapter 3 of this thesis deals the study of heterogeneous catalysts for the fixation of carbon dioxide by means of high throuput experimentation (HTE). This successful technology enables the rapid investigation of catalytic process in supercritical CO_2 medium. This research project was performed during the period from February 2011 to August 2011 in the Centre of Surface Science and Catalysis of *Katholieke Universiteit Leuven* (Belgium)*,* as exchange student under the supervision of Prof. Paolo P. Pescarmona and Prof. Carmela Aprile.

Finally chapter 4 reports the synthesis of new magnetically recyclable and efficient nanocomposite catalysts. These new class of materials combined the advantage of supported ionic liquid with that of magnetic nanoparticles. The materials, which contain a highly cross-linked polymeric network, have

been denoted as magnetic multi-layered supported ionic liquid phase (MML-SILP). They are very versatile materials and have been used for three different kinds of reactions.

Part of the PhD was devoted to a bibliographic activity. It was written in collaboration with Prof. M. Gruttadauria, Prof. R. Noto and Dr. F. Giacalone a chapter in the book edited by Pablo De Maria*, Ionic Liquids in Biotransformations and Organocatalysis: Solvents and Beyond* (Wiley-VCH).

This book addresses the use of ionic liquids in biotransformation and organocatalysis. Its major parts include: an overview of the fundamentals of ionic liquids and their interactions with proteins and enzymes; the use of ILs in biotransformations; non-solvent applications such as additives, membranes, substrate anchoring, and the use of ILs in organocatalysis (from solvents to co-catalysts and new reactivities, as well as non-solvent applications such as anchoring and immobilization).

The chapter regards "Non-solvent" applications of Ionic Liquids in Organocatalysis. It is divided in three part: i) Anchoring organocatalysts to Ionic Liquids, ii) Anchoring substrates to Ionic Liquids, iii) Immobilizing Ionic Liquids and Organocatalysts (102 references).

During the thirst year of PhD a review for the Chemical Society Reviews, with the title "Low Loading asymmetric Organocatalyst" was written in collaboration with Prof. M. Gruttadauria, Prof. R. Noto and Dr. F. Giacalone. This critical review presents the development of chiral organocatalysts which are systematically used in less than 3 mol% loading (193 references).

Palermo, December 2011

Paola Agrigento

Chapter 1

New Simple Hydrophobic Proline Derivatives

for Asymmetric Aldol Reaction in Aqueous Medium

$n= 0$ *anti/syn* 89:11- 96:4 ee 96->99
$n= 1$ *anti/syn* 87:13- >99:1 ee 94->99
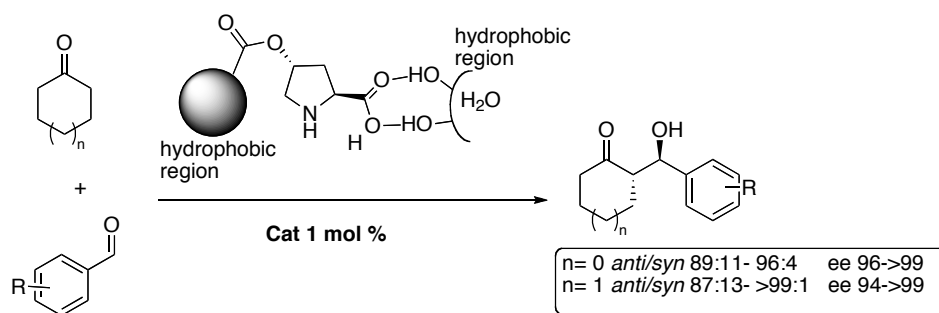
New 4-acyloxy-L-proline derivatives with different hydrophobic properties of the acyl group were easily synthesized and used as catalysts in the direct asymmetric aldol reaction between cyclic ketones and several substituted benzaldehydes. L-proline carrying a simple trans-4-(4-phenylbutanoyloxy) group, employed in only 0.5 mol% at room temperature without additives, was found an excellent catalyst for the aldol reaction between cyclohexanone or cyclopentanone and substituted benzaldehydes. For such catalyst high turn over numbers (TONs) have been obtained, being these among the highest values obtained for enamine organocatalysis. Data reported suggest that such catalytic molecules are organized at ketone/water interface and their organization depend on the nature of the acyl group and on the ratio catalyst/water.

1.1   *Introduction*

The aldol reaction is one of the most important carbon-carbon bond forming reactions, which offers straightforward access to the optically active β-hydroxycarbonyl structural unit found in many natural products and drugs (Figure 1).[1]
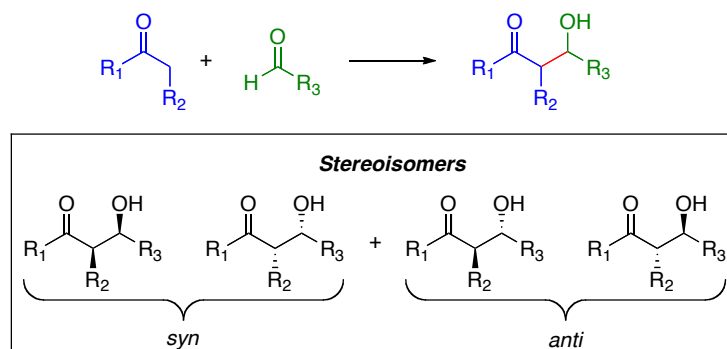
Figure 1. The intermolecular aldol reaction between generic ketone and aldehyde and the four stereoisomers that are *syn* and *anti* diastereomeric pairs of enantiomers

Since List and Barbas[2] reported the direct aldol reaction catalyzed by L-proline in 2000, recent years have witnessed an explosive growth in the field of related asymmetric reactions catalyzed by organocatalysts,[3] especially with L-proline and its derivatives,[4] including prolineamides, prolinethioamides, sulfonamides, chiral amines, and so on.

Organocatalysts are usually used in 5-30 mol% and in some cases also higher catalytic loadings have been reported.[5] For synthetic purposes it is of great interest to have highly active organic catalysts displaying their activity in less than 2 mol% loading. Several examples of organocatalysts employed in low catalytic amount are present in the literature.[5] In the case of organocatalytic reactions via enamine, some catalysts have been employed in low catalytic amount.[6] Few organocatalysts have also been tested in low loading (<2 mol%) for the direct asymmetric aldol reaction. Catalysts **1** and **2** were used in only 0.5 mol% in brine at -5 °C [7] whereas catalyst **3** was used in 1 mol% at 0 °C in brine [8] (Figure 2). In each case, aldol products were obtained in very high ee.

1: X= CH₂, R= *i*-Bu
2: X= CH₂, R= Ph
3: X= S, R= *i*-Bu

4

5

6: R = H or TBSO
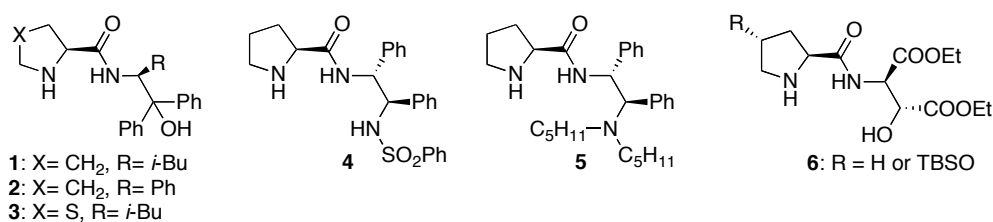
Figure 2. Catalysts **1-6**.

Catalyst **4** was used in 2 mol% at -5 °C in brine with cyclic ketones affording aldol products in 81->99% ee[9] whereas catalyst **5** was used in 2 mol% at -25 °C in neat acetone to give the corresponding aldol products in excellent ee. On the other hand, this catalyst gave poor results when used for cyclic ketones.[10] Good to high ee values were obtained using catalyst **6** (1 mol%) in brine at room temperature, but in this case, an additive was required.[11]

Several more complex catalysts were also reported for aldol reactions in neat acetone. A spiro diamine catalyst was employed in 1 mol% at -25 °C with poor results.[12] Also tripeptide H-Pro-Pro-Asp-NH$_2$ was used in 1 mol% at room temperature affording better ee values.[13] A biphenyl-based axially chiral amino acid was used in only 0.5 mol% at room temperature with long reaction times (2-3 days) but with excellent enantioselectivity.[14] Even very complex dendrimer catalysts were synthesized and used in 1 mol% loading for the aldol reaction with ee up to 65%.[15]

Siloxyproline **7** was the first 4-hydroxy-L-proline derivative used as catalyst in water. It was tested down to 1 mol% with excellent stereoselectivities, although longer reaction times were needed (Figure 2).[16]

The ionic-tagged *cis*-4-hydroxy-L-proline **8** was found to be an efficient catalyst for the aldol reaction in water. [17] Miao and Chan[18] first reported the use of imidazolium ion-tagged catalysts, in which the tag is connected to the 4-OH group of *trans*-4-hydroxy-L-proline. The authors reported the use of catalyst in DMSO or acetone as the solvent but the catalyst loading (30 mol%) was very high resulting in poor TON. Lombardo *et al.* reported the installation of an imidazolium tag *via* acetate connection to the C-4 of *cis*-4-hydroxy-L-proline, providing highly efficient catalyst **8** for the direct asymmetric aldol reaction, that works in a remarkably low catalyst loading (0.1 mol%) affording TONs up to 930 in the case of electron-poor aromatic aldehydes with ee up to >99%. The authors ascribed the better performances of **8** to the occurrence of a "*cis*-effect".[17]
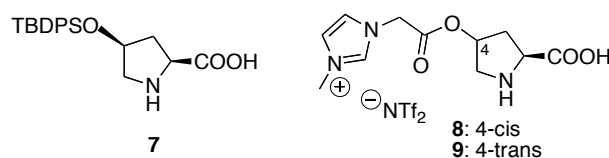
Figure 3. Catalysts **7-9**.

Many of the reported reactions were carried out in water.[19] Indeed it has been found that water is able to promote these reactions with high levels of enantio and diastereoselectivity and in high yields. Usually, these reactions are carried out with an excess of ketone, from 2 to 5 equivalents with respect to the aldehyde, and in the presence of variable amounts of water. In such conditions the aqueous biphasic environment can simulate the hydrophobic pocket of class I aldolases. As a consequence, hydrophobic

aldehydes are forced into the hydrophobic region resulting in increased activity and stereoselectivity of the catalyst. The hydrophobic region can be due to a hydrophobic substituent or to a hydrophobic support such as a polystyrene backbone.

Recently, the research group in which I carried out my doctoral studies has been involved in researches regarding the organocatalytic direct asymmetric aldol reaction both using supported and non-supported catalysts.[20] Use of supported organocatalysts is of great interest because their recovery allows the reuse of catalysts that are employed in high catalyst loading, or in the case of expensive organocatalysts (see Introduction).[21]

In 2008, it was started a project in order to find new organocatalysts, structurally simple, which are able to catalyze the asymmetric aldol reaction in water in low amounts without the need of additives. Simple 4-substituted acyloxyproline derivatives, as catalysts for the aldol reaction, characterized by a different hydrophobicity of the acyl group [20b] were easily synthesized and used as catalyst in direct asymmetric aldol reaction between cyclic ketones (cyclohexanone and cyclopentanone) and several substituted benzaldehydes (Figure 4).
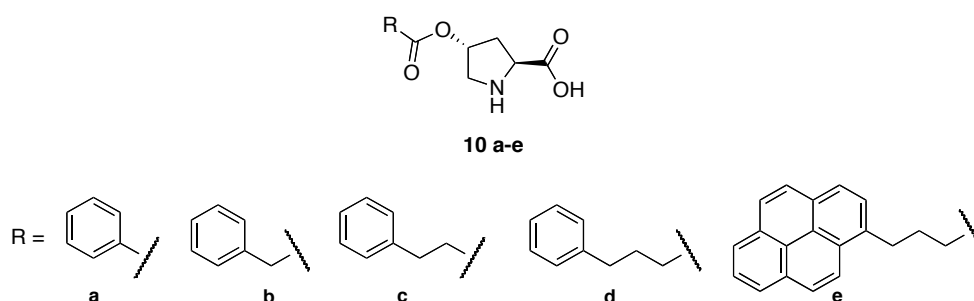
Figure 4. Structure of catalysts **10a-e**

Reactions were carried out using water, this being the best reaction medium examined. Screening of these catalysts showed that compounds bearing the most hydrophobic acyl chains, 4-phenylbutanoate (**10d**) and 4-(pyren-1-yl)butanoate (**10e**), provided better results. The latter catalysts were successfully used in only 2 mol% at room temperature without additives to give aldol products in excellent stereoselectivities. These results demonstrate that derivatization of the proline moiety with the proper simple hydrophobic substituent in the 4-position can furnish highly active and stereoselective catalysts without the need of additional chiral backbones in the molecule.

1.2   *Results and Discussion*

1.2.1   *Synthesis of Catalysts*

In order to develop new simple organocatalysts for the direct asymmetric aldol reaction in water, five new proline derivatives **11a-c**, **12**, **13** and a known catalyst **11d**, were prepared (Figure 5). The new proline derivatives were chosen to have very simple hydrophobic substituents.
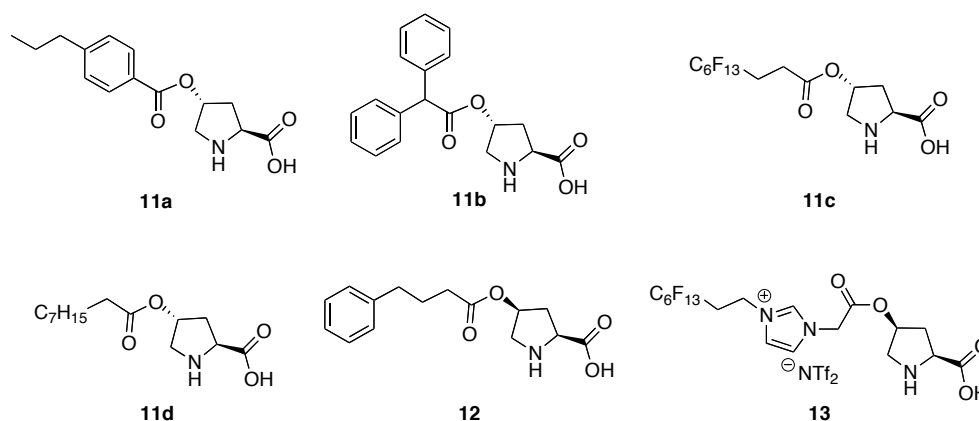
Figure 5. Catalyst **11a-d**, **12**, **13**

These molecules allow the set of known compounds to be expanded, which would make a deeper comparison with them possible. Such a comparison regarded the different hydrophobicity that substituents at the C-4 position give to the molecules. Compound **12** was prepared to investigate the role of the configuration at C-4. In addition considering the good results reported using catalyst **8**, [17] compound **13** was prepared, adopting the ion tag strategy to modify the proline scaffold.

This compound was prepared in order to investigate the role of the hydrophobic fluorous chain in the ionic liquid-modified proline. The fluorous tag could be also useful for recovery and reuse of such catalyst.

Compounds **11a-d** were easily prepared from N-Cbz-4-hydroxyproline by benzylation and subsequent esterification in the presence of 1,3-dicyclohexylcarbodiimide and 4-(dimethylamino)pyridine followed by removal of the protecting groups by catalytic hydrogenolysis (Scheme 1). Products were obtained in 64–98% overall yield.
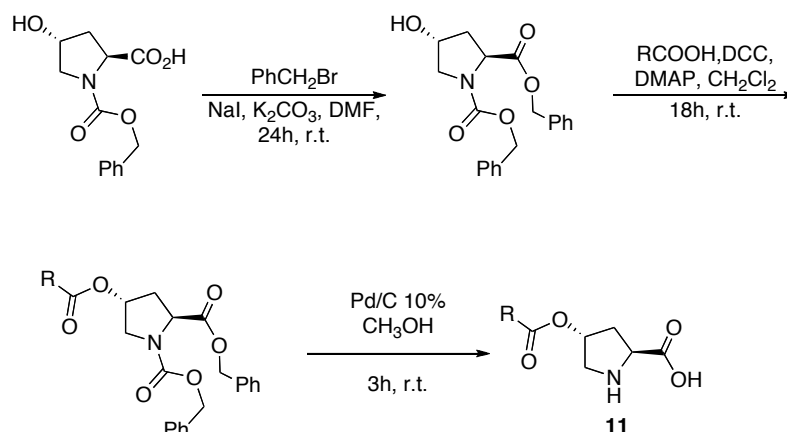
Scheme 1. Synthesis of catalysts **11a-d**

Compound **12** was easily prepared starting from Cbz-protected trans-4-hydroxy-L-proline, benzyl ester and 4-phenylbutyric acid, using a standard Mitsunobu protocol, followed by removal of the protecting groups by catalytic hydrogenolysis.

The synthesis of **13** was smoothly met in just four operations starting from Cbz-protected trans-4-hydroxy-L-proline (Scheme 2).
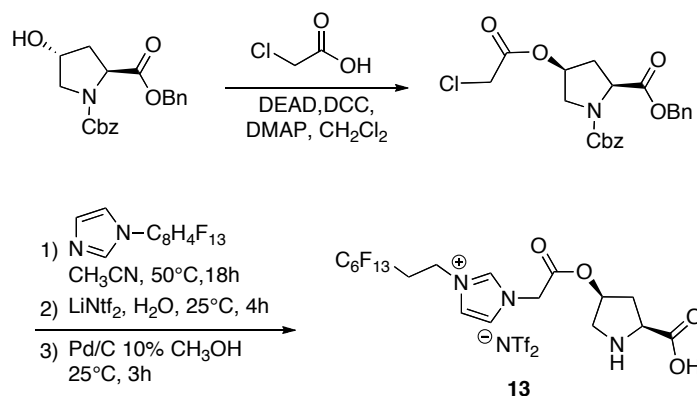
Scheme 2. Synthesis of the ionic-tagged cis-4-hydroxy-L-proline **13**

A reaction between the protected trans-4-hydroxy-L-proline and chloroacetic acid was followed by installation of N-fluoroalkyl-substituted imidazole on the chloro ester moiety and anion exchange with lithium trifilimide. Hydrogenation cleavage of the protective groups completed the synthesis of **13** in 98% yield from Cbz-protected trans-4-hydroxy-L-proline benzyl ester.

1.2.2 Screening of Catalysts

With the aim to discover the more active and stereoselective catalyst, the molecules in Figure 5 were tested for the model aldol reaction between cyclohexanone and 4-nitrobenzaldehehyde. The screening was carried out by using 2, 1 or 0.5% of catalyst and variable amount of water (175 μL, 19 equiv.; or 11 μL, 1.2 equiv.) with the purpose to see how the catalyst/water ratio influenced the reactions.

First the reactions were carried out by using 2 mol% of catalyst and an excess amount (175 μL) of water (Table 1).

Table 1. Screening of catalysts **11a-d, 12** and **13** in the direct asymmetric aldol reaction between cyclohexanone and 4-nitrobenzaldehyde in the presence of water.[a]

Entry	Catalyst		Conv. (%)	Yield[b] (%)	Anti/Syn[c]	e.e.[d] (%)	TON
1		**11a**	>99	99	87/13	86	50
2		**11b**	>99	98	91/9	91	49
3		**11c**	18	16	83/17	11	8
4 [e]		**11c**	98	95	62/38	28	47
5 [f]		**11c**	48	45	78/22	94	23
6		**11d**	>99	98	95/5	97	50
7		**12**	>99	98	96/4	97	49
8		**13**	>99	98	97/3	97	50

[a] Reaction conditions: cyclohexanone (260 μL, 2.5 mmol), aldehyde (0.5 mmol), catalyst (0.01 mmol), H$_2$O (175 μL), room temperature, 24 h. [b] Isolated yield. [c] Determined by ^{1}H NMR of the crude product. [d] *Anti* diastereoisomer, determined by HPLC using a chiral column. [e] Reaction carried out in MeOH. [f] Reaction carried out in *i*-PrOH.

The increased hydrophobicity of **11b** compared to that of **11a** resulted in a moderate increase in stereoselectivity, (Table 1, Entries 1 and 2). In each case, the yield was almost quantitative. Simple fluorous proline derivative **10c** was much less active and stereoselective (Table 1, Entry 3). With the latter catalyst, two others solvents (MeOH and *i*-PrOH) were employed, but again the results were disappointing (Table 1, Entries 4 and 5). This finding could be ascribed to its lower solubility (see the Experimental Section). Catalyst **12** was highly active and stereoselective. In comparison to its diastereoisomer **10e**[19b] a slightly lower enantioselectivity was observed (Table 1, Entry 7). A high efficiency was achieved by working with catalyst **13**, where the counterion was the lipophilic bis(trifluoromethylsulfonyl)imide ion.

Table 2. Screening of catalysts **10a-h, 11** in the direct asymmetric aldol reaction between cyclohexanone and 4-nitrobenzaldehyde in the presence of water.[a]

Entry	Catalyst		Cat. loading mol%	Water mL	Conv. %	Yield[b] %	Anti/Syn[c]	ee[d] %	TON
1		**11a**	1	175	57	54	96.5/3.5	>99	54
2			0.5	175	57	55	93/7	93	110
3			0.5	11	91	90	84/16	99	180
4		**11b**	1	175	>99	99	97/3	>99	99
5			0.5	175	74	72	96/4	97	144
6			0.5	11	>99	98	87/13	80	196
7		**11c**	0.5	175	-	-	-	-	-
8		**11d**	0.5	175	20	18	96/4	98	36
9			0.5	11	43	40	94/6	92	80
10		**12**	1	175	70	69	96.5/3.5	97	69
11			0.5	175	40	39	97.5/2.5	97	78
12			0.5	11	95	93	93.5/6.5	80	186
13		**13**	0.5	175	47	46	97/3	84	93
14			0.5	44	57	54	97/3	88	114
15			0.5	11	44	43	94/6	44	88

[a] Reaction conditions: cyclohexanone (260 μL, 2.5 mmol), aldehyde (0.5 mmol), catalyst, H_2O, room temperature, 24 h. [b] Isolated yield. [c] Determined by ^1H NMR of the crude product. [d] *Anti* diastereoisomer, determined by HPLC using a chiral column

A comparison between these data and the previous reported data[20b] suggests that the best results are achieved when a rigid hydrophobic group (*i.e.*, **11b**) or a long alkyl chain (*i.e.*, **11d**) or, at least, a propyl chain bearing an additional hydrophobic group (*i.e.*, **10d-e, 12**) are present as the acyl substituent.

The main factors that play a role in activity and selectivity are, in addition to the nature of the acyl group, the amount of catalyst and the catalyst/water ratio.

Then, after this preliminary test, we carried out further experiments by lowering the catalyst loading (1–0.1 mol-%) and by using an excess amount (175 µL) or 1.2 equiv. (11 µL) of water (Table 2). Different catalyst loadings and water/catalyst ratios caused different reaction outcomes in both the chemical yields and stereoselectivities. As an example, catalyst **11a** gave excellent enantioselectivity, high diastereoselectivity, and moderate yield when used in 1 mol%. The enantioselectivity decreased when **11a** was used in 0.5 mol%, whereas a lower amount of water caused a higher yield but a decreased diastereoselectivity (Table 2, Entries 1–3). A similar comparison can be done with the remaining catalysts (for example, Table 2, Entries 4–6). Among the catalysts, the diphenyl derivative **11b** gave excellent results when employed in 1 mol% (Table 2, Entries 4). Fluorinated derivative **11c** was inactive (Table 2, Entry 7).

A comparison of the data obtained by using catalysts **12** and **10d** clearly indicated that catalyst **10d**, having a trans configuration, gave better results under the examined conditions. However, catalyst **12** was much less soluble (see the Experimental Section) than **10d**, and probably, the different solubility could make the comparison devoid of significance.

1.2.3   *Screening of aldehydes*

After this screening of catalysts **11a–d** and **12** and **13**, the attention was focused on one of these compounds: the catalyst **11b**, which gave excellent results at 1 mol% loading (Table 2, Entry 4). Then, using catalyst **11b** under the optimized reaction conditions, several aldol reactions were carried out. The results obtained in the aldol reaction between cyclohexanone and several substituted benzaldehydes in the presence of catalyst **11b** are reported in Tables 3. The use of catalyst **11b** gave aldol products in excellent optical purity (98 to >99 %; Table 3, Entries 1– 6), high diastereoselectivities, and high yields. Less-reactive aldehydes furnished products still with high ee values (94– 97 %; Table 3, Entries 7–9) and good yields. Only 4-tolualdehyde gave a moderate yield, whereas 4-methoxybenzaldehyde was non reactive.

Table 3. Direct asymmetric aldol reaction between cyclohexanone and substituted benzaldehydes in the presence of water catalyzed by 10b.[a]

Entry	R	Time (h)	Conv. (%)	Yield[b] (%)	*Anti/Syn*[c]	ee[d]	TON
1	4-NO$_2$	24	>99	99	97:3	>99	100
2	4-CN	24	99	95	96.5:3.5	>99	95
3	2-NO$_2$	24	95	94	99:1	>99	94
4	4-Br	24	86	85	96:4	>99	85
5	4-Cl	24	87	81	95:5	>99	81
6	2,3,4,5,6-F$_5$	24	>99	>99	>99:1	98	100
7	H	24	75	69	93.5:6.5	97	69
8	4-CH$_3$	72	26	25	87:13	94	25
9	3-OCH$_3$	72	78	74	92:8	95	74
10	4-OCH$_3$	72	<5	-	-	-	-

[a] Reaction conditions: cyclopentanone (220 μL, 2.5 mmol), aldehyde (0.5 mmol), catalyst, H$_2$O (175 μL), room temperature. [b] Isolated yield. [c] Determined by ^{1}H NMR spectroscopic analysis of the crude product. [d] The anti diastereoisomer, determined by HPLC by using a chiral column.

Further experiments carried out by employing cyclopentanone confirmed the high performances of these catalysts. Catalyst **11b** gave aldol products with excellent *ee* values (96 to >99%), high diastereoselectivities (89:11 to 96:4), and very high yields (82 to >99%) even with less reactive aldehydes (Table 4).

Table 4. Direct asymmetric aldol reaction between cyclopentanone and substituted benzaldehydes in the presence of water catalyzed by **11b**.[a]

Entry	R	Time (h)	Conv. (%)	Yield[b] (%)	Anti/Syn[c]	ee[d]	TON
1	4-NO$_2$	24	>99	>99	92:8	>99	100
2	4-CN	24	>99	99	91.5:8.5	>99	99
3	2-NO$_2$	24	>99	>99	96:4	>99	100
4	4-Cl	24	93	92	92:8	99	92
5	4-Br	24	96	96	92:8	99	96
6	H	24	87	86	92.5:7.5	98	86
7	4-CH$_3$	72	84	82	89:11	96	82
8	4-OCH$_3$	72	96	96	90:10	97	96

[a] Reaction conditions: cyclopentanone (220 µL, 2.5 mmol), aldehyde (0.5 mmol), catalyst, H$_2$O (175 µL), room temperature. [b] Isolated yield. [c] Determined by ^{1}H NMR spectroscopic analysis of the crude product. [d] The *anti* diastereoisomer, determined by HPLC by using a chiral column.

1.2.4 Mechanistic Aspects

From a mechanistic point of view, water plays a crucial role. Such role was evident when the reactions were carried out in neat conditions showing that water enhances the catalyst activity and stereosectivity.[20b] It was hypothesized that, under the reaction conditions employed, a hydrophobic region and a hydrophilic region can be formed in the presence of catalyst, as depicted in Figure 6.
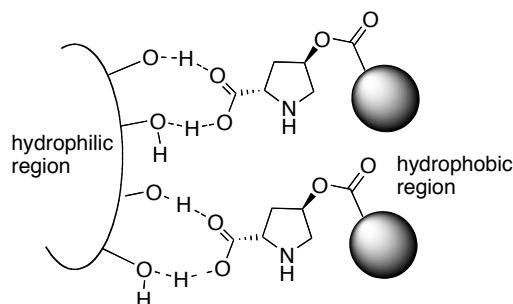
Figure 6. Proposed structure of catalyst in the presence of water

The enhanced activity of organic catalysis on water has been recently theoretically investigated. Free OH groups of interfacial water molecules play a key role in catalyzing reactions via the formation of hydrogen bonds.[22]

Quantum mechanical calculations have predicted the transition state geometries for the reaction of cyclohexanone enamine with benzaldehyde.[23] The transition states involving the *re* attack on the anti-enamine are lower in energy than the transition states for *si* attack on the syn-enamine.[23] Following this mechanism, in order to explain the observed enhanced stereoselectivities, we hypothesize that transition state A (Figure 6) is highly stabilized because the hydrophobic aldehyde attacking the anti-enamine lies in the hydrophobic region. The excellent enantioselectivities observed can be explained by transition state B. In this case the less favoured attack of aldehyde on the syn-enamine is more destabilized because the hydrophobic aldehyde lies in the hydrophilic region. Finally, the high diastereoselectivities observed can be explained by transition state C. In this case the attack of aldehyde on anti-enamine is more destabilized because the hydrophobic part of the aldehyde is directed towards the hydrophilic region. This model can explain the lower stereoselectivity observed when water is absent.
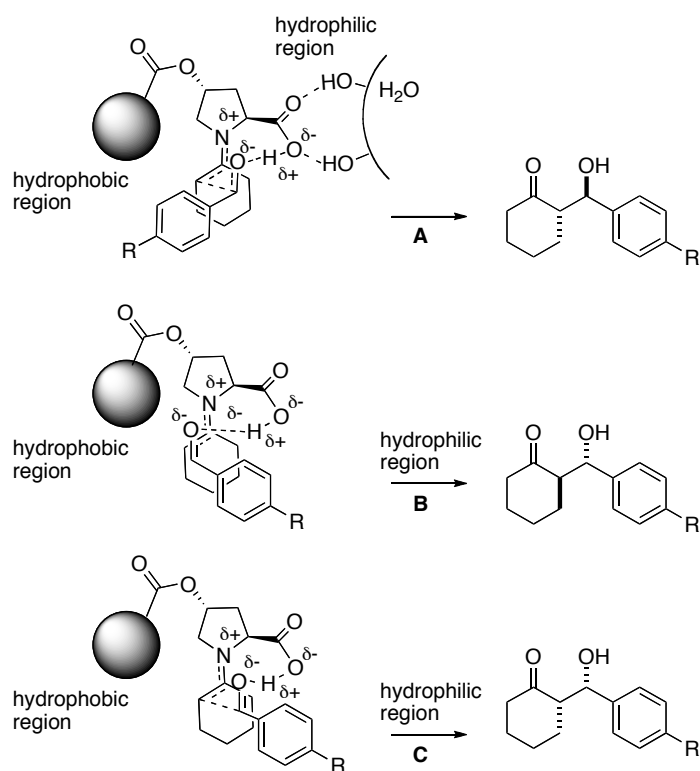
Figure 6. Proposed transition state model for the major steroisomer (A), its enantiomer (B), and the minor diastereoisomer (c)

1.4   *Conclusions*

In conclusion, the data reported represent an update regarding the use of cheap proline-based organocatalysts for the asymmetric aldol reaction in water. Deeper investigations showed the general and wide applicability of hydrophobic 4-acyloxyproline derivatives as catalysts for the direct asymmetric aldol reaction between cyclic ketones and substituted benzaldehydes. Particularly, this chapter presented the outstanding activity and stereoselectivity of *trans*-4-hydroxy-L-prolines bearing a simple 2,2-diphenylacetate (**11b**), which afforded aldol products with high to excellent enantio- and diastereoselectivities, even when cyclopentanone was employed, with as low as 1 mol% catalytic loading. It is important to stress that simple catalysts such as **11b** do not need the use of low temperature or additives, do not need new chiral centers in addition to those of inexpensive *trans*-4-hydroxy-L-proline. Finally, the data reported suggest that such catalytic molecules are organized at the ketone/water interface and their organization depends on the nature of the acyl group and on the catalyst/water ratio (see Tables 1 and 2). Further studies in this field may disclose new simple more active and stereoselective proline catalysts.

1.4   *Experimental Section*

General Methods

The NMR spectra were recorded on a Bruker 300 MHz spectrometer using $CDCl_3$ or DMSO-d_6 as solvent. Solid-state $^{13}C\{H\}$ CP-MAS NMR spectra was recorded on a Bruker AV 400, 400 MHz spectrometer with samples packed in zirconia rotors spinning at 13 kHz. FT-IR spectra were registered with a Shimadzu FTIR 8300 infrared spectrophotometer. Carbon and nitrogen contents were determined by combustion analysis in a Fisons EA 1108 elemental analyzer. Optical rotations were measured in chloroform on a Jasco P1010 polarimeter. Hydrogenation reactions were carried out using a Parr apparatus. Flash chromatography was carried out using Macherey–Nagel (0.04–0.063 mm) silica gel. Melting points were determined using a Köfler hot plate. Chiral HPLC analyses were performed using a Shimadzu LC-10AD apparatus equipped with an SPD-M10A UV detector and Daicel columns (OD-H, AD-H, AS-H) using hexane/2-propanol as eluent. Aldol products, except (S)-2-{(R)-hydroxy[3-methoxyphenyl]methyl}cyclopentanone, are known compounds and showed spectroscopic and analytical data in agreement with their structures (see Table 5 and Table 6). The configurations of products have been assigned by comparison with literature data. N-Cbz-4-hydroxy-proline was commercially available (Aldrich). (2S,4R)-Dibenzyl 4-hydroxypyrrolidine-1,2-dicarboxylate was prepared as reported in the literature.[24] Catalyst 11d[16] is know compound and showed spectroscopic and analytic

data in agreement with its structure. 1,3-Bis(1H,1H,2H,2H-perfluorooctyl)imidazolium iodide was prepared as reported in the literature.[25]

General Procedure for the Synthesis of Catalyst

Compounds 11a-d, 12

<u>Step 1</u>: To a solution of (2S, 4R)-dibenzyl-4-hydroxypyrrolidine-1,2-dicarboxylate (562 mg, 1.58 mmol) in anhydrous dichloromethane (35 mL) the proper carboxylic acid (2.24 mmol) was added. The mixture was stirred for 10 min at 0 °C under an atmosphere of argon. Then, a solution of 1,3-dicyclohexylcarbodiimide (DCC; 2.24 mmol) and 4-(dimethylamino)pyridine (DMAP; 0.224 mmol) in dichloromethane (10 mL) was added, and the mixture was stirred at 0 °C for 15 min. The reaction mixture was stirred overnight at room temperature under an atmosphere of argon. After this period, the dichloromethane solution was washed with water (2 x 30 mL), and the organic phase was dried with $MgSO_4$ and concentrated under reduced pressure.

<u>Step 2</u>: To a solution of compounds **14a–d** or **15** (1.91 mmol) in methanol (65 mL) was added Pd (10 %)/C (308 mg). The reaction mixture was stirred under an atmosphere of hydrogen in a Parr apparatus for 3 h. After this time, the reaction mixture was filtered through a short pad of Celite and then through a short pad of silica, washing with methanol. The organic phase was concentrated under reduced pressure to give compounds **11a–d** and compound **12** (see Scheme 3).
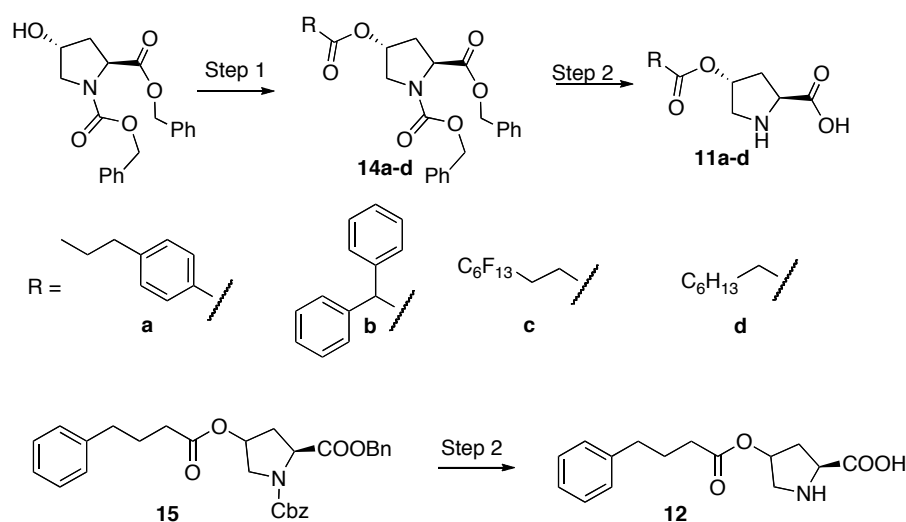
Scheme 3. Synthesis of catalysts 11a-d and 12

*(2S,4R)-dibenzyl 4-(4-propylbenzoyloxy)pyrrolidine-1,2-dicarboxylate (**14a**):* the residue was purified by column chromatography (petroleum ether/ethyl acetate, 5 :1), to give the *title compound* **12d** as a pale yellow oil; yield: 92%; $[\alpha]_D^{29}$ = -33.0 (*c* 0.84, $CHCl_3$); δ_H (300 MHz, $CDCl_3$) 0.87 (t, J= 7.4 Hz, 3 H), 1.57 (s, J=

7.4 Hz, 2H), 2.25 (m, 1H), 2.48 (m, 1H), 2.56 (t, J= 7.4 Hz, 2H), 3.80 (m, 2H), 4.53 (m, 1H), 4.93-5.20 (m, 4H), 5.44 (bs, 1H), 7.14-7.28 (m, 12H), 7.81 (d, J= 7.8Hz, 2H); δ_c (75 MHz, CDCl$_3$; two rotamers) 172.0, 171.8, 165.9, 154.8, 154.2, 148.9, 148.8, 136.2, 136.2, 135.4, 135.6, 129.7, 128.6, 128.4, 128.4, 128.3, 128.2, 128.1, 28.0, 127.9, 127.8, 126.9, 126.9, 72.9, 72.2, 67.3, 67.1, 67.0, 58.1, 57.8, 52.7, 52.4, 38.0, 36.8, 35.7, 30.9, 24.2, 13.7; IR (nujol): ν_{max} = 2959, 2931, 1749, 1715, 1609, 1353, 755, 698 cm^{-1}. [Found: C, 71.5; H, 6.4; N, 2.8. C$_{30}$H$_{31}$NO$_6$ requires C, 71.8; H, 6.2; N, 2.8].

(2S,4R)-4-(4-propylbenzoyloxy)pyrrolidine-2-carboxylic acid (11a): pale yellow liquid-viscous; yield: 85%; $[\alpha]_D^{25}$ = -15.1 (*c* 0.47, DMSO); δ_H (300 MHz, DMSO-d$_6$) 0.79 (t, J= 7.3 Hz, 3H), 1.50 (m, J= 7.3 Hz, 2H), 2.05 (m, 1H), 2.42 (m, 1H), 2.52 (t, J= 7.3 Hz, 2H), 3.28 (bs, 1H), 3.49 (bs, 1H), 3.73 (bs, 1H), 5.28 (m, 1H), 7.24 (d, J= 7.5, 2H), 7.82 (d, J= 7.5, 2H); d$_c$ (75 MHz, DMSO-d$_6$) 172.2, 165.0, 147.9, 129.2, 128.33 127.2, 127.0, 36.9, 35.9, 28.8, 24.2, 23.7, 23.5113, 13.2. [Found: C, 65.1; H, 6.9; N, 5.1. C$_{15}$H$_{19}$NO$_4$ requires C, 64.9; H, 6.9; N, 5.0].

(2S,4R)-dibenzyl 4-(2,2-diphenylacetoxy)pyrrolidine-1,2-dicarboxylate (14b): the residue was purified by column chromatography (petroleum ether/ethyl acetate, 4 :1), to give the *title compound* **12f** as a pale yellow oil; yield: 98%; $[\alpha]_D^{29}$ = -29.8 (*c* 0.64, CHCl$_3$); δ_H (300 MHz, CDCl$_3$) 2.20(m, 1H), 2.44 (m,1H), 3.84 (m, 2H), 4.47 (dt, 1H), 5.05 (s, 2H), 5.11 (s, 1H), 5.23 (m, 2H), 5.40 (bs, 1H), 7.36 (m, 20H); δ_c (75 MHz, CDCl$_3$; two rotamers) 171.8, 171.7, 171.6, 154.5, 153.9, 137.9, 137.9, 137.8, 136.1, 136.0, 135.2, 135.0, 128.5, 128.5, 128.4, 128.3, 128.3, 128.2, 128.2, 128.0, 128.0, 127.9, 127.7, 127.7, 127.3, 127.3, 73.1, 72.4, 69.3, 67.2, 67.1, 66.9, 66.8, 57.7, 56.6, 53.3, 52.2, 51.8, 36.2, 35.2, 31.6, 29.1; IR: ν_{max} = 1715, 1738, 1418, 1186, 1150, 768, 746 cm^{-1}. [Found: C, 74.5; H, 5.8; N, 2.6. C$_{15}$H$_{19}$NO$_4$ requires C, 74.3; H, 5.9; N, 2.5].

(2S,4R)-4-(2,2-diphenylacetoxy)pyrrolidine-2-carboxylic acid (11b): pale yellow solid; yield: 93%; $[\alpha]_D^{29}$ = -2.5 (*c* 0.62, methanol); mp 102-105 °C; δ_H (300 MHz, CD$_3$OD) 1.98 (bs, 2H), 2.95 (d, J = 11.9 Hz, 1H), 3.26 (m, 1H), 3.37 (d, J = 11.9 Hz, 1H), 3.58 (bs, 1H), 5.17 (s, 1H), 7.24 (m, 10H); δ_c (75 MHz, CD$_3$OD) 172.4, 139.6, 129.5, 129.2, 128.0, 75.6, 73.5, 60.6, 56.5, 50.8, 36.3; IR (nujol): ν_{max} = 2853, 2922, 1726, 1456, 1377, 1146 cm^{-1}. [Found: C, 70.3; H, 5.9; N, 4.4. C$_{19}$H$_{19}$NO$_4$ requires C, 70.4; H, 5.9; N, 4.1].

(2S,4R)-dibenzyl4-(4,4,5,5,6,6,7,7,8,8,9,9,9-tridecafluorononanoyloxy)pyrrolidine-1,2 dicarboxylate (14c): the residue was purified by column chromatography (petroleum ether/ethyl acetate, 8:1), to give the *title compound* **12h** as a pale yellow oil; yield: 64%; $[\alpha]_D^{27}$ = -23.7 (*c* 0.90, CHCl$_3$); δ_H (300 MHz, CDCl$_3$) 2.20 (m,1H), 2.35 (m, 3H), 2.54 (m, 2H), 3.55-3.75 (m, 3H), 4.44 (dt, 1H), 5.03 (m, 4H), 5.25 (m, 1H), 7.19

(m,10H); δ_c (75 MHz, CDCl$_3$) 171.9, 171.6, 170.4, 170.4, 154.6, 154.1, 136.2, 136.1, 135.3, 135.1, 128.6, 128.5, 128.4, 128.3, 128.2, 128.1, 128.1, 128.0, 127.9, 120.4-103.8 (22 CF signals), 73.4, 72.7, 67.4, 67.4, 67.1, 67.0, 57.9, 57.6, 52.4, 52.0, 36.4, 35.4, 26.6, 26.3, 26.0, 25.5, 25.4, 25.4037; IR (nujol): ν_{max} = 1746, 1713, 1418, 1354, 1146, 1123, 737, 700 cm^{-1}. [Found: C, 47.9; H, 3.4; N, 2.0. C$_{29}$H$_{24}$F$_{13}$NO$_6$ requires C, 47.7; H, 3.3; N, 1.9].

(2S,4R)-4-(4,4,5,5,6,6,7,7,8,8,9,9,9-tridecafluorononanoyloxy)pyrrolidine-2-carboxylic acid (11c): white-grey powder; yield: 92%; mp 130-135 °C. Since this compound is very poor soluble, it was characterized by solid state ^{13}C NMR (see Figure 5). δ_c 173.5, 170.8, 130-110 (CF signals), 73.7, 62.7, 51.9, 36.4, 25.8, 24.9. IR (nujol): ν_{max} = 2853, 1742, 1460, 1377 cm^{-1}. [Found: C, 33.3; H, 2.9; N, 2.8. C$_{14}$H$_{12}$F$_{13}$NO$_4$ requires C, 33.8; H, 2.4; N, 2.7].
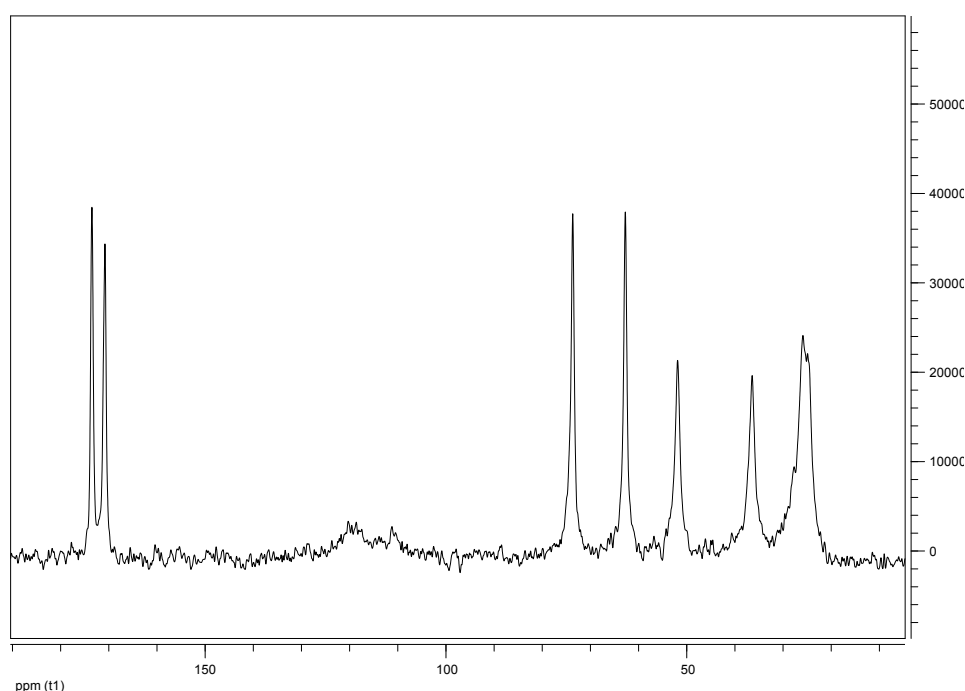
Figure 5. Solid-state ^{13}C NMR spectrum of compound **11c**.

(2S,4S)-dibenzyl 4-(4-phenylbutanoyloxy)pyrrolidine-1,2-dicarboxylate (15): the residue was purified by column chromatography (petroleum ether/ethyl acetate, 3:1), to give the *title compound* **13** as a pale yellow oil; yield: 70%; $[\alpha]_D^{28}$ = -41.5 (*c* 0.73, CHCl$_3$); δ_H (300 MHz, CD$_3$OD) 1.17 (t, J= 5.5 MHz, 1H), 1.69 (m, 2H), 1.96 (m, 2H), 2.20 (dd, 1H), 2.37 (m, 3H), 3.45 (dd, J= 5.0 MHz, 1H), 3.64 (dd, J= 5.0 MHz, 1H), 4.45 (dd, J= 9.4 MHz, 1H), 5.02 (m, 5H), 7.13 (m, 15H); δ_c (75 MHz, CD$_3$OD) 173.1, 171.81, 171.6, 155.3, 155.0, 141.6, 136.6, 136.0, 128.4, 128.3, 128.0, 127.7, 125.9, 73.3, 72.3, 67.3, 66.8, 58.3, 58.1, 52.8, 52.5,

36.0, 35.1, 34.8, 33.1, 26.4; IR ν_{max} = 3030, 2949, 1711, 1496, 1415, 1165, 1070, 1005 cm^{-1}. [Found: C, 74.6; H, 6.2; N, 2.9. $C_{30}H_{29}NO_5$ requires C, 74.5; H, 6.0; N, 2.9].

(2S,4S)-4-(4-phenylbutanoyloxy)pyrrolidine-2-carboxylic acid (12): white-grey powder; yield: 95%; mp 163-167 °C; Since this compound is very poor soluble, it was characterized by solid state ^{13}C NMR (see Figure 6). IR (nujol): ν_{max} = 2924, 2852, 17430, 1597, 1460, 1377 cm^{-1}. [Found: C, 65.1; H, 6.9; N, 5.1. $C_{15}H_{19}NO_4$ requires C, 64.9; H, 6.9; N, 5.0].
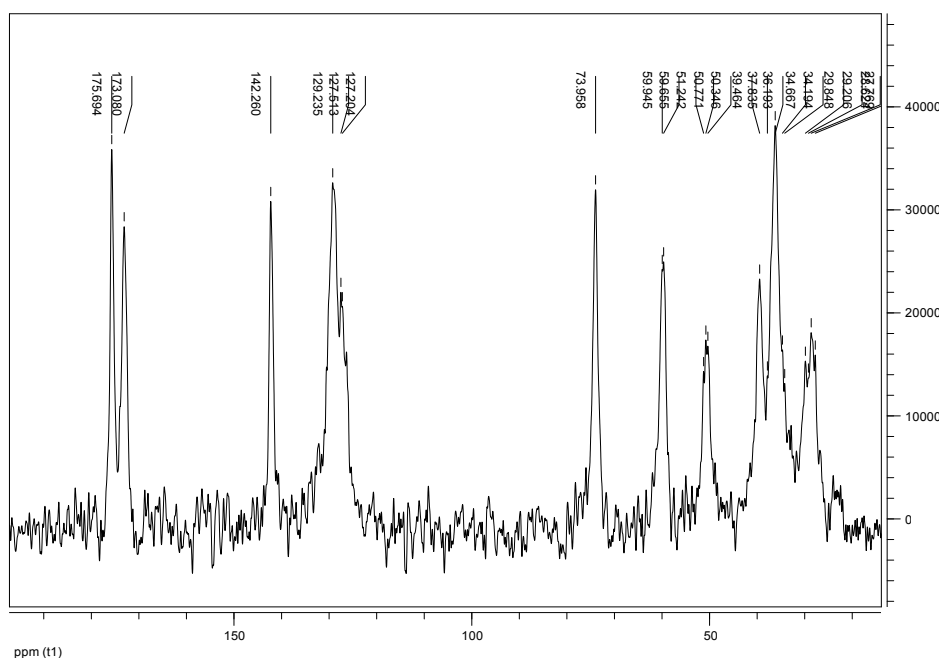
Figure 6. Solid-state ^{13}C NMR spectrum of compound **11**

Compound 14

Step 1: To a solution of (*N* benzyloxycarbonyl-(2*S*,4*R*)-4-hydroxyproline benzyl ester (562 mg, 1.58 mmol) in anhydrous dichloromethane (45 mL) the chloroacetic acid (2.24 mmol) was added. The mixture was stirred for 10 min at 0 °C under an atmosphere of Argon. Then, a solution of 1,3-dicyclohexylcarbodiimide (DCC; 2.24 mmol) and 4-(dimethylamino)pyridine (DMAP; 0.224 mmol) in dichloromethane (10 mL) was added, and the mixture was stirred at 0 °C for 15 min. The reaction mixture was stirred overnight at room temperature under an atmosphere of argon. After this period, the dichloromethane solution was washed with water (2x30 mL), and the organic phase was dried with MgSO$_4$ and concentrated under reduced pressure.

Step 2: To a solution of the above chloroacetate (0.61 g, 1.5 mmol) in CH$_3$CN (10 mL) was added N,N'-difluoroalkyl-substituted imidazolium salt (0.640 g, 1.5 mmol) and the reaction mixture was heated at 50 °C for 18 h. The CH$_3$CN was then removed under reduced pressure. The crude hygroscopic product

was washed with anhydrous ether (5 mL × 4) and vacuum dried to obtain the title imidazolium chloride salt. The imidazolium chloride salt thus obtained (0.839 g, 1 mmol) was dissolved in water (3 mL), a solution of *N*-lithiobis(trifluoromethylsulfonyl)imide (0.3 g, 1.04 mmol) in H_2O (3 mL) was added and the reaction mixture was stirred for 4 h at 65°C. The crude product was extracted with AcOET (15 mL × 4) and the combined organic layer was washed with H_2O (10 mL × 4) (until no precipitate formation was seen with $AgNO_3$). Concentration of the organic layer under vacuum afforded the corresponding imidazolium bis(trifluoromethylsulfonyl)imide salt

Step 3: To a solution of the imidazolium bis(trifluoromethylsulfonyl)imide salt (1.05 g, 1 mmol) in MeOH (32 mL) was added Pd (10 %)/C (156 mg). The reaction mixture was stirred under an atmosphere of hydrogen in a Parr apparatus for 3 h. After this time, the reaction mixture was filtered through a short pad of Celite and then through a short pad of silica, washing with methanol. The organic phase was concentrated under reduced pressure to give compounds **13** (see Scheme 4).
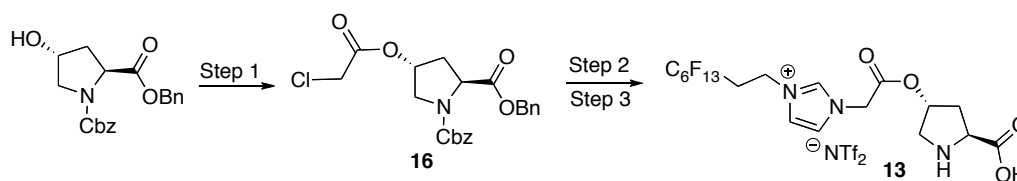
Scheme 4. Synthesis of catalysts 13

N-Benzyloxycarbonyl-(2S,4S)-4-(2-chloroacetyl)proline benzyl ester **(16)**: the residue was purified by column chromatography (petroleum ether/ethyl acetate, 3 :1), to give the compound **16** as a pale yellow oil (0.643 g, 93 % yield). $[\alpha]_D^{20}$ = −63.4 (*c* = 1.2, $CHCl_3$); ^{1}H NMR (200 MHz, CDCl3, two conformational isomers) δ 2.32 - 2.61 (m, 2 H), 3.50 - 3.72 (m, 2 H), 3.72 - 3.91 (m, 2 H), 4.62 (ddd, *J* = 18.31, 8.42, 2.56 Hz, 1 H), 5.07 - 5.26 (m, 4 H), 5.32 (m, 1 H), 7.28 - 7.43 (m, 10 H); ^{13}C NMR (50 MHz, $CDCl_3$, two conformational isomers) δ 34.53, 35.54, 39.9, 51.5, 51.9, 57.1, 57.4, 66.28, 66.33, 66.57, 66.64, 73.2, 74.2, 127.3, 127.4, 127.46, 127.54, 127.70, 127.8, 127.89, 127.94, 128.0, 135.1, 135.2, 135.9, 153.5, 153.9, 166.0, 170.3, 170.5. [Found C, 61.2; H, 5.1; N, 3.2. $C_{22}H_{22}ClNO_6$ requires C, 61.1; H, 5.0; N, 3.6].

Imidazolium chloride salt: pale yellow oil (0.952 g, 76% yield). $[a]_D^{27}$ = -37.32 (*c* 0.7625, $CHCl_3$); ^{1}H NMR (200 MHz, $CDCl_3$, two conformational isomers) d 1.5 (m, 2H), 2.25 - 2.63 (m, 2 H), 3.57 - 3.83 (m, 2 H), 3.61 (m, 2 H), 4.42 - 4.63 (m, 1 H), 4.96 - 5.41 (m, 7 H), 6.78 - 7.69 (m, 12 H), 10.32 (br. s., 1 H); ^{13}C NMR (75 MHz, $CDCl_3$, two conformational isomers) 32.7, 34.1, 35.0, 35.7, 48.9, 51.1, 51.6, 56.7, 57.0, 66.2, 73.2, 74.2, 118.3, 112.7, 109.4 122.4, 123.0, 126.8, 127.1, 127.3, 127.4, 127.6, 127.7, 127.8, 134.9,

135.4, 137.6, 153.2, 153.6, 164.9, 170.4. IR ν_{max} = 3361, 2299, 1711, 1496, 1693, 1119, 1004 cm^{-1}. [Found: C, 61. 2; H, 5.1; N, 3.3 $C_{33}H_{29}ClF_{13}N_3O_6$ requires C, 61.2; H, 5. 3; N, 3. 4].

1-(2-((3R,5S)-5-carboxypyrrolidin-3-yloxy)-2-oxoethyl)-3-(3,3,4,4,5,5,6,6,7,7,8,8,8-tridecafluorooctyl)-1H

*imidazol-3-ium (*compound **13***):* pale yellow oil (0.823 g, 94 % yield). $[\alpha]_D^{27}$ = -10.3 (*c* 0.7625, MeOH); ^{1}H NMR (300 MHz, DMSO) δ 1.6 -1.8 (m, 2H) 2.54 - 2.72 (m, 2 H) 3.61 (m, 2 H), 3.52 - 3.66 (m, 1 H) 3.66 - 3.80 (m, 1 H) 4.33 (dd, *J* = 9.28, 4.64 Hz, 1 H) 5.13 (d, 2 H) 5.51 (d, 1 H) 7.46 (br. s., 2 H) 8.74 (br.s., 1 H); ^{13}C NMR (75 MHz, DMSO) δ 23.1, 34.9, 40.9, 50.0, 51.0, 60.1, 75.5,118.2, 117.4, 112.1, 109.3, 121.6, 123.7, 123.9, 137.6, 167.1, 173.6. IR ν_{max} = 3284, 3099, 1759, 1496, 1639, 1350, 1143 cm^{-1}. [Found: C, 29.3; H, 3.3; N, 10.5 $C_{13}H_{16}F_6N_4O_8S_2$ requires C, 29.2; H, 3.2; N, 10.5].

Typical Procedure for the Aldol Reactions

Catalysts were added to a mixture of the corresponding aldehyde (0.5 mmol) and ketone (2.5 mmol) in distilled water (0.175 mL), and the reaction mixture was stirred at room temperature. The reaction was quenched by adding ethyl acetate, and the organic phase was washed with water. The organic layer was dried (MgSO$_4$) and concentrated under reduced pressure. The crude product was checked by ^{1}H NMR spectroscopy and HPLC and was then purified by chromatography (petroleum ether/ethyl acetate). Enantiomeric excess values were determined by HPLC by using chiral columns (OD-H, AD-H, AS-H) and hexane/2-propanol as eluent.

(S)-2-[(R)-hydroxy(3-methoxyphenyl)methyl]cyclopentanone: pale yellow viscous oil after purification by column chromatography (petroleum ether/ethyl acetate, 6 :1–3 :1); mixture of diastereoisomers. ^{1}H NMR(CDCl$_3$): δ = 1.58– 2.58 (m, 6 H, anti + syn), 2.80–2.83 (m, 1 H, syn), 3.91 (s, 3 H, anti+syn), 4.66 (s, 1H, OH, anti+syn), 4.79 (d, J=9.0 Hz, 1 H, anti), 5.36–5.38 (m, 1 H, syn), 6.88–7.02 (m, 3 H, anti + syn), 7.32–7.38 (m, 1 H, anti + syn) ; ^{13}C NMR (CDCl$_3$; anti diastereoisomer): d =223.0, 159.6, 143.0, 129.3, 118.9, 113.4, 111.8, 75.0, 55.2, 55.1, 38.7, 26.9, 20.3; (syn diastereoisomer): δ =220.3, 159.5, 144.6, 126.3, 117.7, 112.5, 111.1, 71.2, 56.0, 55.1, 39.1, 22.6, 20.4; IR (liquid film): IR ν_{max} =3447, 1724 cm^{-1}. [Found: C 70.9, H 7.4 $C_{14}H_{17}NO_4$ requires C 70.9, H 7.3].

In table 5 and Table 6 are reported same selected spectroscopic data for diastereoisomers and HPLC data for enantiomers compounds.

Table 5. Selected ^{1}H NMR spectroscopic data for diastereoisomers and HPLC data for enantiomers of compounds obtained in the reactions between cyclohexanone and aryl aldehydes.

Entry	Compound	^{1}HNMR (CDCl$_3$)		HPLC				
		Syn 1'H [ppm]	*anti* 1'H [ppm]	Column	Eluent [hexane/ i-PrOH]	Flow [mL·min^{-1}]	t$_R$ Major	t$_R$ Minor
1[a,b,c]	4-NO$_2$	5.4	4.8	AS-H	90:10	1.0	33.8	29.9
2[a,b]	4-CN	5.6	5.0	AS-H	90:10	0.5	86.8	75.2
3'	2-NO$_2$	5.48	4.90	AD-H	95:5	1.0	37	47
4[a,b,c]	4-Br	5.5	4.9	AD-H	90:10	0.5	31.3	36.4
5[a,b]	4-Cl	5.4	4.8	AD-H	90:10	0.5	27.5	31.5
6[d]	2,3,4,5,6-F$_5$	5.4	4.8	AD-H	90:10	1.0	7.8	10.0
7[a,b]	H	5.4	4.8	AS-H	90:10	0.5	27.2	29.4
8[e]	3-OCH$_3$	5.3	4.7	AS-H	90:10	0.5	39.5	48.5
9[b]	4-OCH$_3$	5.33	4.7	AD-H	90:10	0.5	42.7	43.9

[a] Ref. 26, [b] Ref. 27, [c] Ref. 28, [d] Ref. 29, [e] Ref. 30

Table 6. Selected ^{1}H NMR spectroscopic data for diastereoisomers and HPLC data for enantiomers of compounds obtained in the reactions between cyclopentanone and aryl aldehydes.

Entry	Compound	^{1}HNMR (CDCl$_3$)		HPLC				
		Syn 1'H [ppm]	*Anti* 1'H [ppm]	Column	Eluent [hexane/ i-PrOH]	Flow [mL·min^{-1}]	t$_R$ Major	t$_R$ Minor
1[a,b,c]	4-NO$_2$	5.3	5.1	OD-H	90:10	0.5	113.7	98.5
2[c,d]	4-CN	5.2	4.7	AS-H	90:10	0.5	86.8	75.2
3[e]	2-NO$_2$	5.7	5.2	OD-H	95:5	1.0	28.6	32.3
4[f]	4-Cl	5.1	5.0	AD-H	95:5	1.0	16.7	17.9
5[g]	4-Br	5.1	5.0	AD-H	95:5	1.0	27.9	30.3
6[a,b]	H	5.1	5.0	OD-H	90:10	1.0	11.6	14.0
7[h]	4-CH$_3$	5.1	4.9	AD-H	90:10	0.5	28.3	32.3

[a] Ref. 27, [b] Ref. 31, [c] Ref. 26, [d] Ref. 32, [e] Ref. 33, [f] Ref. 34, [g] Ref. 35, [h] Ref. 36

1.4   *References*

1. (a) G. Casiraghi, F. Zanardi, G. Appendino, G. Rassu, *Chem. Rev.* **2000**, *100*, 1929-1972. (b) T. D. Machajewski, C. H. Wong, *Angew. Chem. Int. Ed*. **2000**, *39*, 1352-1374.

2. B. List, R. A. Lerner, C. F. Barbas III, *J. Am. Chem. Soc*. **2000**, *122*, 2395-2396.

3. (a) S. Mukherjee, J. W. Yang, S. Hoffmann, B. List, Chem. Rev. **2007**, *107*, 5471-5569. (b) J. Seayad, B. List, *Org. Biomol. Chem.* **2005**, *3*, 719-724. (c) H. Pellissier, *Tetrahedron* **2007**, *63*, 9267-9331. (d) K. Sakthivel, W. Notz, T. Bui, C. F. Barbas III, *J. Am. Chem. Soc.* **2001**, *123*, 5260-5267. (e) W. Notz, F. Tanaka, C. F. Barbas III, *Acc. Chem. Res.* **2004**, *37*, 580-591 (f) P. Dziedzic, W. B. Zou, J. Hafren, A. Cordova, *Org. Biomol. Chem.* **2006**, *4*, 38-40. (g) S. Adachi, T. Harada, *Eur. J. Org. Chem.* **2009**, 3661-3671.

4. Review on proline–catalyzed reactions: (a) B. List, *Tetrahedron* **2002**, 58, 5573-5590. (b) E. R. Jarvo, S. J. Miller, *Tetrahedron* **2002**, 58, 2481-2495. (c) W. Notz, F. Tanaka, C. F. Barbas III, *Acc. Chem. Res.* **2004**, 37, 580-591.

5. (a) A. Berkessel, H. Gröger (Eds.), *Asymmetric Organocatalysis: From Biomimetic Concepts to Applications in Asymmetric Synthesis*, Wiley-VCH, Weinheim, **2005**. (b) P. I. Dalko (Ed.), *Enantioselective Organocatalysis*, Wiley-VCH, Weinheim, **2007**. (c) B. List (Ed.), *Asymmetric Organocatalysis*, Springer, Berlin, **2010**. (d) S. Mukherjee, J. W. Yang, S. Hoffman, B. List, *Chem. Rev.* **2007**, *107*, 5471-5569. (e) A. Erkkilä, I. Majander, P. M. Pihko, *Chem. Rev.* **2007**, *107*, 5416-5470.

6. For Michael reactions, see: (a) M. Wiesner, G. Upert, G. Angelici, H. Wennemers, *J. Am. Chem. Soc.* **2010**, *132*, 6-7. (b) M. Wiesner, J. D. Revell, H. Wennemers, *Angew. Chem. Int. Ed.* **2008**, *47*, 1871-1874. (c) M. Wiesner, J. D. Revell, S. Tonazzi, H. Wennemers, *J. Am. Chem. Soc*. **2008**, *130*, 5610-5611. (d) S. Zhu, S. Yu, D. Ma, *Angew. Chem. Int. Ed.* **2008**, *47*, 545-548; for Mannich reactions, see: (e) T. Kano, Y. Yamaguchi, O. Tokuda, K. Maruoka, *J. Am. Chem. Soc.* **2005**, *127*, 16408-16409. (f) S. Mitsumori, H. Zhang, P. H.-Y. Cheong, K. N. Houk, F. Tanaka, C. F. Barbas III, *J. Am. Chem. Soc.* **2006**, *128*, 1040-1041. (g) B. Rodríguez, C. Bolm, *J. Org. Chem.* **2006**, *71*, 2888-2891; for α-fluorination, see: (h) M. Marigo, D. Fielenbach, A. Braunton, A. Kjærsgaard, K. A. Jørgensen, *Angew. Chem. Int. Ed.* **2005**, *44*, 3703-3706.

7. M. R. Vishnumaya, V. K. Singh, *Org. Lett.* **2007**, *9*, 2593-2595.

8. M. R. Vishnumaya, V. K. Singh, *J. Org. Chem.* **2009**, *74*, 4289-4297.

9. S. Gandhi, V. K. Singh, *J. Org. Chem.* **2008**, *73*, 9411-9416.

10. Z. Tang, Z.-H. Yang, X.-H. Chen, L.-F. Cun, A.-Q. Mi, Y.-Z. Jiang, L. Z. Gong, *J. Am. Chem. Soc.* **2005**, *127*, 9285-9289.

11. Y.-N. Jia, F.-C. Wu, X. Ma, G.-J. Zhu, C.-S. Da, *Tetrahedron Lett.* **2009**, *50*, 3059-3062.

12. M. Jiang, S.-F. Zhu, Y. Yang, L.-Z. Gong, X.-G. Zhou, Q.-L. Zhou, *Tetrahedron: Asymmetry* **2006**, *17*, 384-387.

13. P. Krattiger, R. Kovasy, J. D. Revell, S. Ivan, H. Wennemers, *Org. Lett.* **2005**, *7*, 1101-1103.

14. T. Kano, O. Tokuda, K. Maruoka, *Tetrahedron Lett.* **2006**, *47*, 7423-7426.

15. J. Kofoed, T. Darbre, J.-L. Reymond, *Org. Biomol. Chem.* **2006**, *4*, 3268-3281.

16. S. Aratake, T. Itoh, T. Okano, N. Nagae, T. Sumiya, M. Shoji, Y. Hayashi, *Chem. Eur. J.* **2007**, *13*, 10246-10256.

17. M. Lombardo, S. Easwar, F. Pasi, C. Trombini, *Adv. Synth. Catal.* **2009**, *351*, 276-282.

18. W. Miao, T. H. Chan, *Adv. Synth. Catal.* **2006**, *348*, 1711-1718.

19. M. Gruttadauria, F. Giacalone, R. Noto, *Adv. Synth. Catal.* **2009**, *351*, 33-57.

20. (a) C. Aprile, F. Giacalone, M. Gruttadauria, A. Mossuto Marculescu, R. Noto, D. J. Revell, H. Wennemers, *Green Chem.* **2007**, *9*, 1328-1334. (b) F. Giacalone, M. Gruttadauria, P. Lo Meo, S. Riela, R. Noto, *Adv. Synth. Catal.* **2008**, *350*, 2747-2760. (c) M. Gruttadauria, A. Salvo, F. Giacalone, P. Agrigento, R. Noto, *Eur. J. Org. Chem.* **2009**, 5437-5444.

21. (a) M. Gruttadauria, F. Giacalone, R. Noto, *Chem. Soc. Rev.* **2008**, *37*, 1666-1688. (b) F. Cozzi, *Adv. Synth. Catal.* **2006**, *348*, 1367-1390. c) M. Benaglia, *New. J. Chem.* **2006**, *30*, 1525-1533.

22. Y. Jung, R. A. Marcus, *J. Am. Chem. Soc.* **2007**, *129*, 5492-5502.

23. S. Bahmanyar, K. N. Houk, H. J. Martin, B. List, *J. Am. Chem. Soc.* **2003**, *125*, 2475-2479.

24. J. K. Robinson, V. Lee, T. D. W. Claridge, J. E. Baldwin, C. J. Schofield, *Tetrahedron* **1998**, *54*, 981-996.

25. L. Xu, W. Chen, J. F. Bickley, A. Steiner, J. Xiao, *Journal of Organometallic Chemistry* **2000**, 598, 409-416.

26. M. Gruttadauria, F. Giacalone, A. Mossuto Marculescu, S. Riela, R. Noto, *Eur. J. Org. Chem.* **2007**, 4688-4698.

27. N. Mase, Y. Nakai, N. Ohara, H. Yoda, K. Takabe, F. Tanaka, C. F. Barbas III, *J. Am. Chem. Soc.* **2006**, *128*, 734-735.

28. A. Yanagisawa, H. Takahashi, T. Arai, *Chem. Commun.* **2004**, 580-581.

29. D. Gryko, W. J. Saletra, *Org. Biomol. Chem.* **2007**, *5*, 2148-2153.

30. L. Zu, H. Xie, H.Li, J. Wang, W. Wang, *Org. Lett.* **2008**, *10* (6), 1211-1214.

31. Y. Hayashi, T. Sumiya, J. Takahashi, H. Gotoh, T. Urushima, M. Shoji, *Angew. Chem. Int. Ed.* **2006**, *45*, 958-961.

32. Z. Jiang, Z. Liang, X. Wu, Y. Lu, *Chem. Commun.* **2006**, 2801-2803.

33. B. Rodríguez, A. Bruckmann, C. Bolm, *Chem. Eur. J.* **2007**, *13*, 4710-4722.

34. G. L. Puleo, A. Iuliano, *Tetrahedron: Asymmetry* **2007**, *18*, 2894-2900.

35. D.-S. Deng, J. Cai, *Helv. Chim. Acta* **2007**, *90*, 114-120.

36. Y.-Y. Peng, H. Liu, M. Cui, J.-P. Cheng, *Chin. J. Chem.* **2007**, *25*, 962-967.

Chapter 2

Silica Coated Iron Oxide Nanoparticles:

Synthesis, Functionalization and

Application in Organocatalysis
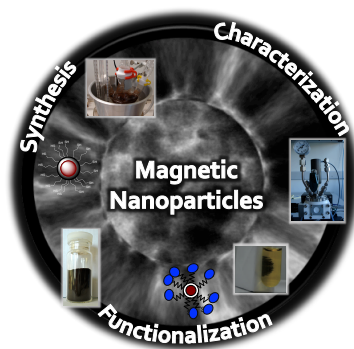
This chapter focuses in the synthesis of magnetic nanoparticles having an iron oxide core, and an outer silica shell. Silica coated iron oxide nanoparticles were synthesized using two different procedures: by co-precipitation using tetraethyl orthosilicate and by flame spray pyrolysis. The obtained materials were grafted with n-propyl thiol functional group. Different conditions were used for the optimization of the silylation reaction of mercaptosilane groups. The surface coverage of the silica with mercaptopropyl-group was analysed by two different way: elemental analysis and the reaction with 2,2'-dipyridyl disulphide followed by UV-Vis analysis of stechiometrically liberated pyridyl-2-thione.

Finally the coupling reaction between the prepared functionalized material and an organocatalyst was investigated. In particular a magnetic nanoparticles supported L-Proline was prepared. This material has been used as organocatalyst in the direct asymmetric aldol reaction between p-nitrobenzaldehyde and cyclohexanone.

2.1   Introduction

Magnetic nanoparticles based on iron oxide have received a great interest in a wide range of disciplines, including catalysis,[1] biotechnology, biomedicine,[2] magnetic resonance imaging data storage.[3]

Silica coating is often applied to magnetic iron oxide nanoparticles to improve their functionality and biocompatibility.[4] For the silica coating, the surface is often terminated using a silanol group that can reacts with various coupling agents to covalently attach specific ligands to the surfaces of these magnetic nanoparticles using conventional silane based chemistry.[5] The silica coating can either be accomplished as a core shell materials where each single iron oxide particle is coated with a silica layer or as a iron oxide nanoparticles embedded in a porous silica matrix. These core-shell type nanoparticles with defined iron oxide core size and silica shell thickness can be produced scalable in one step using flame spray pyrolysis (FSP).[6]

Organic functional groups immobilized in nanoparticles generating multifunctional systems combine in a single material the interesting properties of nanosized systems, magnetism, organic functionality and reactivity. The interest shown for this material depends on several factors: (i) it can be easily separated from a reaction mixture or guide to a target by means of an external magnetic fiels; (ii) it can bind to drugs, proteins, enzymes, antibodies, or nucleotides and can direct to an organ, tissue, or tumor using an external magnetic field; (iii) because of their small size, magnetite particles possess exceptional size-related magnetic properties known as superparamagnetism; they do not show a permanent magnetic moment, but can be readily magnetized upon exposure to an external magnetic field; and (iv) it is simple to prepare in the gram scale. The best known potential applications of such materials are both in the field of biomedicines,[2,7] but also in the field of chemistry, in relation to the preparation of magnetically separable catalyst[8] as well as scavenging of undesirable chemicals.[9] Especially the anchoring of expensive homogenous catalyst onto magnetic nanoparticles has show to be a feasible approach to develop new heterogeneous recyclable catalysts.[7c,10]

Thiol-modified materials are remarkable intermediate for chromatography,[11] leaching of heavy metals,[12] and heterogeneous catalysis.[13] Interestingly, functionalized thiol materials can be attached to chiral catalysts by click chemistry.[14] The thiol-ene click reaction is an excellent synthetic tool for the creation of sulphur-carbon bonds, due to high yields of products, the chemoselectivity and the very simple reaction. In our group the thiol-ene reaction was applied to attach proline-based organic catalysts for direct asymmetric aldol reactions. Such catalysts are applied in rather high amounts (20 mol%), meaning catalyst separation is crucial.[13] Catalyst immobilization has been done on polystyrene particles, which interestingly have shown a higher activity than the heterogeneous material. However to improve separability of the catalyst a magnetic support material is highly desirable.

The functionalization of a magnetic nanoparticles by means of organic molecules allows the powerful combination of the solid-state properties of the carrier to the chemical properties of the functional groups that are attached to it.

Efficient use of such materials requires the understanding of the chemical behavior and availability of organic moieties, which are covalently bound to the solid phase. For fine chemistry or biomedical applications it is an important issue to know "the title" of the material, in a way to say which portion of the organic functionalization actually takes part in an organic reaction. If only a portion of the attached functional group (*e.g.* catalyst or anticancer agent) attached to the particle is able to react it makes a huge difference.

Recently it was shown that there is a discrepancy between the theoretical loading of functional groups grafted on silica coated iron oxide nanoparticles (determined by the total amount of nitrogen by elemental analysis) and the loading of functional groups that is actually available for reactivity.[15] Standard techniques to study functional groups attached to nanoparticles include infrared or Raman spectroscopy, elemental analysis or thermogravimetrical analysis.[16] These solid-state techniques may identify the presence of organic functionalities, and at most an upper bound for the amount of free functional groups on the nanoparticles can be determined. However they generally do not provide any information on the actual behavior in suspensions where they will be used. Some of the functional groups may be unable to react freely due to steric hindrance, deactivation, or limited accessibility. Especially thiol groups are often deactivated, as they are easily oxidized resulting in the formation of disulfide bonds. Typical functional group loadings are in the order of mmol functional groups per gram of material, and the extent of the influence of this bulk upon chemical reactivity cannot be sufficiently evaluated without a technique able to monitor the transformation of such functional groups. Furthermore, techniques like NMR spectroscopy cannot be applied due to the peak broadening caused by the magnetic core.

UV-Vis spectroscopy has been shown to be a powerful technique to measure the concentration of thiol groups using a thiol-disulfide exchange reaction:[11a,17]
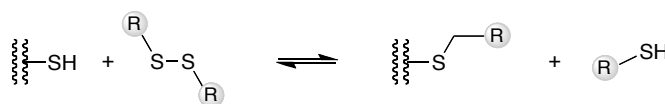
Figure 1. Schematic representation of thiol-disulfide exchange reaction

The thiol attached to the nanoparticle surface reacts with a symmetric disulfide R'SSR' to form a mixed disulfide RSSR' and a thiol product R'SH (Figure 1). Among many disulfides,[17] one disulfide often used is 2,2'-dipyridyl disulfide (DPDS), which was first applied by Grassetti and Murray.[17b] They showed the

reaction between the immobilized thiol and DPDS. The formed 2-pyridyl thiol is tautomerically in equilibrium with its thione form, which is more stable than its thiol form. This shifts the reaction equilibrium to the product side, leading to quantitative transformation.[19] The strong bathochromic shift allows selective detection of the product using UV-Vis spectroscopy, [17b] so the concentration of this product can then be determined spectroscopically using UV-Vis spectroscopy. According to the stoichiometry of the reaction, the number of formed thiol product is equal to the number of thiol groups immobilized originally on the nanoparticle surface. Thus the analysis of the product gives a direct measure for the total active surface coverage. However this analysis is accurate only if the equilibrium is shifted completely towards the mixed disulfide side, *i.e.* if the reaction is quantitative.

Nogueira *et al.* [11a] used DPDS to determine the active thiol content on modified mesoporous silica. They observed a good agreement between the elemental analysis and the spectroscopically determined thiol availability. Radu *et al.*[17e] have functionalized mesoporous silica, and even though they find a higher total loading for thiol groups compared to carboxylic acid or sulfonic acid, a lower chemical availability for the thiols was observed. Very recently Li *et al.*[20] functionalized bare flame-made iron oxide nanoparticles with thiol groups, obtaining an active thiol loading ranging from 0.04-1.15 mmol/g as determined by titration with Ellman's reagent. However no comparison with the total sulfur loading was made.

This chapter describes the synthesis and the thiol functionalization silica-coated iron oxide nanoparticles with different silica contents. The focus is on the difference in actual thiol loading (as determined spectroscopically) as a function of silica content. It describes how applied UV-Vis spectroscopy to study the chemical availability of magnetic thiol-functionalized nanoparticles.

In addition, a magnetic nanoparticle supported proline has been prepared. This material was used as organocatalyst in direct asymmetric aldol reaction between *p*-nitrobenzaldehyde and cyclohexanone.

2.4   *Results and discussion*

2.2.1   *Synthesis of FeO$_x$ Magnetic Nanoparticles and Silica Coating*

Several preparation procedure for silica coated iron oxide nanoparticles have been published in recent years, each one of them yielding a material with different physical and chemical features.[21] One of the most diffused of such procedures is co-precipitation and coating using tetraethyl orthosilicate (TEOS) as silica precursors. This synthesis can yield well defined core–shell structures, with a core composed of the iron oxide particles and a shell of silica, for a diameter of 15–20 nm. Iron oxide nanoparticles were prepared from ferrous and ferric ion solution under alkaline condition. In a subsequent process, the as-precipitated nanoparticles were coated with a layer of silica by hydrolysis of tetraethyl orthosilicate in ethanol/water medium (Figure 1). This procedure yielded the silica coated magnetic nanoparticles (designated as materials M$_1$).
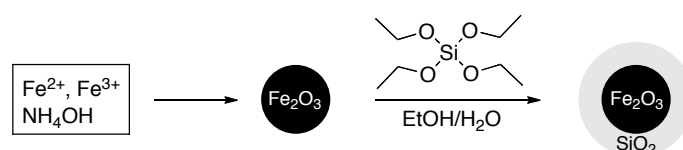

Figure 2. The reaction mechanism of magnetite particle formation from aqueous Fe^{2+}/Fe^{3+} salts solution in the presence of a base, followed by silica coating using tetraethyl orthosilicate (TEOS) in ethanol/water medium.

Silica coated iron oxide nanoparticles were also prepared by flame spray pyrolysis (FSP). This is an interesting dry synthetic approach to silica-coated iron nanoparticles, and an alternative to classical wet synthetic approaches.[6,15b] In this case the iron oxide nanoparticles were produced by flame spray pyrolysis of iron acetylacetonate in xylene/acetonitrile solutions and the resulting aerosol was in situ coated with silicon dioxide by oxidation of hexamethyldisiloxane vapour (HMDSO).

The resulting material shows similarities to that prepared with TEOS, having a well defined core–shell structure and similar dimensions. Among the advantages offered by this synthetic route are tight control of particles properties within a single step synthesis and the scalability of the process. [6,15b] The silica content in the product powder are 0, 8, 14 and 23 wt % SiO$_2$. These materials are referred throughout the text as Material M$_2$, M$_3$, M$_4$ and M$_5$.

2.2.2 *Grafting of Thiol-Modified Magnetic Nanoparticles and Study of the Loading*

The silica coated iron oxide nanoparticles, prepared by co-precipitation and by flame spray pyrolysis, were chemically modified with thiol groups.
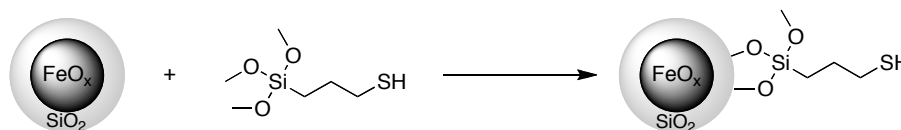
Figure 3. Grafting of 3-(Mercaptopropyl)trimethoxysilane on the silica coated iron oxide nanoparticles

3-(mercaptopropyltrimethoxysilane) was added dropwise to a suspension of SiO_2/FeO_x in dry toluene under Argon atmosphere. The resulting mixture was refluxed. After different hours, the suspension was cooled at room temperature and then magnetically washed with methanol, acetone, hexane, and diethyl ether, indeed the reaction vessel was placed over a permanent magnet until the reaction suspension became transparent and the liquid was then decanted. A light-brown material was obtained. Figure 3 shows the grafting of the 3-(mercaptopropyl)trimethoxysilane on the silica coated iron oxide nanoparticles .

Different conditions were carried out under optimization of the silylation reaction of a mercaptosilane groups. The results were summarized in Table 1. The evaluation of the content of the sulfur was determined by microelemental analysis.

Table 1. Study of loading of Silica Coated FeO_x Nanoparticles with 3-(Mercaptopropyl)trimethoxysilane.

Entry	Time	Materials [a]					
		M_1 [b]	M_1 [c]	M_2 [c]	M_3 [c]	M_4 [c]	M_5 [c]
1	22	0.2703	0.3406	0.8156	0.5844	0.7531	0.7250
2	46	0.2844	-	1.1188	1.0594	0.8063	1.0375
3	70	0.4859	-	1.2000	1.2969	0.9281	1.0469
4	94	0.4532	-	1.1719	1.6594	1.0344	1.1375
5	118	0.4250	-	1.1469	1.4031	1.1313	1.1188
6	142	0.4312	-	1.6063	1.3625	1.1906	1.2531

[a] Materials: M_1 is the material prepared by co-precipitation, M_2-M_5 are the materials obtained by flame made pyrolysis with a silica content that varied respectively from 0, 8, 14 and 23 wt% SiO_2. [b] Solvent used xylene. [c] Solvent used toluene and pyridine as catalyst

As show in Table 1, the best results are achieved with material M_2, using toluene as solvent and pyridine as catalyst (Table 1, entry 6).

In addition, Figure 4 shows the time-dependent total amount of sulfur atoms per gram material as determined by microelemental analysis.
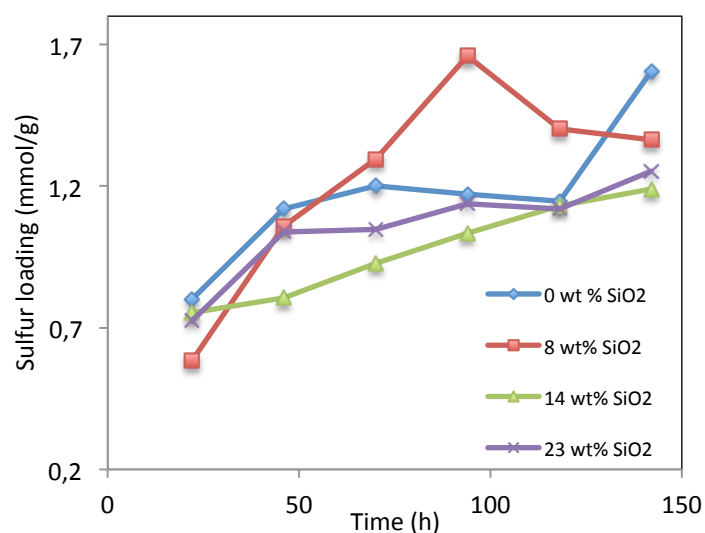
Figure 4. Sulfur loading of thiol-functionalized flame-made SiO_2-coated Fe_2O_3 nanoparticles for different amounts of silica coating.

It appears that there is no significant effect of the variation in silica content on the total sulfur loading. For all materials, the loading after 72 h does not significantly increase. Under the assumption that all sulfur atoms contribute to thiol-functional groups; the total amount of functional groups is that as determined by microelemental analysis. This approximation is often found in literature concerning the preparation of surface functionalized nanoparticles. This value, however, does not necessarily correspond to the number of functional groups that are free to react. In fact, part of the functional groups might be deactivated by the formation of disulfide bonds or might have been oxidized. The determined value by microelemental analysis therefore only shows a theoretical upper bound of the possible loading in terms of chemically available thiol groups.

2.2.3 Characterizations of Materials

Product powders were analysed by transmission electron microscopy (Figure 5), X-ray diffraction (XRD), and nitrogen adsorption at 77K. The results are displayed in Table 2.

Table 2. Specific surface area, particle diameter and theoretical silica coating thickness for iron oxide nanoparticles with different silica contents.

Material	Silica content (wt%)[a]	SSA (m²/g)	d_{BET} (nm)	d_{XRD} (nm)
M_2	0	29	42	22
M_3	8	41	31	22
M_4	14	54	25	15
M_5	23	63	23	15

[a] The silica content in the product powder is defined as $m\mathrm{SiO_2}/(m\mathrm{Fe_2O_3} + m\mathrm{SiO_2})$

Figure 5 shows transmission electron micrograph (TEM) images at low (a) and high (b) magnification of pure, mostly hexagonal Fe_2O_3 particles. Silica coating of these magnetic particles was achieved by injecting HMDSO at various concentrations at 20 cm above the FSP burner. Figure 5 also shows images of these 23 wt % SiO_2-coated Fe_2O_3 at low (c) and high (d) TEM magnification. At higher magnification (Figure 5d) homogeneous and thin amorphous SiO_2 layers around Fe_2O_3 particles could be distinguished.
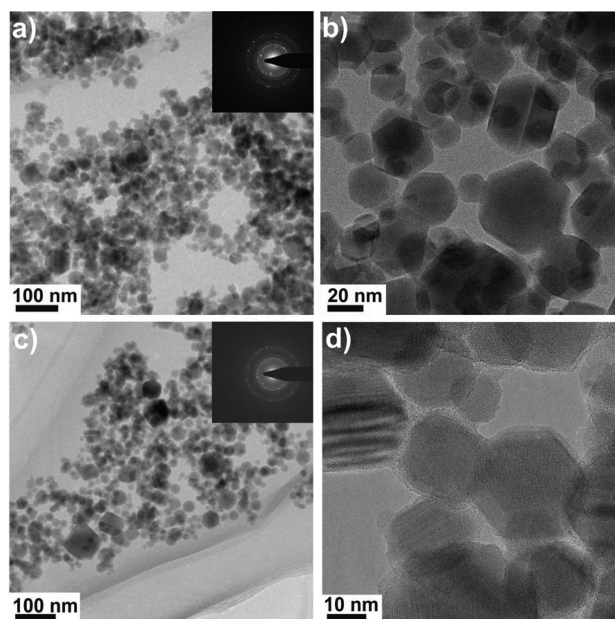
Figure 5. TEM images at low and high magnification of pure Fe_2O_3 (a,b) and 23 wt % SiO_2-coated Fe_2O_3 (c,d).

Figure 7. shows the DRIFT spectra of the functionalized compared to the non-functionalized materials.
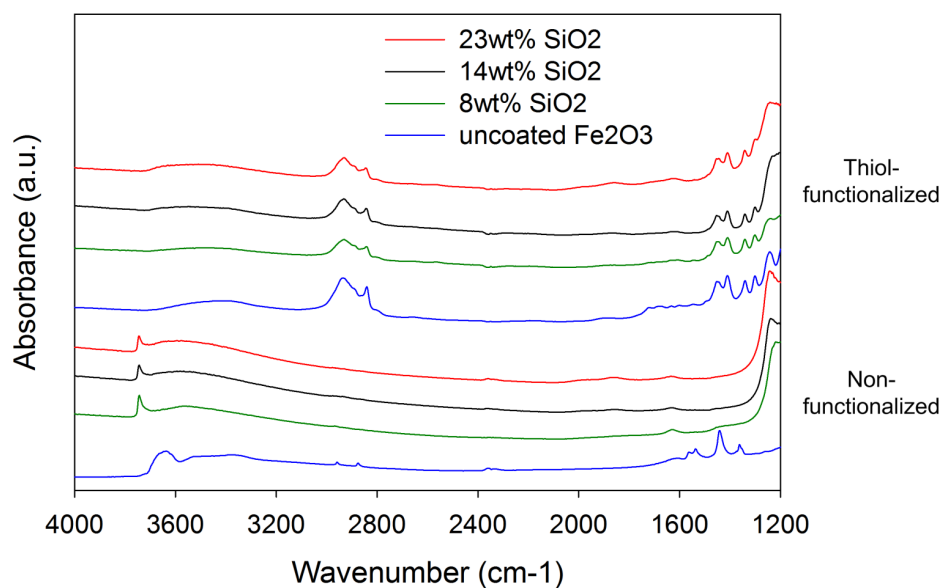
Figure 7. DRIFT spectra of the non-functionalized (bottom) and thiol-functionalized (top) silica-coated nanoparticles.

The sharp absorption edge of silica around 1250 cm^{-1} is clearly visible for the silica-coated materials. The vibrational bonds of respectively asymmetric and symmetric CH_2 stretching are visible at 2932 and 2842 cm^{-1},[22] indicating a successful surface functionalization. This is also confirmed by CH_2 bending vibrations around 1409 and 1454 cm^{-1}.[23] Thiol and disulfide vibrations are typically too weak to be detected by IR spectroscopy.

2.2.4 *UV-Vis spectroscopy*

The functionalization of magnetic nanoparticles with organic molecules allows the powerful combination of the solid solid-state properties of the carrier to the chemical properties of the functional groups that are attached to it. Efficient use of these materials requires the understanding of the chemical behavior and availability of organic moieties that are covalently bound to the solid phase. The actual chemical availability of thiol functional group grafted onto flame-made silica coated iron oxide nanoparticles was determined spectroscopically by UV-vis measurements with a home-built reactor cell (Figure 10).
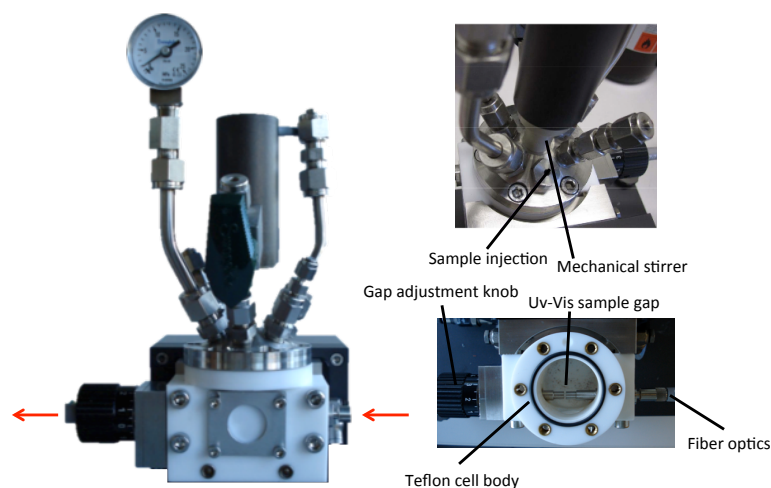
Figure 10. Schematic view of the in situ reactor cell. The red arrows represent the optical path of the IR radiation.

The thiol groups were reacted with an excess of 2,2-dipyridyl disulfide (DPDS) to form 2-pyridyl thiol, which is converted into its tautomeric thione form (Scheme 1).
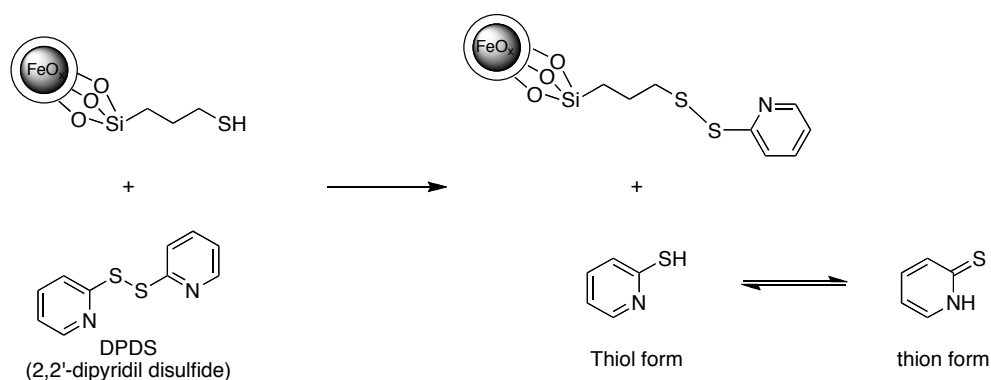
Scheme 1. Thiol-disulfide exchange reaction between DPDS and SH-functionalized nanoparticles.

Since 2-pyridyl thione is clearly detectable with UV-Vis spectroscopy, the amount of thiol groups on the nanoparticle surface was quantified by measuring the concentration of 2-pyridyl thione that is formed. For this purpose, first a calibration curve was established using different concentrations of 2-pyridyl thione in ethanol. The peak area of the product signal at 363 nm corresponds to a given concentration of 2-pyridyl thione. In a second step, a known amount of thiol-functionalized nanoparticles was reacted with excess DPDS for at least 17 h. The nanoparticulate material was separated magnetically and the clear solution was analyzed by UV-Vis spectroscopy. The amount of thiol groups that has reacted corresponds to the number of 2-pyridyl thione groups that are formed, which can be determined quantitatively using the calibration curve that was established previously. The formation of the 2-pyridyl thione is quantitatively determined by integrating the signal at 363 nm, which

is a fingerprint signal for the product. Even though there is a secondary peak at lower wavelengths, there is a strong overlap in that region due to the absorbance by DPDS.[17b]
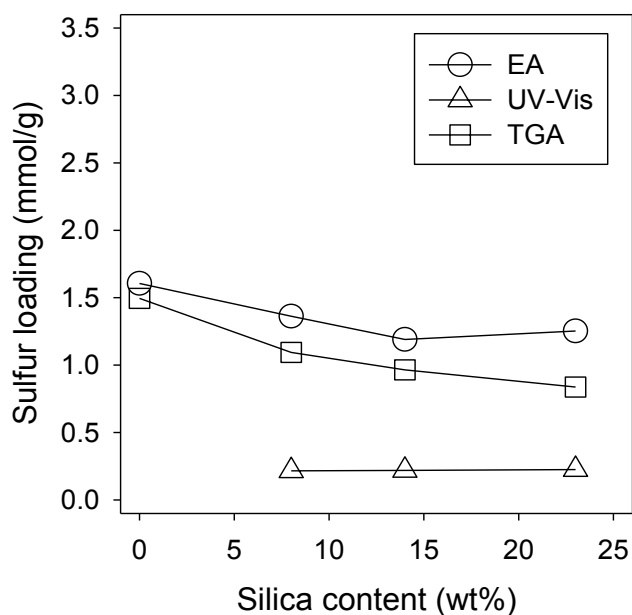

Figure 11. Thiol loading as function of silica content

Figure 11 shows the sulfur loading as determined by UV-Vis spectroscopy compared to the results of elemental analysis (EA) and thermogravimetrical analysis (TGA). There is no significant difference between EA and TGA results, however for high silica contents the values deviate. This could be due to the assumptions made in both methods. Both EA and TGA typically overestimate the chemical availability. What is striking here is that there is an immense difference between the spectroscopically derived loading and the total loading. It therefore appears that a large amount of the thiol groups is not reacting or has been deactivated.

2.2.5 *Magnetic Nanoparticles supported Organocatalyst*

The here prepared thiol functionalized nanoparticles are to be used as a source of immobilized organic catalysts. For the immobilization of the organic catalysts a "click reaction" is done,[24] which couples the catalyst to the sulfur groups immobilized on the nanoparticles. The thiol nanoparticles were derivatized with L-proline. The thus prepared material has been used as organocatalyst in direct asymmetric aldol reactions between p-nitrobenzaldehyde with ciclohexanone. In addition the value of nitrogen of elemental analysis in the magnetic nanoparticles supported L-Proline **6** is in agreement with
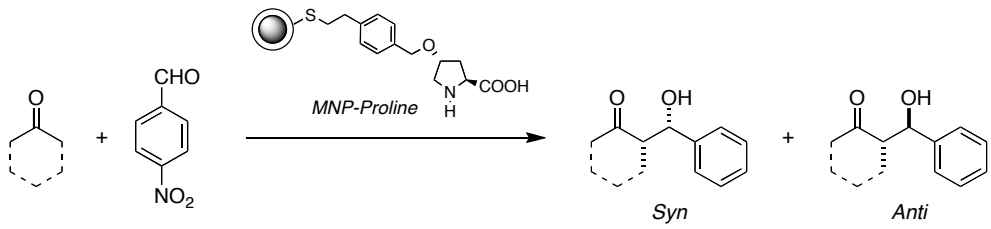
the value found with UV-Vis measurement. This shows that the UV-Vis spectroscopy with a home-built batch reactor cell is a powerful technique to measure the real concentration of thiol groups.
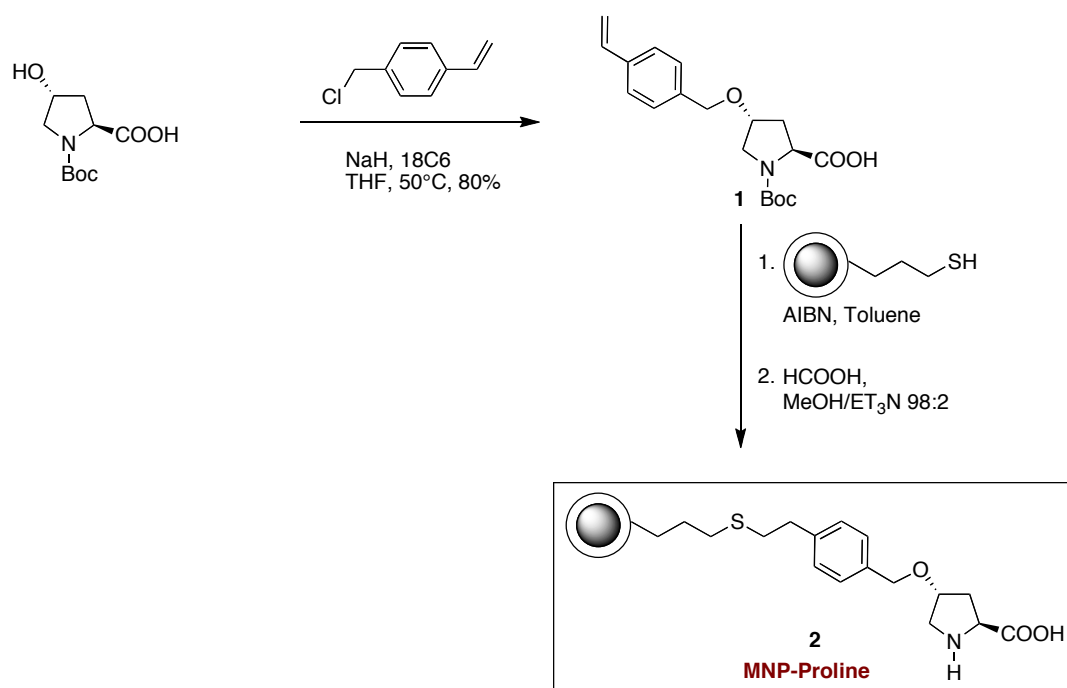
Scheme 1. Synthesis of magnetic nanopaticles supported L-Proline **6**.

Commercially available trans-N-Boc-4-hydroxy-L–proline was used for proline immobilization since the hydroxyl group can be easily functionalized. The anchorage of L-proline was accomplished in three steps accordingly to Scheme 1: (a) synthesis of styrene derivative **1** of hydroxy-L-proline; (b) radical reaction between the as prepared proline derivative and the mercaptopropyl-silica-nanoparticles followed by the deprotection of proline moiety. The removal of *tert*-butoxycarbonyl group was carried out with HCOOH followed by treatment with Et_3N/MeOH 2/98. This procedure gave the nanoparticle-supported L-proline **2** in a high yield and in a very simple way (elemental analysis of nitrogen: 0.3 mmol/g).

In a first approach catalyst was tested under the conditions used by Gruttadauria *et al.* (aldehyde 0.5 mmol; cyclohexanone 5 mmol; catalyst 0.025 mmol; distilled water 0.175 mL), using p-nitrobenzaldehyde as acceptor in the aldol reaction.

Table 3. Direct asymmetric aldol reactions between ketones and *p*-nitrobenzaldehyde with Magnetic Nanoparticle supported Proline 6

Entry	ketone	Loading	Time	Solvent	Conv.	Anti/syn[a]	ee[b]
		(% mol)	(h)		(%)		%
1	cyclohexanone	5	24	water	72	72:28	24
2	cyclohexanone	5	24	water/CHCl$_3$	71	73:27	-
3	cyclohexanone	10	24	water	96	65:35	-
4	acetone	10	24	-	96	-	-

[a]Determined by ^{1}H NMR of the crude product; [b] Determined by HPLC using a chiral column.

Only 5 mol% of L-proline was necessary to achieve good yields of the products. Reactions proceeded with good diastereoselectivity (72:28 *anti: syn* ratios), but low enantioselectivity was observed. Such low enantioselectivity can be explained considering the very low proline loading and because of the presence of free silanol groups on the surface of silica gel.[25] Zamboulis and coworker [25] explained the low enantioselectivity considering the competition of the acidic silanols with the COOH of proline moieties for the positioning of the aldehyde.

2.3   *Conclusions*

Thiol-functionalized flame-made silica-coated iron oxide nanoparticles were prepared and the effect of silica content on the functional group loading was studied. It was found that for lower silica content a higher number of thiol atoms were accommodated on the particle surface. The actual chemical availability of the thiol groups was investigated by reacting the nanoparticles with DPDS to form 2-pyridyl thione, which is sensitive for UV-Vis measurements. The material with a high loading from the elemental analysis (the pure iron oxide) has shown to obtain a low number of free thiol groups on the surface. A possible reason for this could be the formation of disulfide bonds coupled to the reduction of the maghemite core to magnetite. Finally, the synthetic utility of this nanoparticles was demonstrated by derivatization of thiol nanoparticles with L-proline. This material has been used as organocatalyst in direct asymmetric aldol reactions between p-nitrobenzaldehyde with ciclohexanone.

Given the increasing interest in magnetic nanoparticles supported catalysis and in particular in organocatalysis, new investigations of magnetic nanoparticle-supported proline ligands are underway. The successful synthesis of supported L-Proline gives prospect of large applications in the new field of magnetic nanoparticles and organocatalyst. In particular thiolate magnetic nanoparticles can also be useful in biomedicine, biotechnology and drug delivery by acting as an excellent anchors to further immobilized biomolecules and drug candidates by means of thiol-ene coupling reaction.

2.4 *Experimental Section*

Characterization techniques

Diffuse reflectance Fourier transform infrared (DRIFT) spectroscopy was done on a Bruker Vector 22 spectrometer with a Praying Mantis system (Harrick) using ZnSe windows. The samples were purged with 35 mL/min He for 30 min at 200°C, and spectra were measured at 40°C by collecting 64 scans with a resolution of 4 cm^{-1} in the range of 4000-400 cm^{-1}.

An ASAP 2010 instrument was used to measure the nitrogen adsorption-desorption isotherms at 77 K. The BET method was applied for the surface area determination of the materials. Prior to the measurements the samples were outgassed for 3 hours under vacuum at 100 °C. Pore size distributions were derived from the desorption branch of the hysteresis using the Barrer-Joyner-Halenda method.[26]

Thermogravimetric analysis experiments were performed in combination with mass spectrometry on a Netzsch STA 449C thermoanalyzer. Helium was used as a carrier gas with a flow of 50 ml/min and a heating ramp of 10 K/min. Temperature-programmed oxidation (TPO) with 20% O_2 in helium was followed using a Pfeiffer Vacuum (GSD 301O1) quadrupole mass spectrometer for simultaneous monitoring of mass changes and the evolved gases. The mass spectrometer was connected to the thermoanalyzer by a heated (150°C) stainless steel capillary.[27]

For transmission electron microscopy, the probe was dispersed in ethanol and deposited onto a perforated carbon foil supported on a copper grid (Okenshoji Co. Ltd.). The measurements were carried out on a Tecnai F30 FEI microscope with a field emission cathode, operated at 300 kV.

Preparation of iron oxide nanoparticle by flame spray pyrolysis

Silica-coated iron oxide nanoparticles with different silica contents were prepared by flame spray pyrolysis (FSP) and characterized as described by Teleki *et al*.[6] The silica content was varied between 0 and 23 wt% SiO_2. Thus the particles were produced in an enclosed FSP reactor described in detail elsewhere.[22] Precursor solutions, in all cases 0.34 M in total Fe metal concentration, were fed at 5 mL/min and dispersed by 5 L/min O_2 (Pan Gas, purity >99%). The solution spray was ignited by a methane/oxygen (1.5/3.2, total 4.7 L/min) premixed ring-shaped flame and the pressure drop at the nozzle tip was maintained at 1.5 bar. The FSP reactor was enclosed by a 20 cm long quartz glass tube and the spray flame was sheathed by 40 L/min O_2 flowing through the outermost sinter metal plate at the FSP burner.[6] At the top of that tube, a stainless steel metal torus pipe ring with 16 radial equispaced openings was positioned and the reactor was terminated by another 30 cm long quartz tube.[6]

Pure Fe_2O_3 was produced from 0.34 M in total Fe concentration precursor solutions of iron(III) acetylacetonate (Fe(acac)$_3$, Fluka, purity >97%) in xylene (Riedel-de Haën, puriss) and acetonitrile (Riedel-de Haën, puriss) at 3:1 volume ratio. These particles were in situ coated with SiO_2 (SiO_2-coated Fe_2O_3) by introducing N_2 carrying its precursor, hexamethyldisiloxane (HMDSO, Aldrich, purity >98%), vapor from a bubbler at 10 °C along with additional 15 L/min mixing N_2 gas through the above metal torus pipe ring. The silica content in the product powder (defined as $mSiO_2/(mFe_2O_3 + mSiO_2)$ varied from 6.5 to 46 wt % by controlling the N_2 flow rate through the HMDSO bubbler (0.08-0.97 L/min).

Preparation of FeO_x nanoparticles by coprecipitation

Nanoparticles of iron oxide were synthesized. Their composition is better described as $FeO·Fe_2O_3$ therefore with a 1-2 ratio of Fe(II):Fe(III). The magnetite nanoparticles were prepared by co-precipitation according to the synthesis reported by Liu *et al*.[28] 35.01 g of $FeCl_3·6H_2O$ and 12.9 g $FeCl_2·4H_2O$ were dissolved in 600 mL of distilled water. The solution was stirred under constant nitrogen gas flow and heated up at 85 °C. Subsequently 45 ml of 25% $NH_3·H_2O$ were added to the solution which immediately became dark brown indicating the formation of the magnetite particles. The solution was stirred for further 30 min at 358 K under inert atmosphere. After cooling down to room temperature the magnetic nanoparticles were separated from the water solution by centrifugation at 20000 rpm, room temperature, five minutes per batch. A black material is obtained (15.60 gr), which is then dried under vacuum overnight at 343 K.

Preparation of FeO_x and the Silica Coating

Following a described synthesis[15b] a portion of superparamagnetic FeOx nanoparticles were ultrasonically dispersed in a 240 mL anhydrous ethanol and 60 mL deionized water solution. Then the

pH was adjusted to 9 using ammonium hydroxide and 33 ml of TEOS (Tetraethylorthosilicate) was added under vigorous mechanical stirring (300 rpm). The mixed solution was agitated for 10 h and then for 12 h at 323 K. The coated magnetic nanoparticles were then separated by centrifugation and washed with ethanol and distilled water several times. The particles were dried at 330 K.

Functionalization by mercaptopropyltrimethoxysilane and acid dissolution

Surface functionalization of the nanoparticles was done according to the procedure described by Crudden *et al.*[29] Prior to functionalization, 1 g powder was heated overnight at 423 K in a vacuum line in order to remove physically adsorbed water. Next, the material is placed in the flask with 30 mL of toluene (Acros, 99.8%, extra dry) and the suspension is sonicated to break up the agglomerates. The suspension is kept stirring mechanically at 450 rpm and 110 °C under toluene reflux in argon atmosphere. Subsequently, 1 mL mercaptopropyltrimethoxysilane (MPTS, Fluka, ≥97%) and 1 mL pyridine (Acros, 99.5%, extra dry) are added dropwise. After each time interval, an aliquot of 2 mL of the suspension is taken and magnetically washed using methanol, acetone, hexane, and diethyl ether. Then the material is dried under vacuum for 2 hours at 323 K.

Synthesis of (2S,4R)-1-(tert-Butoxycarbonyl)-4-(4-vinylbenzyloxy)pyrrolidine-2-carboxylic Acid

A solution of *trans*-Boc-4-hydroxy-L-proline (2.0 g, 8.65 mmol) in anhydrous THF (30 mL) was added dropwise, under argon, at 0°C to a suspension of NaH (60% mineral oil, 751 mg, 18.77 mmol) in anhydrous THF (20 mL). The mixture was stirred at r.t. for 1 h, and 18-crown-6 (228 mg, 0.86 mmol) and 4-chloromethylstyrene (90 %, 3.66 g, 21.6 mmol) were then added. The mixture was stirred for 1 h at r.t., and then at 50 °C overnight. After cooling to r.t., water (100 mL) was added. The aqueous phase was extracted with cyclohexane (2x250mL) in order to remove the unreacted 4-chloromethylstyrene. The aqueous phase was acidified at pH 2–3 by adding a solution of $KHSO_4$ (2 N), and was then extracted with ethyl acetate (3x100mL). The organic phase was dried ($MgSO_4$) and concentrated under reduced pressure to give compound **4** as a pale yellow, viscous oil (2.151g, 84%). $[\alpha]_D^{28}$ = −61.0 (c = 0.60, $CHCl_3$). ^{1}H NMR (300 MHz, $CDCl_3$): δ = 1.45 (s, 9 H), 2.05–2.50 (m, 2 H, 3-H), 3.60–3.78 (m, 2 H, 5-H), 4.15–4.25 (m, 1 H, 4-H), 4.37–4.60 (m, 3 H, 2-H and CH_2O), 5.25 (d, J = 10.8 Hz, 1 H, HHC=CH), 5.75 (d, J = 17.6 Hz, 1 H, HHC=CH), 6.72 (dd, J = 10.8 and 17.6 Hz, 1 H, HHC=CH), 7.28 and 7.40 (d, J = 8.1 Hz, each 2 H, ArH), 10.22 (br. s, 1 H, OH) ppm. ^{13}C NMR (75 MHz, $CDCl_3$): (two rotamers): δ = 28.2, 28.3, 35.1, 36.6, 51.4, 52.0, 58.1, 70.7, 70.9, 76.0, 76.6, 80.6, 81.0, 113.9, 114.5, 126.3, 126.5, 127.8, 128.8, 136.2, 136.4, 137.2, 137.3, 154.1, 155.4, 176.7, 178.0 ppm. IR (liquid film): ν_{max} = 3450, 2626, 1700, 1674, 1418 cm^{-1}. [Found C 65.77, H 7.33, N 4.10.$C_{19}H_{25}NO_5$ requires C 65.69, H 7.25, N 4.03].

*Synthesis of magnetic nanoparticles supported proline*

Mercaptopropyl magnetic nanoparticles **3** (0.400 g, 0.50 mmol) were added to a degassed solution of styrene derivative **4** (0.523 g, 1.50 mmol) and AIBN (0.0049 g, 0.3 mmol) in toluene (13 mL). The mixture was shaken under mechanical agitation at 450 rpm overnight under toluene reflux in atmosphere of argon. After cooling to room temperature, the reaction was then quenched by addition of toluene. The reaction vessel was then placed over a permanent magnet until the reaction suspension became transparent and the liquid was then decanted. The suspension was then washed using methanol and dichloromethane and finally dried under vacuum for 2 hours at 40°C. A light brown powder was obtained. A portion of such nanoparticles (1.76 g) was suspended in formic acid and kept stirring at room temperature using a Büchi Rotavapor at 140 rpm for 17 hours. After this period, the nanoparticles were taken and magnetically washed using a saturated solution of $NaHCO_3$, water, methanol and diethyl ether. Then the material is dried under vacuum for 2 hours at 40 °C.

UV-Vis spectroscopy Measurements

Liquid phase thiol-disulfide exchange reaction kinetics were determined by reacting 100 µmol of 1-hexanethiol (Fluka, 97%) with 400 µmol 2,2'-dipyridyl disulfide (DPDS; ABCR, 98%) in 2.5 ml ethanol (Merck, abs). The reaction was kept stirring mechanically at room temperature using a Büchi Rotavapor R at 140 rpm. Each hour, an aliquot of 50 µl was taken, diluted with 1 ml ethanol and analyzed by gas chromatography using an Agilent J&W HP-FFAP column. An inlet temperature of 200 °C was used, with a temperature profile from 80 to 230°C. Ethanol was used as good solvent for 1-hexanethiol. It was found that after 3 h of reaction the reactant peak had completely disappeared, confirming[11a] that the reaction is complete and quantitative.

Because 2-pyridyl thione is clearly detectable with UV-Vis spectroscopy, the amount of thiol groups on the nanoparticles was quantified by measuring the concentration of 2-pyridyl thione that is formed. For this purpose the approach comprised the following steps: (i) first a calibration curve was established using different concentrations of 2-pyridyl thione in ethanol. The peak area of the product signal at 363 nm corresponds to a given concentration of 2- pyridyl thione. (ii) in a second step, a known amount of thiol-functionalized nanoparticles was reacted with excess DPDS for at least 17 h. A calibration curve correlating the product concentration to the UV-Vis peak area was prepared by adding different amounts of a 0.1 solution of 2-pyridyl thione (Sigma-Aldrich, 99%) in 25 mL ethanol directly in the cell. The product area at 363 nm is calculated and a total of 14 data points are taken, with concentrations up to 5 µmol/mL 2-pyridyl thione. The nanoparticulate material was separated magnetically and the clear solution was analyzed by UV-Vis spectroscopy. The amount of thiol groups that has reacted corresponds to the number of 2-pyridyl thione groups that are formed, which can be determined quantitatively using

the calibration curve that was established previously. The formation of the 2-pyridyl thione is quantitatively determined by integrating the signal at 363 nm, which is a fingerprint signal for the product. Even though there is a secondary peak at lower wavelengths, there is a strong overlap in that region due to the absorbance by DPDS. To determine the thiol loading of the materials, 1.5 mL ethanol was added to 200 mg of SH-functionalized silica-coated iron oxide. The suspension was sonicated for 15 min and degassed using argon. Next, 1 mL ethanol containing 0.8 mmol DPDS was added to the flask. The flask was rotated mechanically at 140 rpm while covered with aluminum foil. After at least 17 h, the suspension was transferred to a 25 mL flask, filled with ethanol and the powder was separated magnetically. The remaining solution was diluted once with ethanol and analyzed using UV-Vis spectroscopy (see Figure 10). For the analysis all 2-pyridyl thione concentrations were in the range of 0-5 µmol/ml.
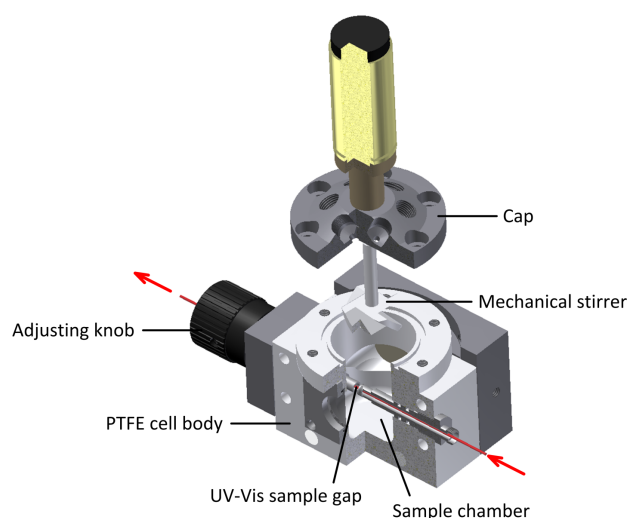
Figure 12. Schematic display of the *in-situ* UV-Vis reactor cell. The red arrows show the optical path of the UV-Vis beam.

UV-Vis measurements were performed with a home-built batch reactor cell. This cell allows measurements of UV-Vis spectra during a reaction. The cell is closed and sealed with a cap equipped with a mechanical axial flow impeller. Liquid samples could be injected through a septum in the cell cap. The UV-Vis sample gap is directly in the cell and is adjustable by a screw cap. Fiber optic wave guides (600 µm thick, length 1 m, Ocean Optics) are connected from the cell to the UV-Vis-NIR light source (DH-2000-BAL, micropack, deuterium and halogen lamps) and the detector. Spectra were recorded at room temperature using the Ocean Optics SpectraSuite software, with an integration time of 3 ms and averaging 100 scans.

2.5   *References*

1. (a) A.-H. Lu, W. Schmidt, N. Matoussevitch, H. B Pnnermann, B. Spliethoff, B. Tesche, E. Bill, W. Kiefer, F. SchVth, *Angew. Chem.* **2004**, *116*, 4403-4410; *Angew. Chem. Int. Ed.* **2004**, *43*, 4303-4306. (b) S. C. Tsang, V. Caps, I. Paraskevas, D. Chadwick, D. Thompsett, *Angew. Chem.* **2004**, *116*, 5763-5767; *Angew. Chem. Int. Ed.* **2004**, *43*, 5645-5649.

2. A. K. Gupta, M. Gupta, *Biomaterials* **2005**, *26*, 3995-4021.

3. (a) S. Mornet, S. Vasseur, F. Grasset, P. Verveka, G. Goglio, A. Demourgues, J. Portier, E. Pollert, E. Duguet, *Prog. Solid State Chem.* **2006**, *34*, 237-247. (b) Z. Li, L. Wei, M. Y. Gao, H. Lei, *Adv. Mater.* **2005**, *17*, 1001.

4. (a) A. Ulman, *Chem. Rev.* **1996**, *96*, 1533-1554; (b) G. Deng, M. A. Markowitz, P. R. Kust, B. P. Gaber, *Mater. Sci. Eng. C.* **2000**, *11*, 165-172.

5. R. Narain, M. Gonzales, A. S. Hoffman, P. S. Stayton, K. M. Krishnan, *Langmuir* **2007**, *23*, 6299-6304.

6. (a) A. Teleki, M. Suter, P. R. Kidambi, O. Ergeneman, F. Krumeich, B. J. Nelson, S. E. Pratsinis, *Chem. Mater.* **2009**, *21,* 2094-2100. (b) A. Teleki, M. C. Heine, F. Krumeich, M. K. Akhtar, S. E. Pratsinis, *Langmuir* **2008**, *24,* 12553-12558.

7. (a) A. Jordan, R. Scholz, P. Wust, H. Fahling, R. Felix, *J. Magn. Magn. Mater.* **1999**, *201,* 413-419. (b) R. Jurgons, C. Seliger, A. Hilpert, L. Trahms, S. Odenbach, C. Alexiou, *J. Phys.: Condens. Matter* **2006**, *18,* S2893-S2902.

8. (a) P. D. Stevens, J. D. Fan, H. M. R. Gardimalla, M. Yen, Y. Gao, *Org. Lett.* **2005**, *7,* 2085-2088. (b) P. D. Stevens, G. F. Li, J. D. Fan, M. Yen, Y. Gao, *Chem. Commun.* **2005**, 4435-4437. (c) A. G. Hu, G. T. Yee, W. B. Lin, *J. Am. Chem. Soc.* **2005**, 127(36), 12486-12487. (d) S. Ko, J. Jang, *Angew. Chem. Int. Ed.* **2006**, *45(45),* 7564-7567.

9. S. C. Halim, W. J. Stark, *Chimia* **2008**, *62(1-2),* 13-17.

10. (a) S. Shylesh, V. Schünemann, W. R. Thiel, *Angew. Chem. Int. Ed.* **2010**, *49*, 3428-3459. (b) Y. Zhu, L. P. Stubbs, F. Ho, R. Liu, C. P. Ship, J. A. Maguire, N. S. Hosmane, *ChemCatChem* **2010**, *2*, 365-374; (c) A.-H. Lu, E.L. Salabas, F. Schüth, *Angew. Chem. Int. Ed.* **2007**, *46*, 1222-1244.

11. (a) R. Nogueira, M. Lammerhofer, N. M. Maier, W. Lindner, *Anal. Chim. Acta* **2005**, *533,* 179-183. (b) R. Dabre, A. Schwammle, M. Lammerhofer, W. Lindner, *J. Chromatogr. A* **2009**, *1216,* 3473-3479.

12. (a) W. Yantasee, C. L. Warner, T. Sangvanich, R. S. Addleman, T. G. Carter, R. J. Wiacek, G. E. Fryxell, C. Timchalk, M. G. Warner, *Environ. Sci. Technol.* **2007**, *41,* 5114-5119. (b) C. Z. Huang, B. Hu, *Spectroc. Acta Pt. B-Atom. Spectr.* **2008**, *63,* 437 (c) P. K. Jal, S. Patel, B. Mishra *Talanta* **2004**, *62,* 1005-1028. (d) G. Z. Fang, J. Tan, X. P. Yan, *Anal. Chem.* **2005**, *77,* 1734-1739. (e) F. Sahin, M. Volkan, A. G. Howard, O. Y. Ataman, *Talanta* **2003**, *60,* 1003-1009.

13. M. Gruttadauria, A. M. P. Salvo, F. Giacalone, P. Agrigento, R. Noto, *Eur. J. Org. Chem.* **2009**, 5437-5444.

14. (a) K. Hayashi, K. Ono, H. Suzuki, M. Sawada, M. Moriya, W. Sakamoto, T. Yogo, *Chem. Mater.* **2010**, *22,* 3768-3772. (b) C. E. Hoyle, C. N. Bowman, *Angew. Chem. Int. Ed.* **2010**, *49,* 1540-1573. (c) A. Dondoni, *Angew. Chem. Int. Ed.* **2008**, *47,* 8995-8997.

15. (a) B. Panella, A. Vargas, D. Ferri, A. Baiker, *Chem. Mater.* **2009**, *21,* 4316-4322. (b) A. Vargas, I. Shnitko, A. Teleki, S. Weyeneth, S. E. Pratsinis, A. Baiker, *Applied Surface Science* **2011**, 257, 2861-2869.

16. (a) S. Mohapatra, N. Pramanik, S. Mukherjee, S. K. Ghosh, P. Pramanik, *J. Mater. Sci.* **2007**, *42*, 7566-7574. (b) A. Teleki, N. Bjelobrk, S. E. Pratsinis, *Langmuir* **2010**, *26,* 5815-5822. (c) H. Schulz, S. E. Pratsinis, H. Rugger, J. Zimmermann, S. U. Klapdohr Salz, *Colloid Surf. A,* **2008**, *315,* 79-88.

17. (a) G. L. Ellman, *Arch. Biochem. Biophys.* **1959**, *82,* 70-77. (b) D. R. Grassetti, , J. F. Murray, *Arch. Biochem. Biophys.* **1967**, *119,* 41-49. (c) G. Gabor, A. Vincze, *Anal. Chim. Acta* **1977**, *92,* 429-442. (d) K. Kuwata, M. Uebori, K. Yamada, Y. Yamazaki, *Anal. Chem.* **1982**, *54,* 1082-1087. (e) D. R. Radu, C. Y. Lai, J. G. Huang, X. Shu, V. S. Y. Lin, *Chem. Commun.* **2005**, 1264-1266.

18. M. R. F. Ashworth, *The determination of sulphur-containing groups*; Academic Press: London, 1976.

19. Z. Glatz, H. Maslanova, *J. Chromatogr. A* **2000**, *895,* 179-183.

20. (a) D. Li, W. Y. Teoh, D. Djunaedi, J. J. Gooding, C. Selomulya, R. Amal, *Adv. Eng. Mater.* **2010**, *12,* B210-B214. (b) D. Li, W. Y. Teoh, J. J. Gooding, C. Selomulya, R. Amal, *Adv. Funct. Mater.* **2010**, *20,* 1767-1777.

21. A.-H. Lu, E. L. Salabas, F. Schuth, *Angew. Chem. Int. Ed.* 46, **2007**, 1222-1244.

22. R. De Palma, S. Peeters, M. J. Van Bael, H. Van den Rul, K. Bonroy, W. Laureyn, J. Mullens, G. Borghs, G. Maes, *Chem. Mater.* **2007**, *19,* 1821-1831

23. G. Socrates, *Infrared Characteristic Group Frequencies; Tables and Charts*; John Wiley&Sons Ltd: Chichester, 1994.

24. H. C. Kolb, M. G. Finn, K. B. Sharpless, *Angew. Chem. Int. Ed.* **2001**, *40,* 2004-2021.

25. A. Zamboulis, N. J. Rahier, M. Gehringer, X. Cattoën, G. Niel, C. Bied, J. J. E. Moreau, M. Wong Chi Man, *Tetrahedron: Asymmetry* **2009**, *20*, 2880-2885.

26. E. P. Barrer, L. G. Joyner, P.P. Halenda, *J. Am. Chem. Soc.* **1951**, *73*, 373–380.

27. M. Maciejewski, C. A. Muller, R. Tschan, W.D. Emmerich, A. Baiker, *Novel Pulse Thermal Analysis Method and Its Potential for Investigating Gas–Solid Reactions*, Elsevier Science BV., Leeds, England, 1996, pp. 167-182.

28. X. Liu, Z. Ma, J. Xing, H. Liu, *J. Magn. Magn. Mater.* **2004**, 270, 1-6.

29. C. M. Crudden, M. Sateesh, R. Lewis, *J. Am. Ceram. Soc.* **2005**, *127,* 10045-10050.

Chapter 3

High-Throughput Study of CO₂ Cycloaddition Reaction Catalyzed by Multi-layered Supported Ionic Liquids
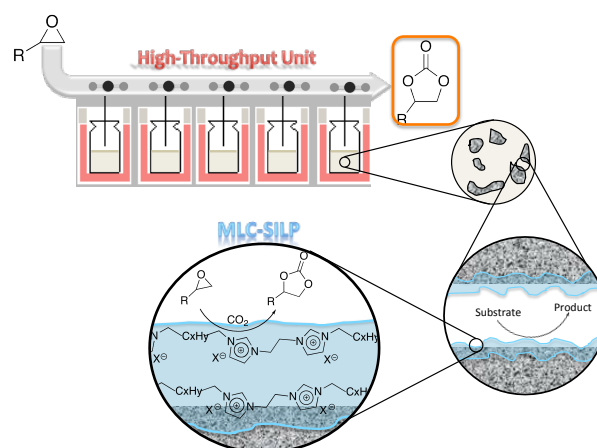
Multi-layered covalently supported ionic liquid phase (mlc-SILP) materials were synthesized using a new approach based on grafting of different bis-vinylimidazolium salts on amorphous silica. These materials, which contain a highly cross-linked polymeric network, were characterized and tested as catalysts in the reaction of supercritical carbon dioxide with various epoxides to produce cyclic carbonates. The material prepared by supporting an iodide bis-imidazolium salt was identified as the most active catalyst for the synthesis of cyclic carbonates and displayed improved productivity compared to known supported ionic liquid catalysts. The catalyst can be successfully reused in consecutive runs. The rapid and parallel screening of the catalysts was efficiently carried out by means of high-throughput (HT) experimentation under supercritical carbon dioxide conditions.

3.1   *Introduction*

Carbon dioxide is the most abundant waste produced by human activities and one of the greenhouse gases. On the other hand, CO$_2$ is recognized to be a naturally abundant, cheap, recyclable and non-toxic carbon source that can sometimes replace toxic chemicals such as phosgene, isocyanates or carbon monoxide. Under these circumstances, chemical fixation of CO$_2$ becomes more and more important from the ecological and economic points of view.[1]

One of the few commercial routes using CO$_2$ as a raw material is the insertion of CO$_2$ into epoxides to produce cyclic carbonates (Scheme 1).
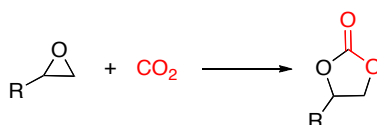
Scheme 1. Cycloaddition of CO$_2$ to epoxide to
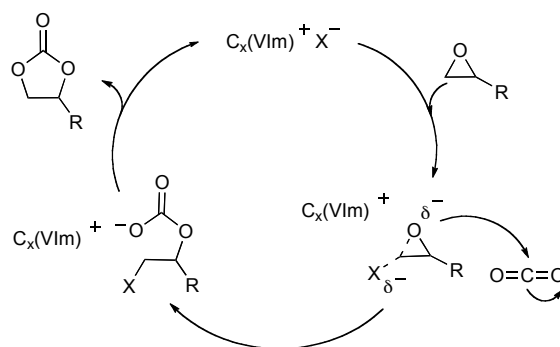produce five membered cyclic carbonates

In terms of *green chemistry* and *atom economy*, the process is promising because CO$_2$ can be incorporated into epoxides with no formation of side products.

Cyclic carbonates have found extensive use as excellent aprotic polar solvents, electrolytes in secondary batteries, sources for reactive polymer synthesis and intermediates in the production of pharmaceuticals and fine chemicals.[2]

Various catalysts have been investigated such as alkali metal halides,[3] organic bases,[4] metal oxides,[5] zeolite, titanosilicates,[6] smectites and metal complexes.[7] In recent years, ionic liquids have been used as catalysts and/or alternative solvents in organic synthesis.[8] The first use of ionic liquids as catalyst for the cycloaddition of cyclic carbonate was reported by Peng and Deng.[9] Since then, numerous ionic liquids such as quaternary ammonium, phosphonium, imidazolium and pyridinium were used for cycloaddition of CO$_2$ to epoxides for the generation of cyclic carbonates.[10]

For better separation and reuse of catalyst, the immobilization of ionic liquids on recyclable solid materials has been a topic of investigation.

Recently, simple supported ionic liquids with halides counter-ions have been successfully employed as catalysts for the chemical fixation of carbon dioxide.[11] The reaction mechanism involves a ring opening by the halogen ion followed by chemical fixation of carbon dioxide (Scheme 2).[11, 12]

Scheme 2. Proposed mechanism for the synthesis of five membered cyclic carbonates via insertion of CO_2 catalyzed by ionic liquid $[C_x(Vim)][X]$; the cation $C_x(Vim)$ is a generic vinylimidazolium and the anion X is a generic halogen.

The concept of Supported ionic liquid phase (SILP) was described for the first time in 2002 by Mehnert[13] and since than the interest for this type of materials increased considerably.[14] SILP is an innovative method to immobilize homogeneous transition metal complexes and organocatalysts. The SILP concept consists of the four major building blocks, namely the support, the ionic liquid, the catalyst and the reactants. In the SILP, the IL layer can act as catalyst and or serve as reaction phase in which the substrate as well as the catalyst are dissolved. The thus obtained full powders material can be employed like any other solid catalyst. By choosing the appropriate combination of catalyst, ionic liquid and support, novel SILP materials can be obtained. These materials have sometimes superior properties compared to conventional catalysts. The advantages of heterogeneous catalytic systems based on supported ionic liquid phase (SILP) compared to the corresponding homogeneous analogous include the easier separation from the reaction media and the possibility of using them in fixed-bed reactors. Several supported ionic liquid materials, mainly based on imidazolium cations, have been employed as catalysts for the cycloaddition of CO_2 to various epoxides. The most used supports are cross-linked polystyrene and silica (amorphous or mesoporous), but other supports have been also investigated (magnetite, toyonite, alumina, chitosan).[11] The ionic liquid phase has been supported on cross-linked polystyrene or linear copolymer by co-polymerization procedure or by post-modification approach and on silica by adsorption, sol-gel method or by grafting.[11]

Usually, these reactions are carried out under supercritical CO_2 (scCO_2) conditions since scCO_2 serves, at the same time, as reactant and as solvent due to its high solvating power towards various epoxides. Supercritical CO_2, due to its low critical pressure (73.75 bar) and temperature (31.0 °C) itself, has received considerable attention as a green alternative to organic solvents and being nonflammable, nontoxic, and abundantly available; in addition scCO_2 offers striking possibilities when combined with ILs. These benefits mainly arise from the fact that scCO_2 is well soluble in ILs (much more than other

common gases), while most ILs are virtually insoluble in CO_2, even at elevated pressures. This phenomenon allows designing very promising bi- and multiphasic reaction systems.

In general, the supported ionic liquid phase is present as a monolayer when it is covalently attached on the surface or as a multilayer when it is adsorbed (Figure 1, *a,b*).
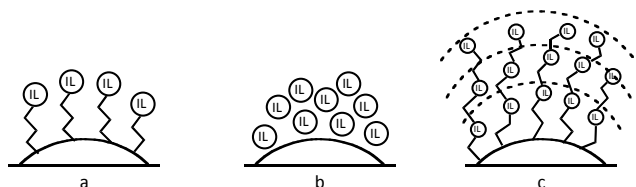

Figure 1. Schematic representation of *a)* covalently attached monolayer of ionic liquid, *b)* adsorbed multilayer of ionic liquid, *c)* covalently attached multilayer of ionic liquid.

On the other hand, paper focused on the synthesis and applications of covalently attached multilayer ionic liquids (Figure 1, c) are still rare.[15]

Recently in our research group was reported for the first time[16] the synthesis of a new class of Multilayered covalently supported ionic liquid phase (mlc-SILP). These materials were synthesized by grafting bis-vinylimidazolium salts on different types of silica or polymeric supports. The obtained materials were characterized and tested as catalysts in the reaction of supercritical carbon dioxide with various epoxides to produce cyclic carbonates. The material prepared by supporting a bromide bis-imidazolium salt on the ordered mesoporous silica SBA-15 was identified as the best catalyst for the synthesis of cyclic carbonates and displayed very good activity and improved productivity compared to known supported ionic liquid catalysts.[16]

Considering this very good result and to further investigate this new interesting class of materials, a series of catalysts using different ionic liquids with iodide and bromide counter-ions supported on amorphous silica were prepared. These materials were characterized and tested as catalysts for the chemical fixation of carbon dioxide on various epoxides under supercritical condition. The rapid and efficient parallel screening of the series of catalysts in the selected reactions was carried out using a novel high-throughput (HT) unit for the study of catalytic systems under supercritical CO_2 (Figure 2).
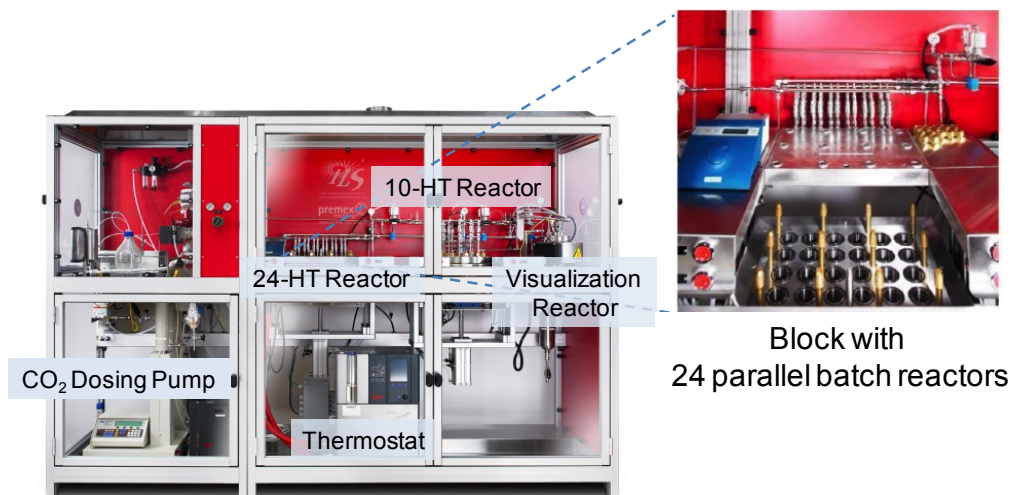
Figure 2. The supercritical CO_2 high-throughput unit.

The parallel catalytic tests were performed in a block consisting of 24 parallel batch reactors (Figure 2), while the recycling tests and the study of the phase behaviour of the systems were carried out in a visualisation batch reactor, equipped with a glass window to allow monitoring the phases present in the reaction mixture (Figures 3).
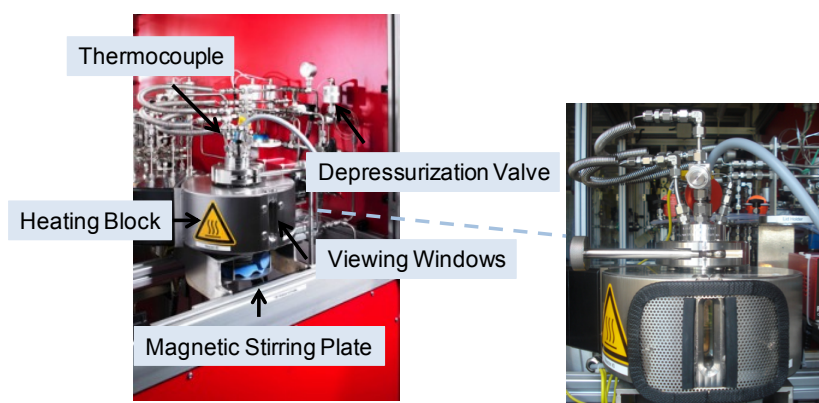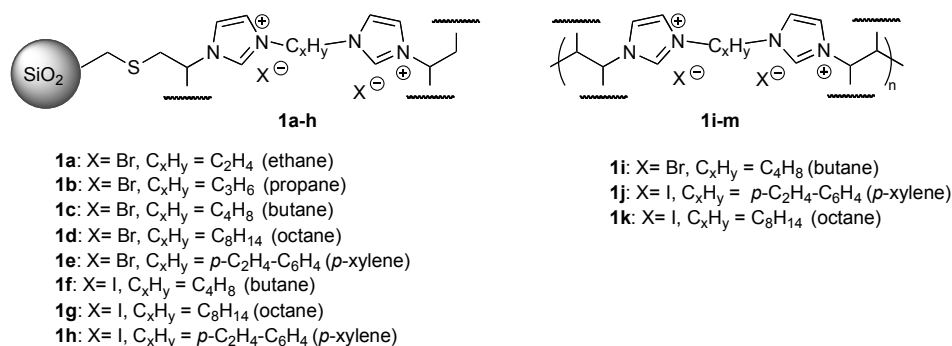

Figure 3. Visualization reactor of the supercritical CO_2 high-throughput unit.

High-throughput experimentation is an established and powerful tool for research in catalysis.[17,18] This is the second time in which high-throughput experimentation techniques are employed in the study of reactions in supercritical CO_2.

3.2   *Results and Discussion*

3.2.1   *Synthesis and Characterization of the mlc-SILP*

With the aim to discover new multi-layered (or high loaded) supported ionic liquid-based materials for the solventless cycloaddition of carbon dioxide to epoxides, a series of new catalysts **1a-k** and two known catalysts **1c** and **1e** were prepared[16c,17] (Figure 4).

1a: X= Br, C_xH_y = C_2H_4 (ethane)
1b: X= Br, C_xH_y = C_3H_6 (propane)
1c: X= Br, C_xH_y = C_4H_8 (butane)
1d: X= Br, C_xH_y = C_8H_{14} (octane)
1e: X= Br, C_xH_y = p-C_2H_4-C_6H_4 (p-xylene)
1f: X= I, C_xH_y = C_4H_8 (butane)
1g: X= I, C_xH_y = C_8H_{14} (octane)
1h: X= I, C_xH_y = p-C_2H_4-C_6H_4 (p-xylene)

1i: X= Br, C_xH_y = C_4H_8 (butane)
1j: X= I, C_xH_y = p-C_2H_4-C_6H_4 (p-xylene)
**1k**: X= I, C_xH_y = C_8H_{14} (octane)

Figure 4. Multi-layered supported ionic liquid-based materials **1a-h** and three highly cross-linked polymer matrix materials **1i-m** for the solventless cycloaddition of carbon dioxide and epoxides. The wavy lines in the scheme symbolize further connections, either by cross-linking to other bis-imidazolium units or by anchoring to the support.

The new materials were obtained starting from amorphous silica functionalized with mercaptopropyl groups and a large amount of bis-vinylimidazolium salts. The anchorage of the salts was carried out in ethanol at 78 °C under argon in the presence of azoibisisobutyronitrile (AIBN) as a radical initiator under magnetic stirring. This approach is a very simple, being based on the thiol-ene coupling (TEC) reaction between a mercaptopropyl modified silica and the double bond of the imidazolium salt. This reaction offers all the desirable features of a click reaction, being highly efficient, simple to execute with no side products and proceeding relatively rapidly to high yield.

Since the bis vinylimidazolium salt is added in excess relatively to the amount of thiol groups (3.62 mol of salt per mol of thiol group), the formation of imidazolium cross-linked networks through self-addition reaction of the double bonds is also expected. The multilayered ionic liquid phase is generated through this oligomerization.

In addition following the same protocol of oligomerization, three materials (**1i-k**) were prepared in the absence of the mercaptopropyl-modified silica gel. These materials were prepared in order to investigate the role of the support.
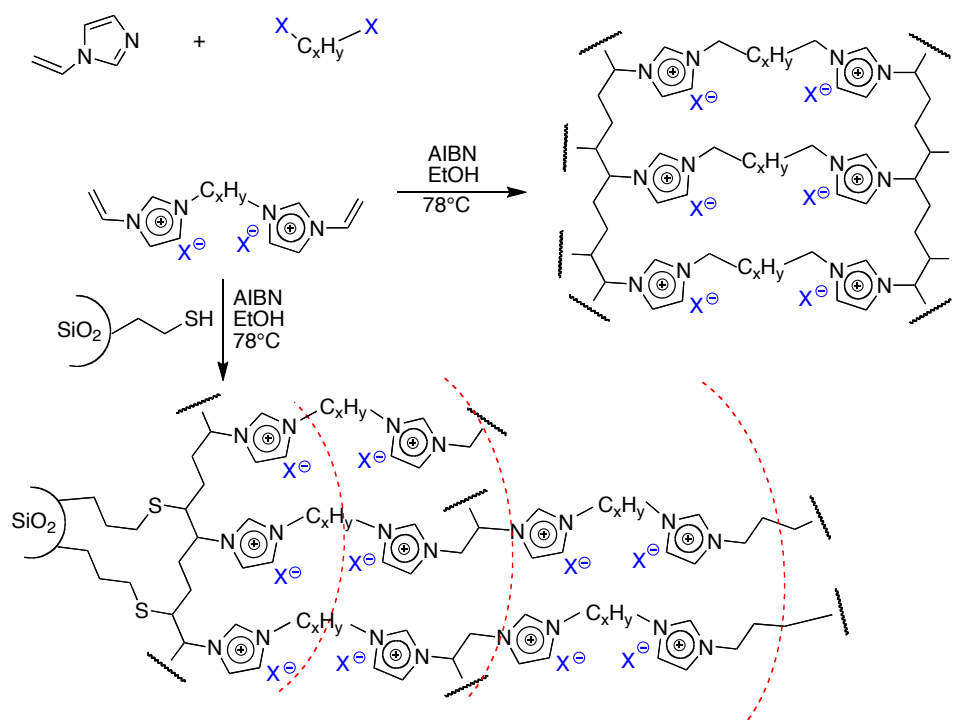
Scheme 3. Representation of the thiol-ene reaction for the preparation of mlc-SILP materials and synthesis of polymer-supported ionic liquid and schematic illustration of the possible domains of mlc-SILP catalyst.

All the materials were characterized through elemental analysis to evaluate the loading of imidazolium units, the molar ratio between ionic liquid and SH and the weight of supported ionic liquid. The results are summarized in Table 1.

Table 1. Loading of imidazolium units in function of the type of bis-vinylimidazoliumsalts (bis-Vim) employed in the synthesis.[a]

Entry	Mlc-SILP	Loading of Vim Units[b] (mmol/g)	Molar ratio IL/SH[c]	Weight of supported IL (%)
1	SiO₂-Ethane-Br	3.20	3.3	60
2	SiO₂-Propane -Br	3.26	3.7	63
3	SiO₂-Butane -Br	2.96	3.1	60
4	SiO₂-Butane -I	2.74	3.6	68
5	SiO₂-Octane-Br-A	1.08	0.6	66
6	SiO₂-Octane-Br-B	2.86	3.5	25
7	SiO₂-Octane-I	2.52	3.5	70
8	SiO₂-*p*-Xylene-I	2.18	2.3	60
9	SiO₂-*p*-Xylene-Br	2.82	3.5	64

[a] *Reaction conditions* : bis-vinyimidazolium salts (3.62 eq), mercaptopropylmodified silica (1.2 mmol/g), ethanol (130 mM), AIBN, 78 °C, 17h. [b] Each bis-vinylimidazolium salt contains two imidazolium units. [c] Molar ratio between the amount of bis-vinylimidazolium salt in the obtained mlc-SILP and the amount of potential anchoring sites on the support (*i.e.* the original amount of –SH groups.

The thiol-ene reactions lead to the almost quantitative anchoring of the employed salt on the surface of the supports to give the mlc-SILP materials, as shown by the high loading of imidazolium units and by the high ratio between supported salt and anchoring sites determined by elemental analysis (Table 1). These results indicate that the synthesis method, in which an excess of salt was used with respect to the thiol groups, leads to the formation of the desired multilayered covalently supported ionic liquid phase.

The morphological properties of mlc-materials were determined by N$_2$ adsorption/desorption measurements (Table 2). The surface areas of these materials significantly decreased after grafting of the ionic liquid phase to about 120 m^2/g in the case of amorphous SiO$_2$. At the same time, a decrease of the cumulative pore volume was observed. This dramatic decrease in surface area and pore volume confirms the successful grafting of the bis-vinylimidazolium salts on the support. In addition, these data indicate that the imidazolium salts were also anchored inside the pores of the support.

Table 2. Morphological properties of mlc-SILP materials

Entry	Mlc-SILP	BET surface area (m^2/g)	Cumulative pore volume (cm^3/g)
1	SiO$_2$	750	0.7
2	SiO$_2$-Ethane-Br	129	0.2
3	SiO$_2$- Propane -Br	128	0.2
4	SiO$_2$- Butane–Br	146	0.2
5	SiO$_2$- Butane-I	134	0.3
6	SiO$_2$-Octane-Br-A	180	0.2
7	SiO$_2$-Octane-Br-B	89	0.2
8	SiO$_2$-Octane-I	121	0.1
9	SiO$_2$-p-Xylene-I-B	133	0.3
10	SiO$_2$-p-Xylene-Br	124	0.1

The characterization of all the catalysts by solid-state ^{13}C NMR spectroscopy confirms the anchorage/polymerization of the imidazolium salts to the support. The disappearance of the signal corresponding to vinyl group of the bis-vinylimidazolium salts is an indication that the organic precursor reacted completely (Figure 5).
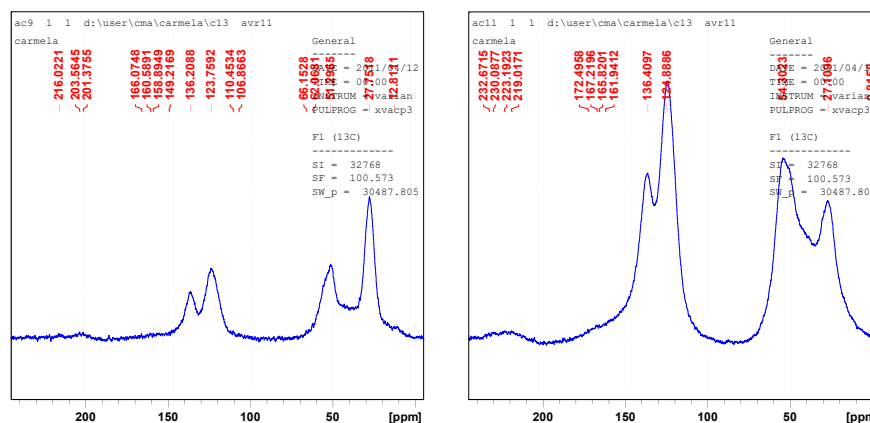
Figure 5. a) Solid State ^{13}C NMR spectrum of materials SiO_2-Octane-Br; b) ^{13}C NMR spectrum of polymeric material Butane-Br .

These results prove that the complete addition reaction of the double bonds occurs both through the reaction with the thiol groups of the functionalized support and by self-addition with other vinyl groups. In addition, there are no proofs of signals around 110 ppm in the case of highly cross-linked polymer matrix materials (Figure 5b).

The signals of carbon atoms of the imidazolium ring are clearly visible at 121–124 and 136 ppm whereas aliphatic carbon atoms resonate in the range 27–60 ppm. A carbon atom close to an Si atom resonates at 12 ppm. There is no evidence of signals around 110 ppm, indicative of presence of the vinyl moiety.

These data also demonstrate that the main structure of the salt is maintained after the grafting process. Although the elemental analysis and the ^{13}C NMR data indicate that the synthesis of the multilayered covalently supported ionic liquid phases was successfully achieved, it is still difficult to define the exact structure of the mlc-SILP materials: a tentative description of the domains formed, based on the characterization data, is given in Scheme 3.

3.2.2 *Catalytic Performance of Multi-layered SILP*

The multi-layered covalently supported ionic liquid materials were tested as catalysts for the chemical fixation of carbon dioxide on various epoxides with CO_2 under supercritical conditions. All the reactions were carried out in the high-throughput unit that enables a rapid and efficient parallel screening of the series of catalysts under supercritical CO_2. The parallel catalytic test was performed in a block consisting of 24 parallel batch reactors. The use of this unique high-throughput unit coupled with fast gas chromatographic (GC) analysis allows the rapid screening of up to 24 catalysts in 24 hours (including both the catalytic test and the GC analysis).

In order to investigate the versatility of our catalysts, two different epoxides were selected as substrates for the reaction with CO_2: a monosubstituted aliphatic epoxide such as hexene oxide (HO) and a monosubstituted aromatic compound like styrene oxide (SO).

As a first test, the catalytic activity of several materials was compared by performing the reaction at 80 bar and 125°C using the high-throughput unit equipped with 24 parallel batch reactors (Table 3).

Table 3. Catalytic test of the mlc-SILP in the reaction of addition of CO_2 to two different epoxide[a]

Entry	Mlc-SILP	Styrene Carbonate			Hexene Carbonate		
		Yield[b] (%)	Prod[c]	TON[d]	Yield[b] (%)	Prod[c]	TON[d]
1	SiO_2-Ethane-Br	18	13	28	12	8	20
2	SiO_2- Propane -Br	25	18	39	11	7	17
3	SiO_2- Butane–Br	11	7	17	9	6	14
4	SiO_2-Octane-Br-A	39	28	159	26	18	114
5	SiO_2-*p*-Xylene-Br	28	21	46	14	8	21
6	SiO_2- Butane -I	39	27	62	7	5	12
7	SiO_2-*p*-Xylene-I	37	29	85	21	13	44

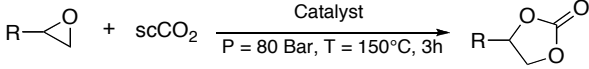[a] *Reaction conditions*: epoxide (46.74), mesitylene (4.67 mmol), 100 mg of catalyst, CO_2 (80 bar), 125 °C, 3h. [b] Carbonate yield determined by GC, using mesitylene as an internal standard. [c] Productivity, calculated as the ratio between the amount of product and the amount of catalyst in grams. [d] TON, calculated as the molar ratio between the mol of product and the mol of halides, calculated using the loading of imidazolium units determined by elemental analysis.

These preliminary data seem to indicate that the materials SiO_2-Octane-Br and the materials SiO_2-*p*-Xylene-I give the highest carbonate yield (Table 3, entries 4 and 7). Also, the SiO_2-Butane-I gives good results for the reaction of cycloaddition in which the epoxide is styrene oxide. (Table 3, entries 6)

Considering this starting results new materials were synthesized, and in particular the material having the C8 linker and iodide as halide and three different cross-linked-polymeric materials.

To further improve the carbonate yield, the test was performed using a higher temperature of 150°C and a Pressure of 80 bar.

Table 4. Catalytic test of the mlc-SILP in the reaction of addition of CO_2 to two different epoxides[a]

$$R\!\!-\!\!\triangleleft^O + scCO_2 \xrightarrow[\text{P = 80 Bar, T = 150°C, 3h}]{\text{Catalyst}} R\!\!-\!\!\langle_O^{O}\!\!\searrow^O$$

Entry	Mlc-SILP	Styrene Oxide			Hexene Oxide		
		Conv.[b] (%)	P[c]	TON[d]	Conv.[b] (%)	P[c]	TON[d]
1	SiO₂-Ethane-Br	48	35	77	20	13	32
2	SiO₂- Propane -Br	59	45	94	13	9	21
3	SiO₂- Butane –Br	56	43	87	20	9	31
4	SiO₂- Butane -I	66	50	112	29	19	48
5	SiO₂-Octane-Br-A	76	57	320	37	25	159
6	SiO₂-Octane-Br-B	83	61	131	26	17	41
7	SiO₂-Octane-I	82	61	148	29[e]	14	53
8	SiO₂-*p*-Xylene-Br	51	38	82	12[e]	8[e]	20
9	SiO₂-*p*-Xylene-I	99	74	215	45	30	98
10	Butane -Br	36	27	34	9[e]	6[e]	10
11	*p*-Xylene-Br	56	41	58	10	4	11
12	Octane-I				13	6	16
13	SiO₂-SH	-	-	-	-	-	-

[a] *Reaction conditions*: epoxide (14.02), mesitylene (1.40 mmol), 30 mg of catalyst, CO_2 (80 bar), 150 °C, 3h. [b] Conversion determined by GC, using mesitylene as an internal standard. [c] Productivity, calculated as the ratio between the amount of product and the amount of catalyst in grams. [d] Calculated as the molar ratio between the mol of product and the mol of halides. [e] Conversion determined by ^{1}H NMR.

The results are summarized in Table 4. As expected on the basis of the accepted reaction mechanism, supported ionic liquids in which the counter ion is represented by iodine provide a higher epoxide conversion than those containing bromide. These differences reflect the nucleophilicity order of the anions. This behaviour can be observed for the materials in which the linker is the butane and the *p*-xylene. (Table 4 entries 3 and 4, 8 and 9). In the case of the C8 linker, the influence of the anion is not so evident.

Comparison between the results with different chain showed that long chain is better. Interesting, there is almost no difference between the catalytic performances of the two different halide, indicating that the long chain influence the conversion.

This could be due to an increase of solubility of CO_2 and epoxide in ionic liquid phase with lengthening alkyl chain of the imidazolium salt.[19]

When comparing the activity of each catalyst with the two substrates, a clear trend can be observed under the conditions used, the highest conversion is always achieved with the material SiO₂-*p*-Xylene-I (Figure 6).
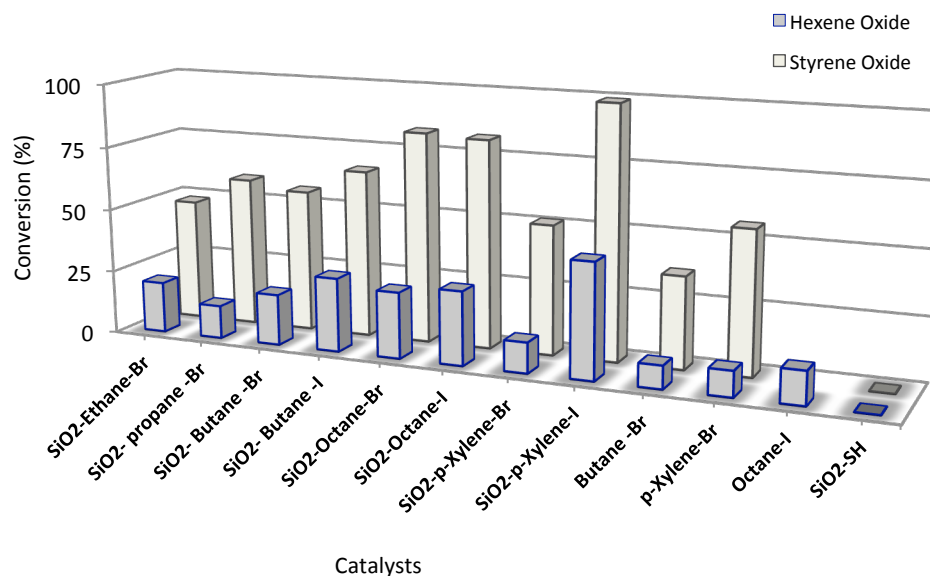
Figure 6. Cycloaddition of carbon dioxide with different epoxide. Reaction conditions: epoxide (14.02), mesitylene (1.40 mmol), 30 mg of catalyst, CO_2 (80 bar), 150 °C, 3h

The reaction carried out with the use of the mercaptopropyl-modified silica was, as expected, unsuccessful (Table 4, Entry 13).

In order to investigate the effect of the supports and the role of multilayered, three different cross-linked-polymeric-supported ionic liquid materials (**1i**-**k**) were employed as heterogeneous catalysts in the cycloaddition reactions. The results show that the support has an effect on the conversion. The conversion for Butane-Br and p-Xylene-Br were 36% and 56%. These results may reflect the high reactivity of styrene oxide. In the case of hexane oxide the influence of support is more evident, for the material SiO_2-octane-I the conversion is 29 % while for the polymeric materials is 13% (Table 4, entries 7 and 12), the same trend is for material SiO_2-butane-Br and the material Butane-Br in which the conversion pass from 20% to 9% (Table 4, entries 3 and 10).

The selectivity was about 100%. Indeed, negligible amounts of by-products such as polycarbonate and homopolymer of styrene oxide and hexene oxide were detected.

3.2.3 *Study of Catalyst Loading*

After the catalytic test, further experiments were carried out by lowering the catalyst loading. The catalyst SiO$_2$-Octane-I and the catalyst SiO$_2$-Octane-Br were used. High catalytic activity of the catalyst in the cycloaddition reaction of styrene oxide was achieved. In particular the catalyst SiO$_2$-octane-I showed not only high TON (324) but also high selectivity (>99%).

Table 5. Catalytic test of the SiO$_2$-octane-X-3.62 in the reaction of addition of CO$_2$ to Styreneoxide[a]

Entry	Catalyst (gr)	Halide X	Conversion[b] %	Productivity[c] %	TON[d] %	Selectivity (%)
1	0.031	I	87	65	157	*>99*
2	0.016	I	72	79	259	*>99*
3	0.008	I	45	98	324	*>99*
4	0.030	Br	74	55	119	*>99*
5	0.015	Br	50	71	156	*>99*
6	0.008	Br	24	73	157	*>99*

[a] *Reaction conditions*: epoxide (14.02), mesitylene (1.40 mmol), catalyst, CO$_2$ (80 bar), 150 °C, 3h. [b] Conversion determined by GC, using mesitylene as an internal standard. [c] Productivity, calculated as the ratio between the amount of product and the amount of catalyst in grams. [d] TON, calculated as the molar ratio between the mol of product and the mol of halides

3.2.4 *Study of Effect of Pressure*

The influence of the pressure on the conversion of hexene oxide was studied. Starting from the good results obtained at 80 bar, it was investigated the possibility to decrease the pressure.

This experiment was performed in a single batch reactor with large, high-pressure viewing windows that enables the direct visualization of the phases during reaction.

The effect of CO$_2$ pressure was examined on the conversion of hexene oxide using SiO$_2$-*p*-xylene-I catalytic system. As shown in Figure 4 when the pressure was 60 bar the conversion was 88%, for a pressure of 80 bar the conversion was 78 %.
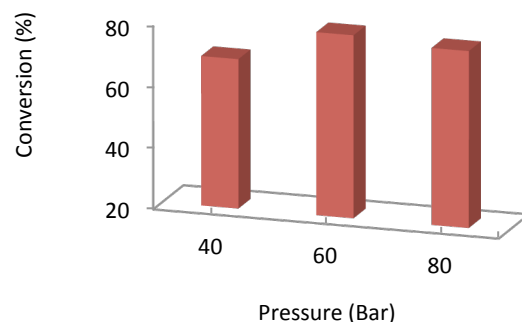
Figure 7. Effect of CO_2 pressure for the cycloaddition reaction of hexene oxide.

This result can be explained on the basis of the structure of the catalyst and of the presence of a multi-layered ionic liquid phase. As it can be clearly seen in Figure 8, two phases are always present in our system, also when working with CO_2 in supercritical conditions: the upper phase is richer in carbon dioxide while the bottom phase is richer in the epoxide. Taking into account the structure of the catalyst, we propose that the reaction takes place in the multi-layered covalently anchored ionic liquid phase (Figure 8). An increase of CO_2 pressure will cause two opposite phenomena: the concentration of carbon dioxide in the bottom phase, and consequently in the mlc-SILP, will increase while the concentration of the organic reactant will decrease. Since both styrene oxide and CO_2 are essential for the formation of the corresponding cyclic carbonate, it is not surprising that an optimum balance between the two opposite phenomena can be reached for certain pressure (60 bar in our case). This behaviour was previously described for others heterogeneous catalysts.[20]
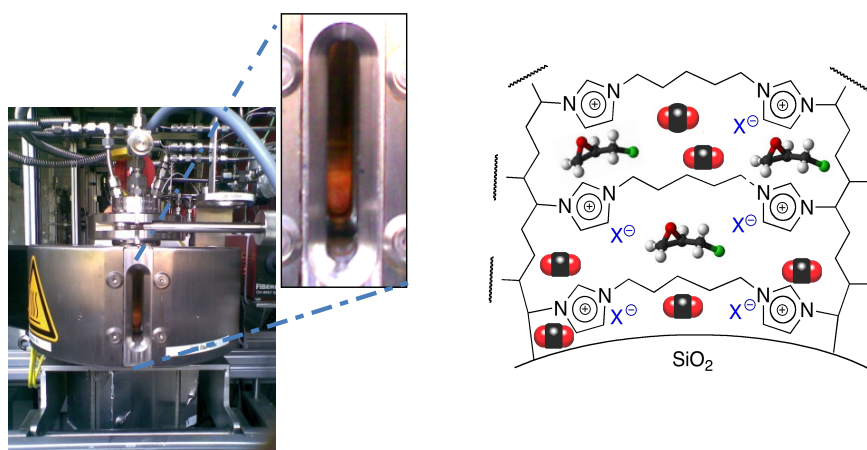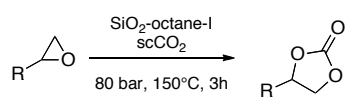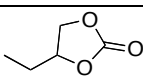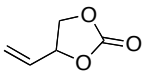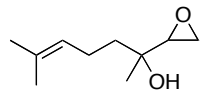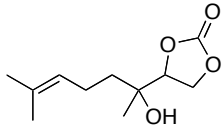

Figure 8. Visualizator reactor of supercritical CO_2 high troughput unit and the phase behaviour during the cycload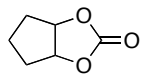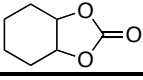dition of carbon dioxide to styreneoxide performed at 80bar. The pictures on the right side show the schematic representation of the possible reaction occurring in the multi-layered ionic liquids phase.

3.2.5 *Synthesis of Cyclic Carbonates from CO₂ and Other Epoxides*

Using the SiO_2-octane-I as catalyst, a series of epoxide substrate were examined for the synthesis of the corresponding carbonate at 80bar and 150°C in the 24-HT reactor block. The results are summarized in Table 6.

Table 6. Results of the catalytic test carried out in the 24-block reactor with SiO_2-octane –I in the reaction of addition of CO_2 to different epoxide [a]

| Entry	Epoxide	Carbonate	Yield %	TON [d]	Productivity [e]
			32 [b]	58	17
2			67 [b]	122	35
3			>99 [b]	185	100
4			5 [b]	9	3
5			10 [c]	9	3

[a] *Reaction conditions*: epoxide (14.02), mesitylene (1.40 mmol), 30 mg of catalyst, CO₂ (80 bar), 150°C, 3h. [b] Conversion determined by ¹H NMR, using mesitylene as an internal standard. [c] Conversion determined by GC, using mesitylene as an internal standard. [d] TON, calculated as the molar ratio between the mol of product and the mol of halides. [e] Productivity, calculated as the ratio between the amount of product and the amount of catalyst in grams.

SiO_2-octane-I was found to be applicable to a variety of epoxides to produce the corresponding cyclic carbonates in good yield. Linalool oxide was found to be the most reactive epoxide, while butadiene monoxide exhibits good conversion. On the other hand, cyclohexene oxide and cyclopentene oxide showed poor reactivity, probably due to the steric effect of the cyclic oxide.

3.2.6 *Studies of Different Loading of Imidazolium Units in the Synthesis of Multi-layer SILP*

In order to understand the role of the multilayered ionic liquid, new mlc-SILP were synthesized using a different excess of liquid ionic respect to thiol group: 4.8, 2.4, 1.2 eq salt per eq of –SH. The SiO_2-octane-I was used since these materials gave very good results in the previous catalytic tests.

In the synthesis, the mercaptopropylmodified silica (1.2 mmol/g), a bis-vinyimidazolium salts (1.2, 2.4, 3.62 or 4.8 eq), AIBN (60 mg) and ethanol (130 mM) were placed in a flask. Argon was bubbled for 10 minutes and the reaction mixture was magnetically stirred under argon. The flask was heated to 78°C to favour the dissolution of the bis-imidazolium salt. At the end of the reaction, we noticed the presence of an additional solid precipitate with different colour and form (white grey for iodide salts). Part of the materials were separated through analytical sieves of 200 µm and used for the catalytic test (so-called *sieve(<200* µm*)*). In order to compare the new materials with the previous mlc-SILP, we also performed the catalytic test using a part of material prepared as in the last test (so-called *as synth*).
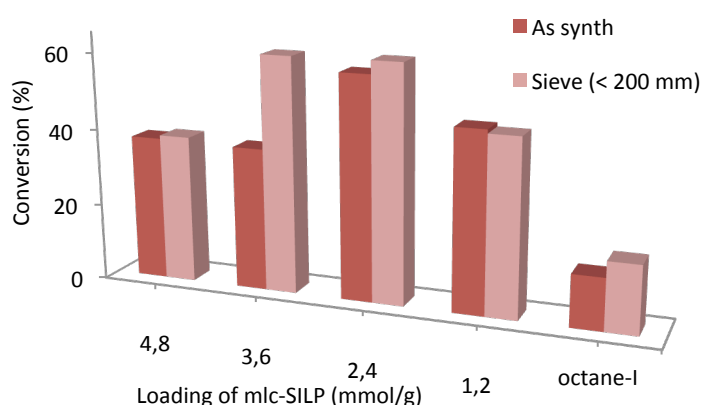

Figure 9. Study of loading of of imidazolium units in the synthesis of SiO$_2$-octane-I

The catalytic test using the large particles separated with sieve of 200 µm was also performed for the high cross-linked polymeric material Octane-I, with a conversion of 5.1 %. The calculated percentage of polymeric part respect to the entire materials was around 30% for all the materials. The materials prepared using 3.6 eq of bis-vinyimidazolium salts respect to thiol group gave the best results. This seems to indicate that the multi-layered covalently supported ionic liquid phase plays an important in the conversion of styrene oxide to carbonate.

3.2.7 *Study of Catalyst Recycling*

Heterogeneous catalysts are clearly advantageous compared to homogeneous ones in terms of separability from the reaction mixture. Ideally, after separation the solid catalyst should be reusable in consecutive cycles without losing its catalytic properties. Recycling tests on one of the most active

supported ionic liquid catalyst, SiO$_2$-p-xylene-Br, were performed. At the end of each cycle, the catalyst was easily recovered by filtration, washed with toluene and ethanol, dried and reused. The recycling tests performed on the reaction with styrene oxide show that the catalyst is stable and can be used for at least four cycles without loss in catalytic activity. Characterization of the catalyst by solid-state ^{13}C NMR at the end of the fourth cycle provides a further confirmation that the morphology of the catalyst as well as the content of the imidazolium salt remained unchanged during the catalytic tests. In order to assess the reusability of our catalysts also under more stringent conditions, we performed a recycling test of SiO$_2$-p-xylene-Br-B employing a four-fold lower catalyst loading (0.25 mol %). In the first run, the catalyst gave 22% yield of styrene carbonate. Upon recycling, the yield gradually increased until the third run (Figure 5), and then stabilized in the following runs (46% yield in the fifth run). These results confirm the reusability of the mlc-SILP catalysts, although the observed trend of increasing activity in the course of the initial recycling runs suggests that some modification of the material occurred. Still, no leaching of imidazolium salt was detected by ^{1}H NMR analysis of the reaction solution at the end of any of the catalytic tests. Future research efforts will try to unravel the nature of these modifications. Finally, it is worth noting that in these tests in which intermediate levels of conversion of the epoxide were achieved, the selectivity towards the carbonate was slightly lower (90-95%) compared to tests with higher catalysts loading, due to the formation of a styrene oxide dimer as by-product, detected by gas chromatography-mass spectrometry analysis (GC-MS).
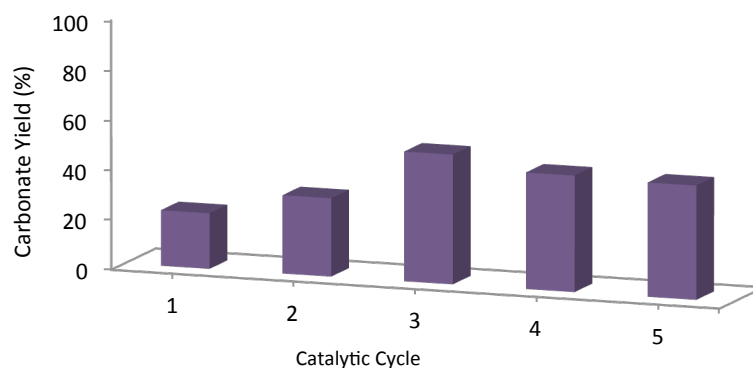
Figure 10. Recycling experiments of SiO$_2$-pxylene-Br as catalyst for the cycloaddition of carbon dioxide to styrene oxide. Conditions: epoxide (58.4 mmol), mesitylene (5.84 mmol, as internal standard), catalyst (0.25 mol %), 3h at 80 bar and 150°C; carbonate yields were calculated by ^{1}H NMR and confirmed by GC.

3.3   Conclusions

Multilayered covalently supported ionic liquid phase (mlc-SILP) materials were synthesized using the thiol-ene coupling reaction to covalently anchor bis-vinylimidazolium salts to amorphous silica functionalized with mercaptopropyl groups. Cross-linked polymers of three bis-vinylimidazolium salts were also synthesized. The characterization of the prepared materials demonstrated the successful anchoring of the ionic liquid phase and strongly suggested the formation of multilayers generated by self-addition reaction of the double bonds of the bis-vinylimidazolium salts. The mlc-SILP materials were tested as heterogeneous catalysts for the addition of carbon dioxide to various epoxides to yield cyclic carbonates. The catalytic tests were carried out under supercritical carbon dioxide in a unique high-throughput unit, which allows performing simultaneously 24 reactions in parallel batch reactors. One of the best catalysts identified in this work was prepared by supporting an iodine bis-imidazolium salt on silica. This catalyst achieved very high conversion and selectivity in the conversion of styrene oxide to the cyclic carbonates and displayed improved productivity compared to known supported ionic liquid catalysts.

3.4   *Experimental Section*

General Methods

The ^{1}H NMR and ^{13}C NMR spectra were recorded on a Bruker 300 MHz spectrometer. The chemical shifts for ^{1}H and ^{13}C are given in ppm to residual signals of the solvents (CD$_3$OD). The following abbreviations are used to indicate the multiplicity: s, singlet; d, doublet; t, triplet; q, quartet; m, multiplet; bs, broad signal. Solid-state ^{13}C CP MAS NMR spectra of the mlc-SILP materials were recorded on a Bruker Avance DSX400 spectrometer (9.4 T). 14000 to 22000 scans were accumulated with a recycle delay of 10 s. The CP contact time was 4 ms. The samples were packed in 4 mm zirconia rotors. The spinning frequency of the rotor was 6000 Hz. Tetramethylsilane was used as chemical shift reference. Carbon and nitrogen contents were determined by combustion analysis with a Fisons EA 1108 elemental analyser. FT-IR spectra were registered with a Shimadzu FTIR 8300 infrared spectrophotometer. Melting points were determined by using a Kofler hot plate. The content of imidazolium salt was determined by chemical combustion analysis carried out on an EAS Vario Max CN equipment.
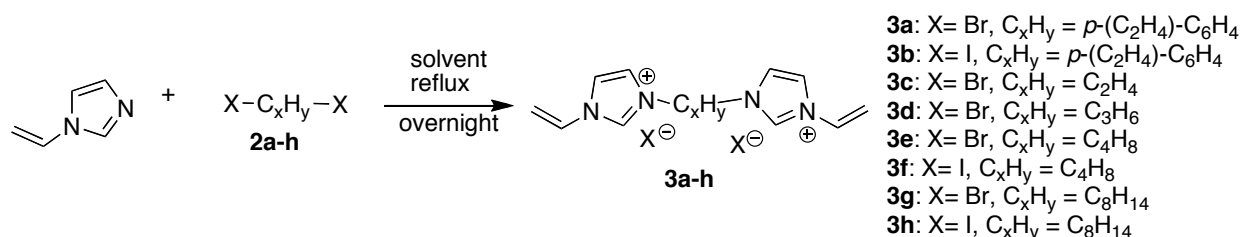
The specific surface areas and pore volumes of the silica-based materials, before and after supporting the ionic liquid phase, were determined from the N$_2$ adsorption/desorption isotherms

measured at -196°C on a Sorptomatic 1900 (Carlo Erba) instrument. The specific surface areas were determined by applying the BET method[21] to the nitrogen adsorption isotherm. The cumulative pore volume was calculated by BJH method[22] applied to the desorption curve in the range p/p$_0$: 0.2-0.98 (Table 2).

Gas chromatography (GC) data were obtained using a Trace GC Ultra from Interscience (RTX-5 column, 5 m, 0.1 mm), equipped with an ultrafast module allowing the rapid analysis of the samples (less than 2.5 min per sample). Instrument conditions-inlet temperature: 250°C; detector temperature: 250°C; hydrogen flow: 35 ml/min; air flow: 350 ml/min; constant col + makeup flow: 30 ml/min. Method: 50°C for 0.50 min., followed by a temperature increase of 10 °C/min to 250°C, hold 0.5 minutes and a subsequent isothermal period at 250°C for 0.50 minutes (total run time = 1.80 minutes). Gas chromatography-mass spectrometry analysis (GC-MS) was obtained on an Agilent 6890N Gas Chromatograph (WCOT fused silica column, 30 m, 0.25 mm) coupled to an Agilent 5973 MSD Mass Spectrometer. The cyclic carbonates are known compounds and showed spectroscopic and analytical data in agreement with their structures. The configurations of these products were assigned by comparison with literature data. The compound 1,4-Bis(iodomethyl)benzene **2b** was prepared as reported in literature.[23] Derivatives **3a**[16] and **3e**[15c] are known compounds and showed spectroscopic and analytical data in agreement with their structures.

General Procedure for the synthesis of bis-vinylimidazolium salts 3a-3g

The procedures to prepare the salts **3a**-**3g** were similar to that reported.[15c, 16] Thus, a solution of compound 2 (0.01 mol) and 1-vinylimidazole (0.021 mol) in toluene (10 mL, in the case of compounds 2a-2b) and in chloroform (5mL, in the case of compound 2c-2g) was heated at reflux for 24 h in an oil bath at 90°C and 50°C (respectively for the toluene and chloroform solution) with magnetic stirring. After cooling at room temperature, the mixture was filtered and washed several times with diethyl ether; the solid product was dried at 40 °C.

3a: X= Br, C$_x$H$_y$ = *p*-(C$_2$H$_4$)-C$_6$H$_4$
3b: X= I, C$_x$H$_y$ = *p*-(C$_2$H$_4$)-C$_6$H$_4$
3c: X= Br, C$_x$H$_y$ = C$_2$H$_4$
3d: X= Br, C$_x$H$_y$ = C$_3$H$_6$
3e: X= Br, C$_x$H$_y$ = C$_4$H$_8$
3f: X= I, C$_x$H$_y$ = C$_4$H$_8$
3g: X= Br, C$_x$H$_y$ = C$_8$H$_{14}$
**3h**: X= I, C$_x$H$_y$ = C$_8$H$_{14}$

**Scheme 4.** Synthesis of bis-vinylimidazolium salts

Diiodide salt 3b: Pale yellow powder. Yield: 88%; mp 232°C; ^{1}H NMR (300 MHz, CD$_3$OD) δ: 5.46 (2H, dd, J = 8.7 and 2.7 Hz, *cis*-CH=CH$_2$), 5.52 (4H, s, CH$_2$Ph), 5.95 (2H, dd, J = 15.6 and 2.7 Hz, *trans*-CH=CH$_2$), 7.29 (2H, dd, J = 15.6 and 8.7 Hz, CH=CH2), 7.60 (4H, s, Ph), 7.77 (2H, d, J = 1.8 Hz, 4-H or 5-H), 8.05 (2H, d, J = 1.8 Hz, 4-H or 5-H), 9.46 (2H, s, 2-H). ^{13}C NMR (CD$_3$OD) δ: 53.9, 110.3, 121.1, 124.4, 129.8, 128.8, 130.9, 136.1. [Found: C, 39.6; H, 3.7; I, 46.5; N, 10.3; C$_{18}$H$_{20}$I$_2$N$_4$ requires C, 39.4; H, 3.5; I, 46.4; N, 10.2].
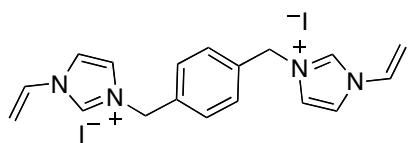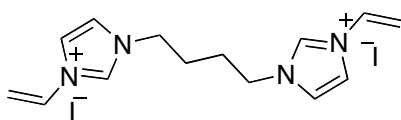
Dibromide salt 3c [C$_2$(vim)$_2$][Br]$_2$: White powder. Yield: 75%; mp> 300°C; ^{1}H NMR (300 MHz, CD$_3$OD) δ: 4.96 (4H, m, CH$_2$CH$_2$), 5.49 (2H, dd, J = 10.4 and 3.0 Hz, *cis*-CH=CH$_2$), 5.98 (2H, dd, J = 18.9 and 3.6 Hz, *trans*-CH=CH$_2$), 7.31 (2H, dd, J = 10.4 and 18.8 Hz, CH=CH$_2$), 7.85 (2H, d, J = 2.2 Hz, 4-H or 5-H), 8.09 (2H, d, J = 2.3 Hz, 4-H or 5-H), 9.54 (2H, s, 2-H). ^{13}C NMR (CD$_3$OD) δ: 50.0, 110.8, 121.4, 124.6, 129.8, 130.9, 137.4. [Found: C, 38.3; H, 4.3; Br, 42.5; N, 14.9 C$_{12}$H$_{16}$Br$_2$N$_4$ requires C, 38.3; H, 4.4; Br, 42.5; N, 14.9].
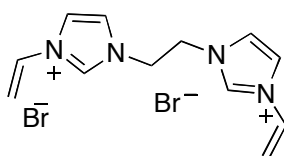
Dibromide salt 3d [C$_3$(vim)$_2$][Br]$_2$: Viscous pale yellow oil. Yield: 83%; ^{1}H NMR (300 MHz, CD$_3$OD) δ: 2.67-262 (2H, m, CH$_2$(CH$_2$)CH$_2$), 4.51-4.46 (4H,m, CH$_2$(CH$_2$)CH$_2$), 5.48 (2H, dd, J = 8.7 and 2.7 Hz, *cis*-CH=CH$_2$), 5.98 (2H, dd, J = 15.6 and 2.7 Hz, *trans*-CH=CH$_2$), 7.31 (2H, dd, J = 15.6 and 8.7 Hz, CH=CH$_2$), 7.89 (2H, d, J = 1.8 Hz, 4-H or 5-H), 8.07 (2H, d, J = 1.8 Hz, 4-H or 5-H), 9.51 (2H, s, 2-H). ^{13}C NMR (CD$_3$OD) δ: 31.1, 47.9, 110.2, 120.9, 124.4, 129.8. [Found: C, 40.0; H, 4.7; Br, 41.5; N, 14.4; C$_{13}$H$_{18}$Br$_2$N$_4$ requires C, 40.0; H, 4.5; Br, 41.4; N, 143].
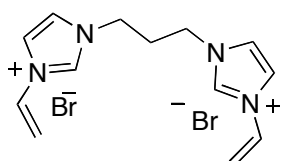
Diodide salt 3f [C$_4$(vim)$_2$][I]$_2$: Pale yellow powder. Yield: 95%; mp 160°C .^{1}H NMR (300MHz, CD$_3$OD): δ=2.12–2.07 [4H, m, CH$_2$ (CH$_2$)$_2$CH$_2$), 4.42 [4H, m, CH$_2$(CH$_2$)$_2$CH$_2$)], 5.46 (2H, dd, J=8.7 and 2.7Hz, *cis*-CH=CH$_2$), 5.97 (2H, dd, J=15.6 and 2.7Hz, *trans*-CH=CH$_2$), 7.30 (2H, dd, J=15.6 and 8.7 Hz, CH=CH$_2$), 7.86 (2 H, d, J = 1.5 Hz, 4-H or 5-H), 8.02 (2H, d, J=1.5 Hz, 4-H or 5-H), 9.48 (2H, s, 2-H); ^{13}C NMR (CD$_3$OD): δ=27.7, 50.4, 110.1, 120.9, 124.5, 129.8, 136.5; IR (nujol) ν$_{max}$/cm^{-1}: 921, 1154, 1377, 1458, 1550, 2854, 2922. [Found: C, 33.8; H, 4.1; I, 50.9; N, 11.3; C$_{14}$H$_{20}$I$_2$N$_4$ requires C, 33.5; H, 4.5; I, 50.3; N, 11.2].

*Dibromide salt **3g** [C₈(vim)₂][Br]₂*Pale yellow powder. Yield: 78%; mp>178°C; ^{1}HNMR (300MHz, CD₃OD):
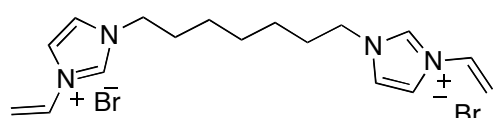
δ=1.42 (8H, bs, CH₂ CH₂(CH_2)₄CH₂CH₂), 1.97-1.93 [4H, m, CH₂CH_2(CH₂)₄CH_2CH₂)], 4.32-4.28 [4H, m, CH_2CH₂(CH₂)₄CH₂CH_2)], 5.45 (2H, dd, J=15.9 and 2.7Hz, *cis*-CH=CH₂), 5.96 (2H, dd, J=15.9 and 2.7Hz, *trans*-CH=CH₂), 7.29 (2H, dd, J=15.6 and 8.7 Hz, CH=CH₂), 7.82 (2 H, d, J = 1.8 Hz, 4-H or 5-H), 8.03 (2H, d, J=1.8 Hz, 4-H or 5-H), 9.44 (2H, s, 2-H); ^{13}C NMR (CD₃OD): δ=27.1, 29.7, 30.9, 51.2, 109.9, 120.7, 124.5, 129.8, 136.5. [Found: C, 46.9; H, 6.1; Br, 34.7; N, 12.2; C₁₈H₂₈Br₂N₄ requires C, 46.8; H, 6.2; Br, 34.5; N, 12.1].

*Diodide salt salt **3h** [C₈(vim)₂][I]₂*Pale yellow powder. Yield: 94%; ^{1}H NMR (300 MHz, CD₃OD) δ=1.42 (8H,
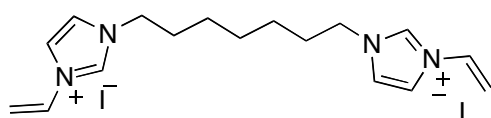
bs, CH₂ CH₂(CH_2)₄CH₂CH₂), 1.97-1.93 [4H, m, CH₂CH_2(CH₂)₄CH_2CH₂)], 4.31-4.26 [4H, m, CH_2CH₂(CH₂)₄CH₂CH_2)], 5.44 (2H, dd, J=9.0 and 2.7Hz, *cis*-CH=CH₂), 5.93 (2H, dd, J=15.6 and 2.4Hz, *trans*-CH=CH₂), 7.26 (2H, dd, J=15.6 and 8.7 Hz, CH=CH₂), 7.79 (2 H, d, J = 1.2 Hz, 4-H or 5-H), 8.00 (2H, d, J=1.5 Hz, 4-H or 5-H), 9.44 (2H, s, 2-H); ^{13}C NMR (CD₃OD): δ=27.1, 29.8, 30.9, 51.3, 110.0, 120.8, 124.6, 129.9, 136.2. [Found: C, 39.1; H, 5.2; I, 45.8; N, 10.1 C₁₈H₂₈I₂N₄ requires C, 39.3; H, 5.4; I, 45.1; N, 10.8].

Sinthesis of mercaptopropyl-modified silica

Mercaptopropyl-modified silica was prepared starting from Sigma-Aldrich silica (403563) as silica source. In the synthesis, 1.5 g of silica gel were initially heated overnight at 423 K in a vacuum line, in order to remove physically adsorbed water, subsequently treated with 3-(mercaptopropyl)-trimethoxysilane (2 mL) in 10 mL toluene. The mixture was heated under reflux in argon atmosphere for 24 h. After cooling to room temperature, the material was isolated by filtration and washed with methanol (50 mL) and diethyl ether (50 mL). The solid was dried under reduced pressure to give the final material (1.9 g, 1.2 mmol of SH group). The loading of thiol group was determinated by means of elemental analysis, elemental analysis of sulfur: 1.2 mmol/g.

Synthesis of mlc-SILP materials 1a-g

The mlc-SILP materials were synthesized using an excess of salts with respect to the -SH groups: 3.62 mol of salt per mol of -SH. In a typical synthesis, the mercaptopropyl-modified silica, a bis-imidazolium salt, AIBN (60 mg) and ethanol were placed in a three-necked round bottom flask. The reactions were carried out employing a concentration of 130 mM for all the salts, but in the case of SiO₂-*p*-xylene-I, the iodide salt was used in a 40mM solution. The suspension was degassed by bubbling argon for 10

minutes and the reaction mixture was magnetically stirred under argon The flask was heated to 78°C to favour the dissolution of the bis-imidazolium salt. The mixture was stirred for 20 h. After cooling down to room temperature, the solid was filtered and washed with hot methanol, diethyl ether and then dried in a oven at 40°C overnight.

Synthesis of cross-linked-polymer-supported ionic liquid materials 1h-l

The materials were prepared by radical polymerization. In a typical synthesis, the bis-imidazolium salt (1.09 mmol), AIBN (0.16 mmol) and ethanol (130 mM) were placed in a three-necked round bottom flask. The suspension was degassed by bubbling argon for 10 minutes and the reaction mixture was magnetically stirred under argon. The flask was heated to 78°C to favour the dissolution of the bis-imidazolium salt. The mixture was stirred for 20 h. After cooling down to room temperature, the solid was filtered and washed with hot methanol, diethyl ether and then dried in a oven at 40°C overnight followed by grinding before use.

Catalytic test

The catalytic tests were performed in a custom made high-throughput supercritical carbon dioxide unit (Integrated Lab Solutions, ILS). The tests were carried out in the 50 mL stainless steel of the 24-HT reactor block and in the 70 mL stainless stell of Visualization reactor in the supercritical CO$_2$ high-throughput unit using the same protocol described in our previous paper.[17] A schematic overview of the unit is given in Figure 11. The set-up consists of four modules: a visualization batch reactor, a block with 10 parallel batch reactors, a block with 24 parallel batch reactors, and a fixed-bed reactor. The four modules can be used simultaneously. The batch reactors in the 10 and 24 blocks are fed in parallel while check valves protect against back-flow. The individual batch reactors are stirred using magnetic stirring bars and heated with electric heating elements. Throughout the system, protection against overpressure is ensured by automated depressurization protocols and by the presence of rupture disks. The 24-HT reactor block consists of 24 parallel batch reactors with individual magnetic stirring, which have been designed to operate with glass or Teflon liners easily removable from the reactor to facilitate the working up of the reaction or the separation of the catalyst. The temperature of the 24-HT block is regulated using a Huber Thermostat. The pressurization of the reactors is achieved by means of two ISCO pumps.
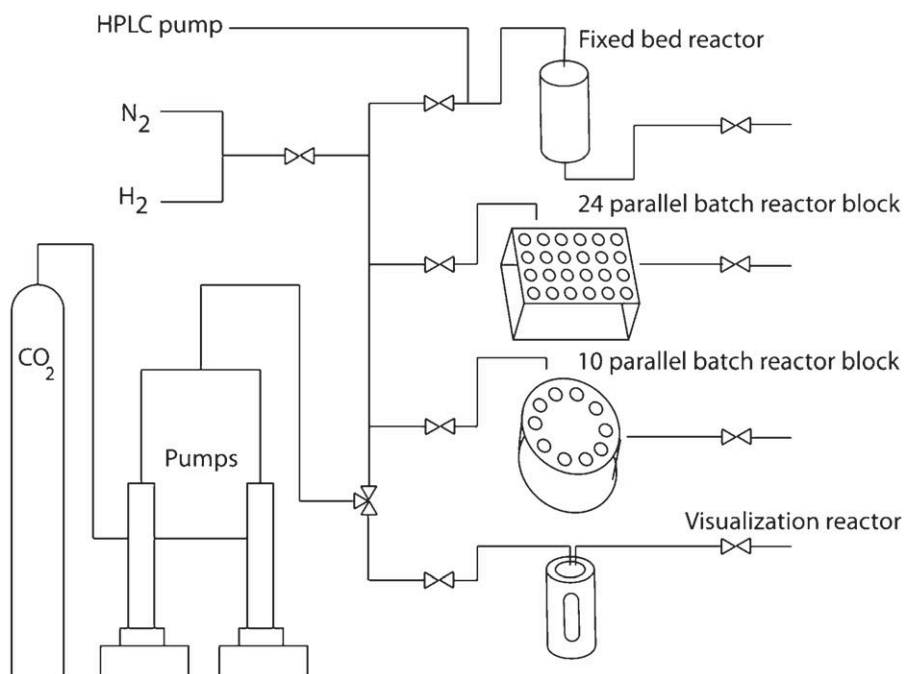
Figure 11. Schematic overview of the high-throughput scCO$_2$ unit.

In a typical experiment, the epoxide (14.02 mmol), the catalyst (30 mg) and mesitylene (1.40 mmol, as GC internal standard) were introduced in the glass liner. The reaction block, either the 24-HT reactor block or the visualization reactor, was closed and the lines and the reactor were purged with N$_2$ for 10 min. Each reactor was pressurized with CO$_2$ at 40 bar while keeping the block at room temperature; then, the temperature was increased to 150°C with a rate of 10°C/min. During this process, the pressure inside the reactor increased to 60 bar. Once a stable pressure value was reached, the reactor was filled with CO$_2$ until the selected pressure (80 bar). The reactor was kept under the selected conditions for 3 h with a stirring speed of 900 rpm. After 3 h (t$_{end}$) the stirring speed was decreased to 100 rpm and the reactors were cooled down. The depressurization was started when the carbon dioxide was not anymore under supercritical conditions (T = 40°C, p = 69 bar; these conditions were reached in 4h after the t$_{end}$ when the 24-HT reactor was used and 3 h after t$_{end}$ when the visualization reactor was used). The system was allowed to depressurize until the reactors were at room temperature with an internal pressure < 2 bar (these conditions were reached in further 90 min). It should be noted that the reaction of carbon dioxide with the epoxide is expected to continue, though at a lower rate, during the cooling down and depressurization phases. This does not affect the comparison among the catalysts tested in the 24-HT reactor block, in which each reactor experiences the same temperature and pressure conditions during the whole experiment. For the experiments in the Visualization reactor, care was taken to maintain the same conditions in the cooling down and depressurization phases in the various tests.

In Figure 12 is represented the trend of pressure in function of the time for a typical experiment in the 24-HT reactor block. In particular it describes the experiment of cycloaddition reaction of styreneoxide and carbon dioxide at 80 bar and 150°C

Once the depressurization was complete, the reactor block was opened and the glass liners were directly removed from the block and centrifuged.
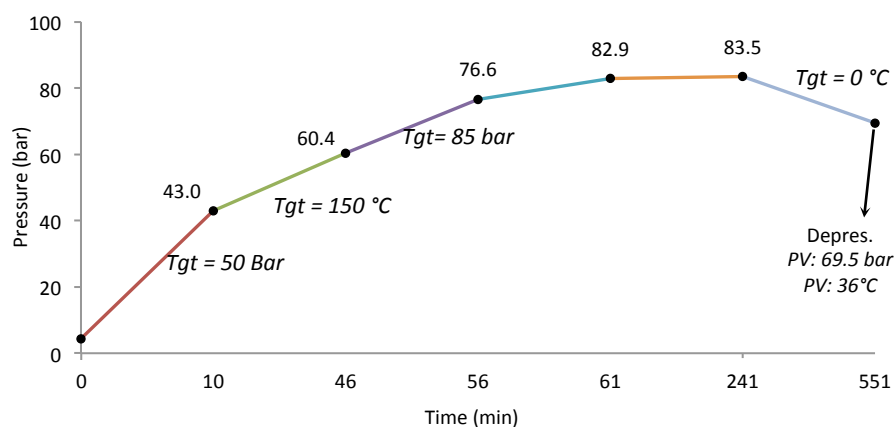
Figure 12. Schematic representations of the values of pressure in function of time for a typical experiment in the supercritical CO$_2$ high-throughput unit. *Reaction conditions*: epoxide (14.02), mesitylene (1.40 mmol), 30 mg of catalyst, CO$_2$ (80 bar), 150 °C, 3h.

The samples were diluted with toluene (in the case of styrene oxide) and with ethyl acetate (in the case of hexane oxide and the others epoxides) and analysed by Gas chromatography (GC) The assignment of peaks due to unknown products was performed by gas chromatography-mass spectrometry analysis (GC-MS). The structures of the products were further identified comparing retention times and fragmentation patterns with those of authentic samples. The reaction mixtures at the end of the catalytic test of selected samples were analysed by ^{1}H NMR to confirm the absence of ionic liquid in the solution and to determine the ratio carbonate/epoxide, which was used to calculate the GC response factor for compounds that are not available commercially (hexene carbonate and cyclohexene carbonate).

3.5 References

1. (a) M. Mikkelsen, M. Jørgensen, F. C. Krebs, *Energy Environ. Sci.* **2010**, *3*, 43-81. (b) T. Sakakura, Jun-Chul Choi, H. Yasuda, *Chem. Rev.* **2007,** *107*, 2365-2387. (c) M. North, R. Pasquale, C. Young, *Green Chem.* **2010**, *12*, 1514-1539. (d) K. M. Yu, I. Curcic, J. Gabriel, S. C. Tsang, *ChemSusChem* **2008**, *1*, 893-899.

2. (a) J. H. Clements, *Ind. Eng. Chem. Res.* **2003,** *42,* 663-674. (b) D. J. Darensbourg, M. W. Holtcamp, *Coordin. Chem. Rev.* **1996**, *153*, 155-174. (c) M. Ratzenhofer, H. Kisch, *Angew. Chem. Int. Ed. Engl.* **1980**, *19*, 317-318. (d) H. Kish, R. Millim, I. Wang, *J. Chem. Ber.* **1986**, *119*, 1090. (e) D. H. Gibson, *Chem. Rev.* 1996, **96**, 2063-2095. (f) J. Sun, S.-I. Fujita, M. Arai, *Journal of Organometallic Chemistry* 690, **2005**, 3490-3497. (g) Xu Xiaoding, J. A. Moulijn, *Energy Fuels* 10, **1996**, 305-325.

3. (a) N. Kihara, N. Hara, T. Endo, *J. Org. Chem.* **1993**, *58,* 6198-6202. (b) T. Zhao, Y. Han, Y. Sun, *Phys. Chem. Chem. Phys.* **1999**, *1,* 3047-3049.

4. (a) A. Barbarini, R. Maggi, A. Mazzacani, G. Mori, G. Sartori, R. Sartorio, *Tetrahedron Lett.* 2003, *44*, 2931-2934*.* (b) M. Shen, W.L. Duan, M. Shi, *Adv. Synth. Catal.* **2003**, *345*, 337-340.

5. (a) T. Yano, H. Matsui, T. Koike, H. Ishiguro, H. Fujihara, M. Yoshihara, T. Maeshima, *Chem. Commun.* **1997**, 1129-1130. (b) K. Yamaguchi, K. Ebitani, T. Yoshida, H. Yoshida, K. Kaneda, *J. Am. Chem. Soc.* **1999**, *121*, 4526–4527. (c) H. Yasuda, L.-N. He, T. Sakakura, *J. Catal.* **2002**, *209,* 547-550. (d) B. M. Bhanage, S. Fujita, Y. Ikushima, M. Arai, *Appl. Catal. A:Gen*. **2001**, *219*, 259-266.

6. (a) E.J. Doskocil, S.V. Bordawekar, B.C. Kaye, R.J. Davis, *J. Phys. Chem. B***, 1999**, *103*, 6277-6282. (b) R. Srivastava, D. Srinivas, P. Ratnasamy, *Catal. Lett.* **2003**, *91*, 133-139. (c) B. M. Bhanage, S. Fujita, Y. Ikushima, K. Torii, M. Arai, *Green Chem.* **2003**, *5*, 71-75.

7. (a) H. S. Kim, J. J. Kim, B. G. Lee, O. S. Jung, H. G. Jang, S. O. Kang, *Angew. Chem. Int. Ed. Engl.* **2000**, *39*, 4096-4098. (b) R. L. Paddock, S. T. Nguyen, *J. Am. Chem. Soc.* **2001**, *123*, 11498-11499.

8. (a) V. I. Parvulescu, C. Hardacre, *Chem. Rev.* **2007**, *107*, 2615-2665. (b) D. Zhao, M. Wu, Y. Kou, E. Min, *Catalysis Today* **2002***, 74,* 157–189 (c) T. Welton, *Chem. Rev.* **1999**, *99*, 2071-2083.

9. J. Peng, Y. Deng, *New J. Chem.* **2001**, *25*, 639-641.

10. W.-L. Dai, S.-L. Luo, S.-F. Yin, C.-T. Au, *Applied Catalysis A: General* **2009**, *366*, 1, 2-12.

11. For a comprehensive review on ionic liquids and dense carbon dioxide: F. Jutz, J.-M. Andanson, A. Baiker, *Chem. Rev.* **2011**, *111*, 322-353.

12. (a) T. Seki, J.-D. Grunwaldt, A. Baiker, *J. Phys. Chem. B* **2009**, *113*, 114-122. (b) J. H. Clements, *Ind. Eng. Chem. Res.* **2003**, *42,* 663-674.

13. (a) C. P. Mehnert, R. A. Cook, N. C. Dispenziere, M. Afeworki, *J. Am. Chem. Soc.* **2002**, *124*, 12932-12933.

14. A. Riisager, R. Fehrmann, M. Haumann, P. Wasserscheid, *Eur. J. Inorg. Chem.* **2006**, 695-706.

15. (a) P. D. Stevens, J. Fan, H. M. R. Gardimalla, M. Yen, Y. Gao, *Org. Lett.* **2005**, *7*, 2085-2087. (b) A. Taher, J.-B. Kim, J.-Y. Jung, W.-S. Ahn, M.-J. Jin, *Synlett* **2009**, 2477-2482. (c) M. Gruttadauria, L. F. Liotta, A. M. P. Salvo, F. Giacalone, V. La Parola, C. Aprile, R. Noto, *Adv. Synth. Catal.* **2011**, *353*, 2119-2130.

16. C. Aprile, F. Giacalone, P. Agrigento, L. F. Liotta, J. A. Martens, P. P. Pescarmona, M. Gruttadauria, *ChemSusChem*, **2008**, 4, 1830-1837.

17. P. P. Pescarmona, J. C. van der Waal, I. E. Maxwell, T. Maschmeyer, *Catal. Lett.* **1999**, *63*, 1-11.

18. W. F. Maier, K. Stöwe, S. Sieg, *Angew. Chem. Int. Ed.* **2007**, *46*, 6016-6067.

19. (a) H. Kawanami, A. Sasaki, K. Matsui, Y. Ikushima, *Chem Comm*, **2003**, 896-897. (b) D.-W. Park, N.-Y. Mun, K.-H. Kim, I. Kim, S.-W. Park, *Catalysis Today*, **2006**, *115*, 130-133

20. (a) Y. Xie, Z. F. Zhang, T. Jiang, J. L. He, B. X. Han, T. B. Wu, K. L. Ding, *Angew. Chem. Int. Ed.* **2007**, *46*, 7255-7258. (b) W.-L. Dai, L. Chen, S. F. Yin, W.-H. Li, Y.-Y. Zhang, S. L. Luo, C. T. Au, *Catal. Lett.* **2010**, *137*, 74-80. (c) J.-Q. Wang, X.-D. Yue, F. Cai, L.-N. He, *Catal. Commun.* **2007**, *8*, 167-172. (d) T. Takahashi, T. Watahiki, S. Kitazume, H. Yasuda, T. Sakakura, *Chem. Commun.* **2006**, 1664-1666.

21. S. Brunauer, P. H. Emmett, E. Teller, *J. Am. Chem. Soc.* **1938**, *60*, 309-319.

22. E. P. Barrett, L. G. Joyner, P.-J. Halenda, *J. Am. Chem. Soc.* **1951**, *73*, 373-380.

23. T. Kida, A. Kikuzawa, H. Higashimoto, Y. Nakatsuji, M. Akashi, *Tetrahedron* **2005**, *61*, 5763-5768.

Chapter 4

Magnetic Nanoparticles Supported Ionic Liquid Phases

Highly Versatile and Recyclable New Catalytic System
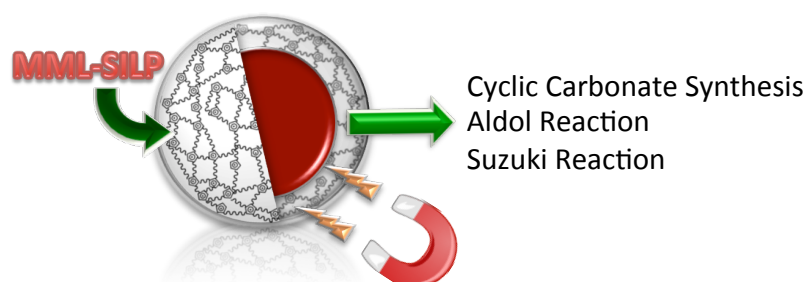
Magnetic nanoparticles supported ionic liquid were synthesized using a simple reaction between an excess of bis-vinylimidazolium salts and iron oxide magnetic nanoparticles in the presence of azoisobutyronitrile (AIBN). This straightforward synthetic approach allowed the obtainment of high loaded imidazolium salts frameworks in presence of magnetic nanoparticle. The versatility of materials was demonstrated in three different kinds of reactions. The material is recyclable and reusable at least for four cycles with good results especially in the case of aldolic reaction of 4-nitrobenzaldehyde and acetone. The catalytic activity of the new materials was tested in the addition of carbon dioxide to propylene oxide to produce the five members cyclic carbonate without any solvent. This catalyst can be easily recovered and recycled in consecutive catalytic runs without loss of activity.

4.1   *Introduction*

In recent years, ionic liquids (ILs) have received a lot of interest owing to their unique features such as negligible vapor pressure, non-flammability, good solvating ability, variable polarity and recyclability.[1] The large number of possible cations and anions combination allow the synthesis of tailor-made ionic liquids that can be useful for various functional applications.[2] Specially ionic liquid have shown great potential as catalyst.[3] In this context, a great deal of attention has been paid to the synthesis, design and application of supported ionic liquid materials.[4]

As it was mentioned in the chapter 3, supported ionic liquid phase (SILP) have gained considerable attention. The SILP involves the presence of support material that is modified with a layer of ionic liquid[5] (see Figure 1 and Chapter 3).
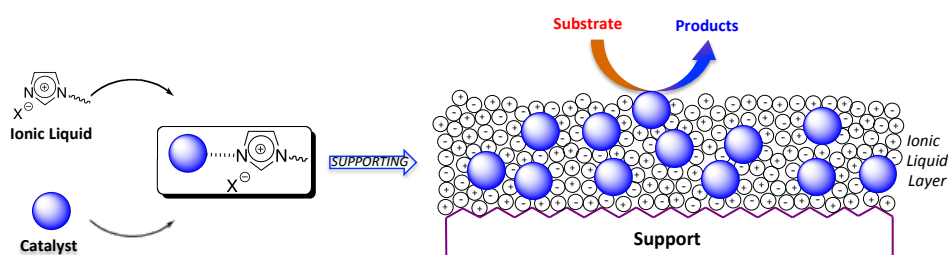

Figure 1. Supported ionic liquid materials

Several examples have been reported, and both organic polymers, such as polystyrene, and inorganic matrices, such as silica, have been frequently employed as the solid support.[6] Therefore, ionic liquid phases have been supported on silica gel by adsorption, sol-gel method, grafting on a preformed silica gel, polymerization, encapsulation or pore trapping.[7]

During the last decade, magnetic nanoparticles have been widely studied for various catalytic applications.[8] In particular the steps of separation and recycling are essential in catalytic technology and frequently affect the overall process economy. A possible solution of these steps is offered by magnetic nanoparticle derived catalysts.[9] They have been employed in such industrially important reaction as hydrogenation, hydroformylation, Suzuki-Miyaura and Heck coupling, and olefin metathesis.[10] In addition, to metal-base catalysts, organocatalysts have also been immobilized on magnetic nanoparticles.[10] These hybrid nanocomposite materials have sometimes-superior properties compared to conventional catalysts.

This chapter describes a new class of material in which the advantage of supported ionic liquid are combined with those of magnetic nanoparticles. The new concept of magnetic nanoparticles supported ionic liquid involves a multi-layered of ionic liquid supported on magnetic nanoparticles. Iron oxide

nanoparticles were chosen for use as magnetic supports since they can be readily prepared by flame synthesis.

These new materials, which contain a highly cross-linked polymeric network, have been denoted as magnetic multi-layered supported ionic liquid phase (MML-SILP). They are very versatile materials, and have been used to immobilize both the organocatalyst L-proline, for asymmetric aldolic reaction, and the metal palladium catalyst for Suzuki and Heck coupling reactions. Finally the catalytic activity of the new materials was tested in synthesis of cyclic carbonate. In all the case good catalytic activity and recyclability was observed.

## 4.2   *Results and Discussion*

New materials bases on the concept of Magnetic multi-layered supported ionic liquid phase (MML-SILP) were developed. These materials were easily prepared via polymerization reaction of suitable bis-vinylimidazolium salt (**1-3**) in the presence of magnetic nanoparticles. The synthesis of the MML-SILP was carried out employing iron oxide nanoparticles. These magnetic materials were produced from flame spray pyrolysis of iron acetylacetonate in xylene/acetonitrile solutions and the resulting aerosol was *in situ* coated with silicon dioxide by oxidation of swirling hexamethyldisiloxane vapour. In this study two different kinds of magnetic nanoparticles were used: pure Fe_2O_3 and 23 wt % SiO_2-coated Fe_2O_3.

As bis-vinylimidazolium salts, the 3,3'-(1,4-phenylenebis(methylene))bis(1-vinyl-1H-imidazol-3-ium) dibromide (**1**) or dichloride (**2**), and 1,4-Bis(3-vinylimidazolium-1-yl) bromide (**3**) were used. These are easily obtained by reaction between 1-vinylimidazole and 1,4-bis(chloromethyl)benzene, 1,4-bis(bromomethyl)benzene and 1,4-dibromobutane, respectively (see chapter 3).

The overall synthesis of the catalytic materials is represented in Scheme 1. This straightforward approach involves the radical polymerization of an excess of bis-vinylimidazolium salt in the presence of magnetic nanoparticles, using azobis(isobutyronitrile) (AIBN) as radical initiator in refluxing ethanol. In Figure 2 are reported two schematic representations of the obtained materials.
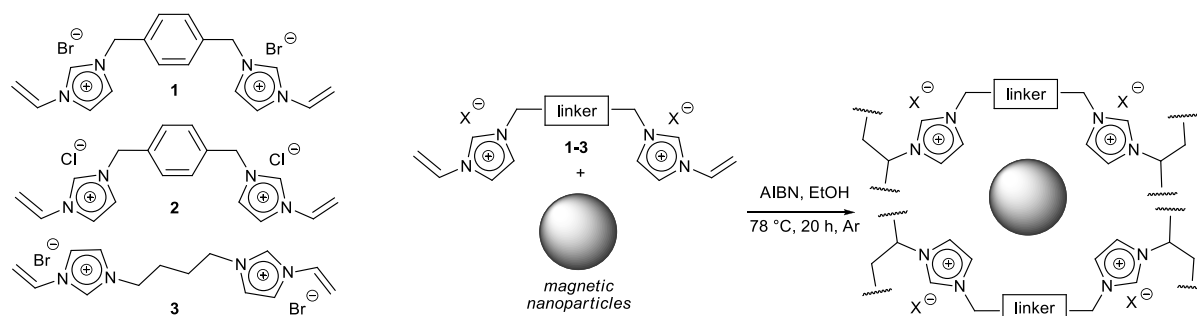
Scheme 1. Synthesis of highly cross-linked imidazolium network on magnetic nanoparticles and schematic representation of the final materials. The wavy lines in the scheme symbolize further connection by cross-linking to other bis-imidazolium unit.
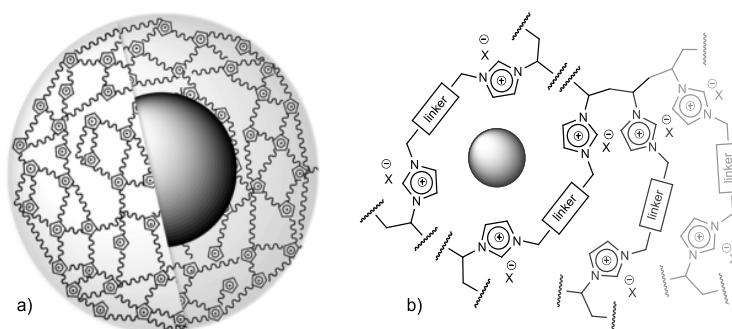
Figure 2. Two schematic (*a* and *b*) representations of MML-SILP materials showing the entrapment of magnetic nanoparticles and their multi-layer nature.

The new catalytic system consists of an oligomeric network of imidazolium unit as a multi-layered ionic liquid phase in the presence of magnetic nanoparticles. The synthetic approach allowed the preparation of a high loaded imidazolium salts framework on the surface of magnetic nanoparticles. The materials prepared using 23 wt % SiO_2-coated Fe_2O_3 as magnetic support and the bis-vinyl imidazolium salts **1-3** were denoted as **MML-SILP$_1$, MML-SILP$_2$, MML-SILP$_3$**. The materias prepared using pure Fe_2O_3 and bis-vinyl imidazolium **3** were called **MML-SILP$_4$ and MML-SILP$_5$.** The latter material was prepared using a higher amount of pure Fe_2O_3, respectively 50 and 200 mg for **MML-SILP$_4$** and **MML-SILP$_5$**. In Table 1 are shown all the experimental conditions for the synthesis of MML-SILP materilas.

**Table 1.** Experimental condition for the synthesis of MML-SILP [a]
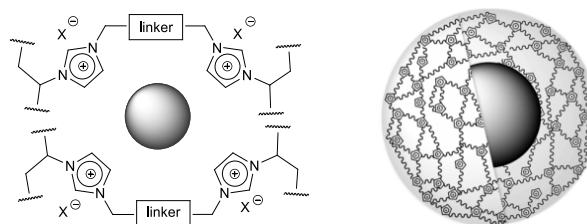
Name	Support[b]	Support (gr)	Linker	Halide	Ethanol (mM)	MML-SILP gr[c]
MML-SILP$_1$	Fe_2O_3 23wt% SiO_2	0.050	p-C_2H_4-C_6H_4	Br	404	1.025
MML-SILP$_2$	Fe_2O_3 23wt% SiO_2	0.050	p-C_2H_4-C_6H_4	Cl	130	0.942
MML-SILP$_3$	Fe_2O_3 23wt% SiO_2	0.050	C_4H_8	Br	130	0.890
MML-SILP$_4$	Fe_2O_3	0.050	C_4H_8	Br	130	0.822
MML-SILP$_5$	Fe_2O_3	0.200	C_4H_8	Br	130	1.123

[a] Reaction Condition: magnetic nanoparticles (indicated amount), the bis-vynilimidazolium salt (2.75 mmol) AIBN (40 mg) and ethanol, 78°C, 20 h. [b] The silica content in the product powder is defined as $m_{SiO_2} / (m_{Fe_2O_3} + m_{SiO_2})$. [c] it is the amount of final material after dried under vacuum for 2 hours at 40 °C.

These materials were tested in different applications: (*i*) as support for the L-proline organocatalyst; (*ii*) as support for palladium nanoparticles, in particular this material was used for Suzuki and Heck reaction; (iii) in the cycloaddition of propylene oxide to carbon dioxide to give cyclic carbonate.

4.2.1   *Magnetic Nanoparticles Supported L-Proline*

In order to test the catalytic activity of new materials based on multilayer supported ionic liquid phase, L-proline has been supported, by adsorption, onto the surface of modified magnetic nanoparticles, **MML-SILP$_1$** (Schema 2).
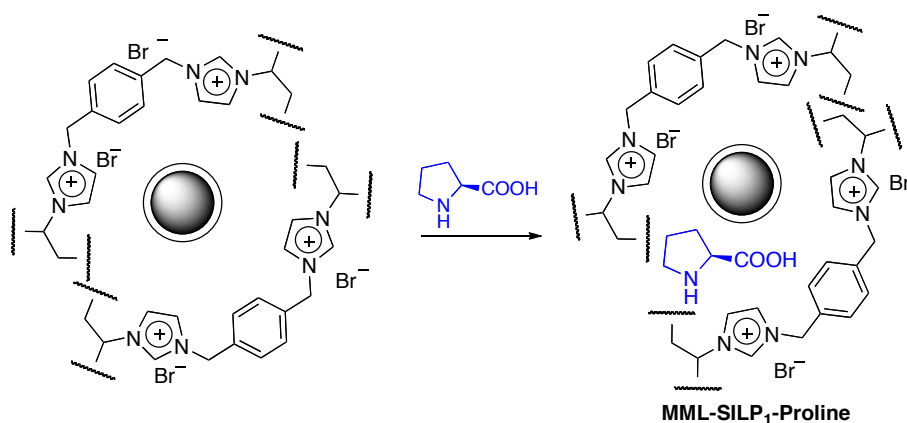
MML-SILP₁-Proline

Schema 2. Schematic representation of L-proline adsorbed
into Magnetic multi-layered supported ionic liquid phase

The resulting material **MML-SILP₁-Proline** was employed in the asymmetric aldol reaction. The reaction was carried out by mixing the supported L-proline (30 mol%) with acetone and 4-nitrobenzaldehyde at room temperature for 3.5 h. The supported proline gave the aldol product in 90% yield and 69% ee (Table 2, entry 1). Then the reuse of the supported proline was investigated.

Table 2. Aldol reaction between acetone and substituted
para-nitrobenzaldehyde and recycling studies

Entry	Cycle	Yield [b] (%)	ee [c] (%)
1	1	90	69
2	2	90	69
3	3	90	60
4	4	70	69
5[d]	5	90	70

[a] Reaction condition: Acetone (2mL), p-nitrobenzaldehide (0.5 mmol), catalyst (30 mol %), r.t., 3.5 h. [b] Isolated yield. [c] Determined by chiral HPLC, (R) configuration. [d] after regeneration

After the reaction, the catalyst was concentrated on the sidewall of the reaction vessel using an external magnet (Figure 2), the organic phase was separated by decantation, concentrated *in vacuo* and analyzed by ¹H NMR and HPLC on chiral column to get the aldolic yield and the enantiomeric excess (ee). The residual catalyst in the reaction vessel was washed and dried and then subjected to the next run directly. Each cycle gave the same ee value and yield, the material was easy recovered, and reused in four consecutive runs with reproducible results (Table 2).

Figure 2. Magnetic separation and recycling of the MML-SILP-Proline

Noteworthy, good yield and enantioselectivity, compared with the parent homogenous catalyst were obtained. In the fourth cycle a decrease in yield was observed, probably due to a leaching of proline. However, the catalytic material can be regenerated after washing with methanol, drying and recharging with fresh proline. Indeed, in the fifth cycle activity was restored. Therefore the most advantageous feature of this new catalytic material is the easy and rapid separation by external magnet and the possibility to use the support in several consecutive cycles.

4.2.2 *Palladium Nanoparticles for Suzuki Reaction.*

In order to develop a supported metal nanoparticles species the material **MML-SILP$_1$** was used for palladium immobilization. An aqueous solution of Na$_2$PdCl$_4$ was stirred with the starting material. Water was removed and Pd^{2+} reduced with NaBH$_4$ in ethanol. This approach allowed the immobilization of Palladium (Schema 2).
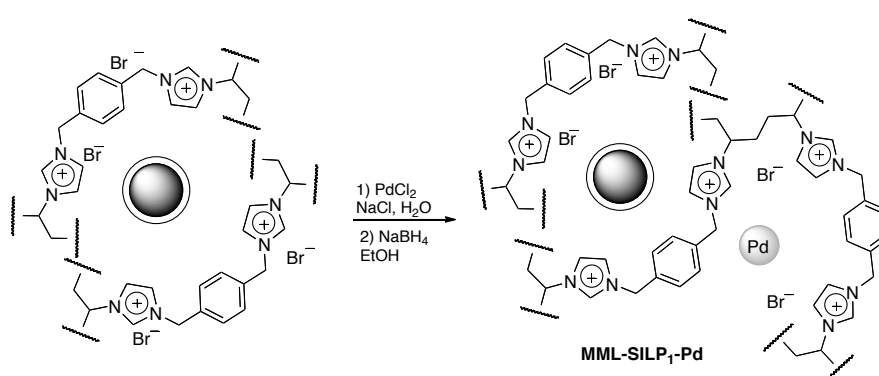
Schema 3. Synthesis of supported Palladium nanoparticles species and schematic representation of magnetic multilayered supported ionic liquid phase Palladium nanoparticles

The catalytic material **MML-SILP$_1$-Pd** was used in several Suzuki reactions in 0.1 mol % at 50 °C in EtOH/H$_2$O affording biphenyls in good yields (see Table 3). It is noteworthy to stress that, because of the

high loading of Pd, we needed only 1 mg of catalyst (reactions were carried out in 1 mmol scale) and this is useful for large scale synthesis.
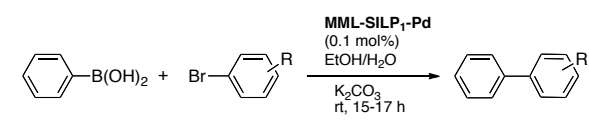
Table 3. Suzuki reactions between phenylboronic acid and aryl bromides catalyzed by MML-ILP-Pd[a]

Entry	R	Isolated yield (%)
1	4-CHO	95
2 [b]	4-CHO	85
3	4-OMe	84
4	3,5-(CF$_3$)$_2$	65
5 [c]	4-Me	72
6 [c]	1-naphthyl	92

[a] Reaction Condition: catalyst MML-ILP-Pd (0.1 mol %), phenylboronic acid (0.5 mmol), K$_2$CO$_3$ (0.6 mmol), aryl bromid (0.55 mmol), ethanol (0.6 mL) and water (0.6 mL).

In addition the Catalyst **MML-ILP-Pd** was used in the Heck reaction between 4-iodoanisole and methyl acrylate in DMF/H$_2$O 4/1 at 90 °C using 1 mg of catalyst (0.1 mol%). Product was isolated in 98% yield (Schema 3).
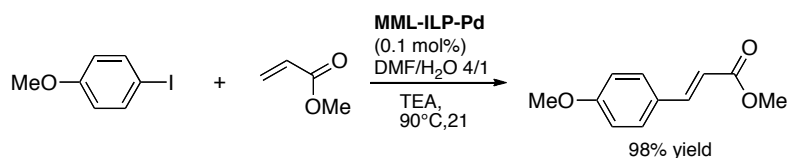
Schema 4. Heck reaction using supported Palladium nanoparticles.

The Palladium catalyst-magnetic nanoparticles are used in rather low amount (only 0.1 mol %), meaning that efforts in catalyst reuse are not crucial.

4.2.3 *Catalysts for Conversion of Epoxides to Cyclic Carbonates*

Since multi-layered covalently supported ionic liquid phase (mlc-SILP) materials were tested as heterogeneous catalysts for the addition of carbon dioxide to various epoxide to yield cyclic carbonate, it was investigated the catalytic activity of these new nanocomposite catalysts for the cyclic carbonates synthesis. Among different carbonate, Propylene carbonate (PC) has attached much attention recently, since it could be used as electrolytic element of lithium secondary batteries, polar aprotic solvent,

intermediates for organic and polymeric synthesis, and ingredients for pharmaceutical/fine chemicals in biomedical applications.[11] In a typical procedure the autoclave glass inset was charged with catalyst and epoxide, using a temperature of 120 °C and a pressure of 40 bar, for 8 h. The results are reported in Table 4 and are the mean values of duplicate experiments. The reported yields were reproducible within ± 2 %.

**Table 4.** Addition of CO_2 to propylene oxide in the presence of MML-ILP

Entry	Catalyst	Yield (%)[b]	TON[c]
1	MML-SILP$_1$	21	9
2	MML-SILP$_2$	42	17
3	MML-SILP$_3$	22	9
4	MML-SILP$_4$	37	15
5	MML-SILP$_5$	42	17
6	No catalyst	0	0

[a] Reaction conditions: 1 mL propylene oxide (14.3 mmol), 30 bar CO_2 (at 20 °C, ca. 17 mL autoclave, ca. 24 mmol), 2.5 mol-% catalyst (based on the imidazolium units), 120 °C (8h), ~900 rpm stirring, 50 mg biphenyl (applied after the reaction). [b] Determined by GC using an internal standard techinique. [c] Based on the halide ions

As expected on the basis of the accepted reaction mechanism,[12] supported ionic liquids in which the counter ion is represented by bromide provide a higher epoxide conversion than those containing chloride. These differences reflect the nucleophilicity order of the anions.

Among the ILs with butyl linker, the purely Fe_2O_3 supported catalyst (entry 4 and 5), gave higher conversion than those with mixed Fe_2O_3/SiO_2. The TON remained almost constant even at higher loading.

After these preliminary results the reusability of the new materials was investigated. Therefore, the recycling tests were performed on the most active supported ionic liquid catalyst, MML-SILP$_5$ using the same reaction condition. At the end of each cycle, the catalyst was easily separated from the product by exposure to an external magnet and decantation of the reaction solution. The remaining magnetic nanoparticles were further washed with ethyl acetate and dried and subjected to the next run. In the first run the catalyst gave 46% yield of propylene carbonate. In the second cycle the yield slowly decrease to 41% but then stabilized in the following run, 46 and 48% respectively in the third and fourth cycle (Figure 3).
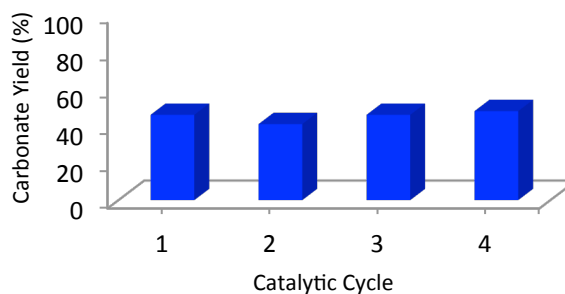
Figure 3. Recycling experiment of material as catalyst for the cycloaddition of carbon dioxide to propylene oxide.

Figure 3 shows the performance of the catalyst, the magnetic multi-layered supported ionic liquid phase (MML-ILP) can be reused up to four runs without any significant loss of activity.

4.3   *Conclusion*

Five new magnetically recyclable and efficient nanocomposite catalysts have been described. These new class of materials combined the advantage of supported ionic liquid with that of magnetic nanoparticles. Iron oxide nanoparticles were chosen for use as magnetic supports since they could be readily prepared by flame synthesis.

The materials, which contain a highly cross-linked polymeric network, have been denoted as Magnetic multi-layered supported ionic liquid phase (MML-SILP). They are very versatile materials and have been used to immobilize an organocatalyst. Therefore, L-proline was adsorbed in the magnetic nanocomposite material and used for asymmetric aldolic reaction between acetone and 4-nitrobenzaldehyde. The catalytic system gave the aldol products in good yield and stereoselectivity. In addition the materials was reused for five times without loss of catalytic activity and stereosectivity.

The materials appeared also to be interesting support for Pd immobilization. The palladium magnetic nanoparticles displayed good activity allowing the synthesis of different set of biphenyl compounds in high yield working with only 0.1 mol % of Pd loading at low temperature.

The catalytic activity of the new materials was tested as heterogeneous catalyst for the addition of carbon dioxide to propylene oxide to produce the five memberes cyclic carbonate without any solvent. The best catalyst identified was prepared by supporting a bromide bis-imidazolium salt on 23 wt% SiO_2-coated Fe_2O_3. This catalyst can be easily recovered and recycled in consecutive catalytic runs without loss of activity.

Finally, although the data presented in this chapter could be further developed since many parameters can be changed. In fact this simple synthetic route can be used to support other ILs on different magnetic nanoparticles to prepare novel magnetic nanocomposite catalyst system, which are stable and can find applications in many other important catalytic process.

4.4 *Experimental part*

Preparation of iron oxide nanoparticle by flame spray pyrolysis

Silica-coated iron oxide nanoparticles with different silica contents were prepared by flame spray pyrolysis (FSP) and characterized as described by Teleki *et al.*[13] The silica content was varied between 0 23 wt% SiO_2. Precursor solutions, in all cases 0.34 M in total Fe metal concentration, were fed at 5 mL/min and dispersed by 5 L/min O_2 (Pan Gas, purity >99%). The synyhesis and characterization of flame made nanoparticles is described in the experimental part of chapter 2.

General Procedure for the synthesis of bis-vinylimidazolium salts 1-3

The procedures to prepare the salts 1-3 were similar to that reported.[7t-u] Thus, a solution of compound 2 (0.01 mol) and 1-vinylimidazole (0.021 mol) in toluene (10 mL, in the case of compounds 2a-2b) and in chloroform (5mL, in the case of compound 2c-2g) was heated at reflux for 24 h in an oil bath at 90°C and 50°C (respectively for the toluene and chloroform solution) with magnetic stirring. After cooling at room temperature, the mixture was filtered and washed several times with diethyl ether; the solid product was dried at 40 °C.

Dibromide salt 1: White powder. Yield >95%; mp >250 °C. ^{1}H NMR (300 MHz, CD_3OD) δ: 5.46 (2H, dd, J = 7.3 and 3.2 Hz, *cis*-CH=CH$_2$), 5.55 (4H, s, CH$_2$Ph), 5.96 (2H, dd, J = 18.8 and 3.2 Hz, *trans*-CH=CH$_2$), 7.30 (2H, dd, J = 18.8 and 7.3 Hz, CH=CH$_2$), 7.61 (4H, s, Ph), 7.78 (2H, d, J = 2.1 Hz, 4-H or 5-H), 8.05 (2H, d, J = 2.1 Hz, 4-H or 5-H), 9.50 (2H, s, 2-H). ^{13}C NMR (CD_3OD) δ: 53.8, 110.3, 121.1, 124.5, 129.8, 130.9, 136.1, 136.7. IR (nujol) ν_{max}/cm^{-1}: 730, 766, 927, 966, 1161, 1550. [Found: C, 47.9; H, 4.5; Br, 35.3; N, 12.4. $C_{18}H_{20}Br_2N_4$ requires C, 47.8; H, 4.4; Br, 35.3; N, 12.4].

Dichloride salt 2: White powder. Yield >95%; mp >250 °C. ^{1}H NMR (300 MHz , CD_3OD) δ: 5.47 (2H, dd, J = 8.7 and 2.7 Hz, *cis*-CH=CH$_2$), 5.58 (4H, s, CH$_2$Ph), 5.99 (2H, dd, J = 15.6 and 2.7 Hz, *trans*-CH=CH$_2$), 7.33 (2H, dd, J = 15.6 and 8.7 Hz, CH=CH2), 7.63 (4H, s, Ph), 7.81 (2H, d, J = 1.8 Hz, 4-H or 5-H), 8.09 (2H, d, J = 1.8 Hz, 4-H or 5-H), 9.57 (2H, s, 2-H). ^{13}C NMR (CD_3OD) δ: 53.8, 110.1, 121.0. 124.4, 129.8, 130.9, 136.1,

136.7. IR (nujol) ν_{max}/cm^{-1}: 724, 750, 930, 962, 1162, 1547. [Found: C, 59.6; H, 5.4; Cl, 19.6; N, 15.5. $C_{18}H_{20}Cl_2N_4$ requires C, 59.5; H, 5.5; Cl, 19.5; N, 15.4].

Dibromide salt 3: White powder; yield: 83%; mp 147°C. ^{1}HNMR (300MHz, CD_3OD): d=1.92–1.96 [4H, m, CH_2 $(CH_2)_2CH_2$], 4.26–4.31 [4H, m, $CH_2(CH_2)_2CH_2$], 5.34 (2H, dd, J=8.7 and 2.7Hz, cis-CH=CH_2), 5.85 (2H, dd, J=15.6 and 2.7Hz, trans-CH=CH_2), 7.18 (2H, dd, J=15.6 and 8.7 Hz, CH=CH_2), 7.73 (2 H, d, J = 1.9 Hz, 4-H or 5-H), 7.92 (2H, d, J=1.9 Hz, 4-H or 5-H), 9.37 (2H, s, 2-H); ^{13}C NMR (CD_3OD): δ=27.7, 50.4, 110.1, 120.9, 124.5, 129.9, 136.6; [Found: C 41.7, H 5.1, Br 39.3, N 13.7; $C_{14}H_{20}Br_2N_4$ requires C 41.6, H 4.9, Br 39.5, N, 13.8].

Synthesis of SILP-encapsulated magnetic nanoparticles

The materials were prepared by radical polymerization. In a typical synthesis, the magnetic nanoparticles, the bis-imidazolium salt AIBN and ethanol (see Table 1 for the amount of magnetic nanoparticle and other chemicals) were placed in a three-necked round bottom flask. The suspension was degassed by bubbling argon for 10 minutes and the reaction mixture was magnetically stirred under argon. The flask was heated to 78°C to favour the dissolution of the bis-imidazolium salt. The mixture was stirred for 20 h. After cooling down to room temperature, the reaction vessel was then placed over a permanent magnet until the reaction suspension became transparent and the liquid was then decanted. The suspension was then washed using methanol and dichloromethane and finally dried under vacuum for 2 hours at 40 °C.

General Procedure for the Supported Proline Materials

In a round-bottom flask L-proline (17.5 mg, 0.15 mmol) were dissolved in methanol (2 mL). To this solution the modified magnetic nanoparticles was added (100 mg). The mixture was shaken for few minutes then evaporated under reduced pressure for 25 h to give a light brown powder.

General procedure for aldol reaction

A solution of p-nitrobenzaldehyde (0.5 mmol) in acetone (2 mL) was added to supported proline material system (L-proline 30% mol). The mixture was stirred at room temperature for 24 h. After this time, the reaction vessel was then placed over a permanent magnet until the reaction suspension became transparent and the liquid was then decanted. The liquid solution was evaporated, checked by ^{1}H NMR and finally purified by chromatography (light petroleum/ethyl acetate) to give the aldol product. The catalytic system was dried for a few minutes and then reused.

General Procedure for the Synthesis of the Palladium Catalyst Material

In a round-bottom flask were placed $PdCl_2$ (95mg, 0.536 mmol), NaCl (626 mg, 10.72 mmol, 20 equiv.) and water (13.6mL). The flask was heated at 80°C until the $PdCl_2$ was dissolved. This clear reddish solution was cooled at room temperature and added to a suspension of MML-SILP$_1$ (500 mg) in water (4.5 mL). The suspension was stirred at room temperature for 20 h, then filtered under reduced pressure, washed with water and dried overnight under reduced pressure at room temperature.

The material was suspended in ethanol (12 mL) and to this suspension a solution of $NaBH_4$ (142 mg, 3.75 mmol, 7 equiv.) in ethanol (12 mL) was added dropwise. The suspension turned black and it was stirred at room temperature for 6 h, then filtered under reduced pressure, washed with water and dried overnight under reduced pressure at room temperature

Typical Procedure for the Suzuki Reaction

In a round-bottom flask catalyst (0.1 mol %), phenylboronic acid (61 mg, 0.475 mmol), K_2CO_3 (83.6 mg, 0.6 mmol, 1.27equiv.), the aryl bromide (0.55mmol), ethanol (0.6mL) and water (0.6mL) were placed. The reaction mixture was stirred at 50°C. After 19 h, the solvent was removed under reduced pressure and the residue was checked by ^1H NMR to calculate the conversion and purified by column chromatography.

General Procedure for Synthesis of Carbonates

In a typical synthesis, the 17 mL autoclave glass inset was charged with catalyst and epoxide. The autoclave was sealed and cooled with liquid N_2 to ca. -30 ˚C after which the atmosphere was replaced three times with CO_2. The reactor was then heated to ca. 20 ˚C and charged with the desired pressure of CO_2. The reaction was started by stirring and initializing reactor heating. Note that it took ca. 2 h to reach the desired reaction temperature of 120 ˚C (pressure was ca. 40 bar). After the desired reaction time, the reactor was removed from the heater and allowed to cool down to RT. Using liquid N_2, the reactor was cooled down to ca. – 30 ˚C and vented slowly. The interior of the reactor and the rubber O-rings were carefully washed with acetone to extract all products and biphenyl was added to the solution as an internal standard. Product yields were determined by GC analysis (model: HP 6950, HP-5 column). The reaction conditions are similar to and were adapted from Zhang *et al.*[14]

At the end of each cycle, the material was easily separated from the product by exposure to an external magnet and decantation of the reaction solution. The remaining magnetic nanoparticles were further washed with (ethyl acetate?) and dried and subjected to the next run.

4.5 *Reference*

1. (a) T. Sakakura, J. C. Choi, H. Yasuda, *Chem. Rev.* **2007**, *107*, 2365-2387. (b) W. L. Dai, S. F. Yin, C. T. Au, *Appl. Catal. A: Gen.* **2009**, *366*, 2-12. (c) J. J. Peng, Y. Q. Deng, *New. J. Chem.* **2001**, *25*, 639-641. (d) H.S. Kim, J.J. Kim, H. Kim, H.G. Jang, *J. Catal.* **2003**, *220*, 44-46. (e) H. Kawanami, A. Sasaki, K. Matsui, Y. Ikushima, *Chem. Commun.* **2003**, 896-897. (f) J. M. Sun, S. I. Fujita, F. Y. Zhao, M. Arai, *Green Chem.* **2004**, *6*, 613-616. (g) F. W. Li, L. F. Xiao, C. G. Xia, B. Hu, *Tetrahedron Lett.* **2004**, *45*, 8307-8310. (h) J. Palgunadi, H. S. Kim, *Catal. Today* **2004**, *98*, 511-514. (i) Y. J. Kim, R. S. Varma, *J. Org. Chem.* **2005**, *70*, 7882-7891. (l) J.Sun, S. J. Zhang, *Tetrahedron Lett.* **2008**, *49*, 3588-3591. (m) Y. X. Zhou, S. Q. Hu, X. M. Ma, S. G. Liang, T. Jiang, B. X. Han, *J. Mol. Catal. A: Chem.* **2008**, 284, 52-57. (n) J. Sun, J. Y. Ren, S. J. Zhang, W. G. Cheng, *Tetrahedron Lett.* **2009**, *50*, 423-426.

2. (a) K. Fukumoto, H. Ohno, *Chem. Commun.* **2006**, 3081-3083. (b) D. M. Li, F. Shi, S. Guo, Y. Q. Deng, *Tetrahedron Lett.* **2004**, *45*, 265-268. (c) G. H. Tao, L. He, N. Sun, Y. Kou, *Chem. Commun.* **2005**, 3562-3564. (d) S. Anjaiah, S. Chandrasekhar, R. Gree, *Tetrahedron Lett.* **2004**, *45*, 569-571. (e) S. G. Lee, *Chem. Commun.* **2006**, 1049-1063. (f) P. B. Webb, M. F. Sellin, T. E. Kunene, S. Williamson, A. M. Z. Slawin, D. J. Cole -Hamilton, *J. Am. Chem. Soc.* **2003**, *125*, 15577-15588.

3. (a) J. A. Boon, J. A. Levinsky, J. L. Pflug, J. S. Wilkes, *J. Org. Chem.* **1986**, *51*, 480-483. (b) V. V. Namboodiri, R. S. Varma, *Chem. Commun.* **2002**, 342-343. (c) T. Welton, *Coord. Chem. Rev.* **2004**, *248*, 2459-2477. (d) J. M. Xu, B. K. Liu, W. B. Wu, C. Qian, Q. Wu, X. F. Lin*, J. Org. Chem.* **2006**, *71*, 3991-3993. (e) S. Z. Luo, X. L. Mi, L. Zhang, S. Liu, H. Xu, J. P. Cheng, *Angew. Chem.* **2006**, *118*, 3165-3169. *Angew. Chem. Int. Ed.* **2006**, *45*, 3093-3097.

4. A. Riisager, R. Fehrmann, M. Haumann, P. Wasserscheid, *Eur. J. Inorg. Chem.* **2006**, 695-706.

5. C. P. Mehnert, R. A. Cook, N. C. Dispenziere and M. Afeworki, *J. Am. Chem. Soc.* **2002**, *124*, 12932-12933.

6. For example, see: (a) R. T. Carlin, J. Fuller, *Chem. Commun.* **1997**, 1345-1346. (b) M. H. Valkenburg, C. DeCastro, W. F. H lderich, *Green Chem.* **2002**, *4*, 88-93 (c) M. H. Valkenburg, C. DeCastro, W. F. Hölderich, *Appl. Catal*. A, **2001**, *215*, 185-189. (d) C. DeCastro, E. Sauvage, M. H. Valkenburg, W. F. Hölderich, *J. Catal.* **2000**, *196*, 86-94. (e) C. P. Mehnert, E. J. Mozeleski, R. A. Cook, *Chem. Commun.* **2002**, 3010-3011. (f) A. Riisager, K. M. Eriksen, P. Wasserschied, R. Fehrmann, *Catal. Lett.* **2003**, *90*, 149-153. (g) R. Sebesta, I. Kmentova, S. Toma, *Green Chem.* **2008**, *10*, 484-496. (h) D. Q. Xu, S. P. Luo, Y. F. Wang, A. B. Xia, H. D. Yue, L. P. Wang, Z. Y. Xu, *Chem. Commun.* **2007**, 4393-4395. (i) D.-Q. Xu, L.-P. Wang, S.-P. Luo, Y.-F. Wang, S. Zhang, Z.-Y. Xu, *Eur. J. Org. Chem*. **2008**, 1049-1053. (l) P. Li, L. Wang, Y. Zhang, G. Wang, *Tetrahedron* **2008**, *64*, 7633-7638. (m) P. Li, L. Wang, Y. C. Zhang, *Eur. J. Org. Chem.* **2008**, 1157-1160. (n) H.-L. Shim, M.-K. Lee, K.-H. Kim, D.-W. Park, S.-W. Park, *Polym. Adv. Technol.* **2008**, *19*, 1436-1440.

7. Selected examples: (a) Y. Gu, G. Li, *Adv. Synth. Catal.* **2009**, *351*, 817-847. (b) A. Riisager, R. Fehrmann, S Flicker, R. van Hal, M. Haumann, P. Wasserscheid, *Angew. Chem.* **2005**, *117*, 826-830. (c) M. Haumann, A. Riisager, *Chem. Rev.* **2008**, *108*, 1474-1497. (d) C. Aprile, F. Giacalone, M. Gruttadauria, A. Mossuto Marculescu, R. Noto, J. D. Revell, H. Wennemers, *Green Chem.* **2007**, *9*, 1328-1334. (e) M. Gruttadauria, S. Riela, C. Aprile, P. Lo Meo, F. D'Anna, R. Noto, *Adv. Synth. Catal.* **2006**, *348*, 82-92. (f) A. Riisager, P. Wasserscheid, R. van Hal, R. Fehrmann, *J. Catal.* **2003**, *219*, 452-455. (g) U. Kernchen, B. Etzold, W. Korth, A. Jess, *Chem. Eng. Technol.* **2007**, *30*, 985-994. (h) P. Virtanen, T. O. Salmi, J.-P. Mikkola, *Top. Catal.* **2010**, *53*, 1096-1103. (i) M. I. Burguete, E. García-Verdugo, I. Garcia-Villar, F.

Gelat, P. Licence, S. V. Luis, V. Sans, *J. Catal.* **2010**, *269*, 150-160 (j) U. Hintermair, Z. Gong, A. Serbanovic, M. J. Muldoon, C. C. Santini, D. J. Cole-Hamilton, *Dalton Trans.* **2010**, *39*, 8501-8510. (k) H. Hagiwara, T. Kuroda, T. Hoshi, T. Suzuki, *Adv. Synth. Catal.* **2010**, *352*, 909-916. (l) M. H. Valkenberg, C. de Castro, W. F. Hçlderich, *Green Chem.* **2002**, *4*, 88-93. (m) C. P. Mehnert, *Chem. Eur. J.* **2005**, *11*, 50-56. (n) B. Karimi, A. Maleki, D. Elhamifar, J. H. Clark, A. J. Hunt, *Chem. Commun.* 2010, *46*, 6947-6749. (o) H. Hagiwara, Y. Sugawara, K. Isobe, T. Hoshi., T. Suzuki, *Org. Lett.* **2004**, *6*, 2325-2328. (p) P. Virtanen, H. Karhu, G. Toth, K. Kordas, J.-P. Mikkola, *J. Catal.* **2009**, *263*, 209-219 (q) S. Werner, N. Szesni, A. Bittermann, M. J. Schneider, P. Härter, M. Haumann, P. Wasserscheid, *Appl. Catal. A: General* **2010**, *377*, 70-75. (r) A. Riisager, R. Fehrmann, S. Flicker, R. van Hal, M. Haumann, P. Wasserscheid, *Angew. Chem.* **2005**, *117*, 826-830; *Angew. Chem. Int. Ed.* **2005**, *44*, 815-819. (s) V. Sans, F. Gelat, N. Karbass, M. I. Burguete, E. García-Verdugo, S. V. Luis, *Adv. Synth. Catal.* **2010**, *352*, 3013-3021. (t) M. Gruttadauria, L. F. Liotta, A. M. P.Salvo, F. Giacalone, V. La Parola, C. Aprile, R. Noto *Adv. Synth. Catal.* **2011**, *353*, 2119–2130. (u) C. Aprile, F. Giacalone, P. Agrigento, L.F. Liotta, J. A. Martens, P. P. Pescarmona, M. Gruttadauria *ChemSusChem* DOI: 10.1002/cssc.201100446.

8. For recent reviews, see: (a) A.-H. Lu, E. L. Salabas, F. Schüth, *Angew. Chem. Int. Ed.* **2007**, *46*, 1222-1244. (b) J. Fan and Y. Gao*, J. Exp. Nanosci.* **2006**, 457-475. (c) Y.-W. Jun, J.-S. Choi, J. Cheon *Chem. Commun.* **2007**, 1203-1214. (d) S. Shylesh, V. Schünemann, W. R. Thiel, *Angew. Chem. Int. Ed.* **2010**, *49*, 3428-3459. (e) A. Schätz, R. N. Grass, W. J. Stark, O. Reiser, *Chem. Eur. J.* **2008**, *14*, 8262–826.

9. For example, see: (a) S. Ko, J. Jang, *Angew. Chem.* **2006**, *118*, 7726-7729; *Angew. Chem. Int. Ed.* **2006**, *45*, 7564–7567 (b) D. K. Yi, S. S. Lee, J. Y. Ying, *Chem. Mater.* **2006**, *18*, 2459-2461. c) T. Wendy, A. B. Ageeth, W. G. John, *Catal. Today* **1999**, *48*, 329-336.

10. Y. Zhu, L. Paul Stubbs, F. Ho, R. Liu, C. Peng Ship, J. A. Maguire, N. S. Hosmane, *ChemCatChem* **2010**, *2*, 365-374.

11. (a) T. Seki, J.-D. Grunwaldt, A. Baiker, *J. Phys. Chem. B* **2009**, *113*, 114-122. (b) J. H. Clements, *Ind. Eng. Chem. Res.* **2003,** *42,* 663-674.

12. J.-Q. Wang, X.-D. Yue, F. Cai, L.-N. He, *Catal. Commun* **2007**, *8*, 167-172.

13. (a) A. Teleki, M. Suter, P. R. Kidambi, O. Ergeneman, F. Krumeich, B. J. Nelson, S. E. Pratsinis, *Chem. Mater.* **2009,** *21,* 2094-2100. (b) A. Teleki, M. C. Heine, F. Krumeich, M. K. Akhtar, S. E. Pratsinis, *Langmuir* **2008**, *24*, 12553-12558. (c) A. Teleki, B. Buesser, M. C. Heine, F. Krumeich, M. K. Akhtar, S. E. Pratsinis, *Ind. Eng. Chem. Res.* **2009**, *48*, 85-92.

14. X. L. Zhang, D. F. Wang, N. Zhao, A. S. N. Al-Arifi, T. Aouak, Z. A. Al-Othman, W. Wei, Y. H. Sun, *Catal. Commun.* **2009**, *11*, 43-46.

Curriculum Vitae of Agrigento Paola

Personal Information

Date of birth: 27/09/1983

Place of birth: Palermo (Italy)

e-mail: paola.agrigento@gmail.com; paola.agrigento@unipa.it

Nationality: Italian

Education

01.2009-31.2011
PhD student in Chemistry

02.2011-08.2011
Visiting PhD student in the *Centre of Surface Science and Catalysis* of University of Leuven (Belgium), under the supervision of Prof. P. Pescarmona and Prof. C. Aprile

01.2008-07.2011
Visiting PhD student in the Baiker research group in Institute for Chemical and Bioengineering, Department of Chemistry and Applied Biosciences, ETH Hönggerberg, Zürich (Switzerland), under the supervision of Prof. A. Baiker and Dr. A. Vargas.

2008
Master's Degree in Chemistry in "Advanced methodology for the synthesis and characterization of organic molecules" Faculty of Science, University of Palermo.

2008
Professional Chemistry Qualification

2007
Bachelor of Science in Chemistry, Faculty of Science, University of Palermo

2002
Liceo Classico Statale "Umberto I", Secondary School certificate.

Publications

- C. Aprile, F. Giacalone, <u>P. Agrigento</u>, L. F. Liotta, J. A. Martens, P. P. Pescarmona, M. Gruttadauria, "*Multilayered supported ionic liquids as catalysts for chemical fixation of carbon dioxide: a high-throughput study in supercritical conditions*" ChemSusChem*,* 2011, 4, 1830-1837.

- F. Giacalone, M. Gruttadauria<u>, P. Agrigento</u>, V. Campisciano, R. Noto, *"Polystirene-supported organocatalysts for a-selenenylation and Michael reactions. A common post-modification approach for catalytic differentiation"* Catalysis Communications*,* **2011**, *16*, 75-80.

- M. Gruttadauria, F. Giacalone, <u>P. Agrigento</u>, P. Lo Meo, R. Noto, "*Advances towards highly active and stereoselective simple and cheap proline-based organocatalysts*" Eur. J. Org. Chem, **2010**, 5696-5704.

- M. Gruttadauria, F. Giacalone, A. M. P. Salvo,<u> P. Agrigento</u>, R. Noto, *"Asymmetric aldol reaction with polystyrene-supported proline-based catalysts*" Synfacts, **2010**, 120.

- M. Gruttadauria, F. Giacalone, A. M. P. Salvo, <u>P. Agrigento</u>, R. Noto, "*Enhanced activity and stereoselectivity of polystyrene-supported proline-based organic catalysts for direct asymmetric aldol reaction in water"* Eur. J. Org. Chem, **2009**, 5437-5444.

- F. Giacalone, M. Gruttadauria, <u>P. Agrigento</u>, R. Noto, *"Low-loading asymmetric Organocatalysis"* ChemSocRev*,* **2012***, Doi: 10.1039/C1CS15206H.*

- <u>P. Agrigento</u>, M. BaiJ. T. N. Knijnenburg, S. E. Pratsinis, , A. Baiker, M. Gruttadauria *"Highly Cross-linked Imidazolium Salts entrapped Magnetic Nanoparticles-preparation and uses",* manuscript in preparation.

- **BOOKCHAPTER:** M. Gruttadauria, F. Giacalone, P. Agrigento, R. Noto, *"Non-solvent Applications of Ionic Liquid in Organocatalysis*, chapter in the book "Ionic Liquids in Biotransformations and Organocatalysis: Solvents and Beyond" editor Pablo Dominguez de Maria, 2010, Wiley-VCH.

Congress Communications

- Poster Presentation al Convegno Congiunto delle Sezioni Calabria e Sicilia, Messina 1-2 December 2011, <u>Paola Agrigento</u>, Carmela Aprile, Paolo P. Pescarmona, Francesco Giacalone, Michelangelo Gruttadauria *"High-Throughput Study of CO_2 Cycloaddition Reaction catalysed by Multilayered supported ionic Liquid"*

- Poster Presentation al XXIV Congresso Nazionale della Società Chimica Italiana Lecce 11-16 September 2011: Michelangelo Gruttadauria, Francesco Giacalone, Anna Maria Pia Salvo, <u>Paola. Agrigento</u>, Leonarda F. Liotta, Valeria La Parola, Carmela Aprile, Paolo P. Pescarmona, Renato Noto *"Sali di imidazolio multistrato supportati covalentemente: attività catalitica per la produzione di carbonati ciclici in $scCO_2$ e nuovi supporti per catalizzatori di palladio".*

- Oral Presentation al Convegno Congiunto delle Sezioni Calabria e Sicilia, Palermo 2-3 December 2010, Francesco Giacalone, <u>Paola Agrigento</u>, Michelangelo Gruttadauria, Paolo Lo Meo, Renato Noto "*Simple and highly active organocatalysts for direct asymmetric aldol reaction in water".*

- Oral Presentation al EuropaCatIX, Salamanca, Spagna, 31 Agosto-04 September 2009, Michelangelo Gruttadauria, Francesco Giacalone, Anna Maria Pia Salvo, <u>Paola Agrigento</u>, Paolo Lo Meo, Serena Riela, Renato Noto "*New proline derivatives as recyclable catalysts for aldol reaction*".

- Oral Presentation al EuropaCatIX, Salamanca, Spagna, 31 Agosto-04 September 2009, Michelangelo Gruttadauria, Francesco Giacalone, Anna Maria Pia Salvo, <u>Paola Agrigento</u>, Paolo Lo Meo, Serena Riela, Renato Noto "*New proline derivatives as recyclable catalysts for aldol reaction*".

- Poster Presentation al **XXIII** Congresso Nazionale della Società Chimica Italiana**,** Sorrento 5-10 July 2009: Michelangelo Gruttadauria, Francesco Giacalone, Anna Maria Pia Salvo, Renato Noto, <u>Paola Agrigento</u> *"Simple and low loading catalysts for asymmetric aldol reaction under aqueous condition".*

- Poster Presentation al **XXIII** Congresso Nazionale della Società Chimica Italiana, Sorrento 5-10 July 2009: Michelangelo Gruttadauria, <u>Paola Agrigento</u>, Anna Maria Pia Salvo, Renato Noto, Francesco Giacalone *"Proline- and prolinamide-supported polystyrene: powerful and highly recyclable organocatalysts for the asymmetric aldol reaction".*

- Poster Presentation al **XXIII** Congresso Nazionale della Società Chimica Italiana**,** Sorrento, 5-10 July 2009, Michelangelo Gruttadauria, Francesco Giacalone, Renato Noto, <u>Paola Agrigento</u>, Anna Maria Pia Salvo "*Novel supported dipeptides as recyclable catalysts for asymmetric aldol reaction*".

- Poster Presentation al 2nd EuChems Chemistry Congress, Torino 16-20 September 2008: Francesco Giacalone, <u>Paola Agrigento</u>, Adriana Mossuto Marculescu, Michelangelo Gruttadauria, Renato Noto "*Novel Hydroxyproline-Derivatives as Powerful Aldolase-I Mimics".*

Lectures and Seminars

- 25 September 2009, Seminar *"NMR spectroscopy and chemometrics in food analysis"* Prof. Apostolos Spyros, Department of Chemistry, University of Crete.

- 24 September 2009, Seminar *"Biosorption. Low cost sorbents for metal ions removal from aqueous solution"* Prof. Isabel Villaescusa Gil, Department di Enginyeria Quimica, Agraria y Tecnologia Agroalimentaria de la Escola Politecnica Superior, Universitat de Girona.

- 16 September, Seminar *"Morphologyand properties of sol-gel prepared LDPE-silica nanocomposites"* Prof. A.S. Luyt, University of Free State South Africa.

- 1 July 2009, Lecture *"In silico tools in drug research for prediction of efficacy and ADMET e Chemistry and Biology of Quinones"* Prof. Peter Matyus – Semmelweis, University - Budapest – Ungheria.

- 26 and 27 May 2009, Conference *"Developments in the Synthesis of Biologically Active Heterocycles* e *Chemistry and Biology of Quinones"* Prof. Christopher J. Moody School of Chemistry, University of Nottingham, - UK

- 5 March 2009, Conference *"Gold Catalysis and its Application"* Prof. David Thompson (World Gold Council Consultant)**.**

- 14-17 April 2009, Seminar *"Molecular Organic Material"* Prof. Nazario Martín León, Università Complutense di Madrid.

- 21 October 2010, Seminar *"On the use of calorimetry to study interactions in aqueous solutions containing for instance surfactants and polymers"* Prof. Gerd Olofsson, Università di Lund (Svezia).

- 19 October 2010, Seminar *"Association behaviour of block copolymers under the influence of surfactants and hydrophobically-modified polyelectrolytes"* Prof. Karin Schillén , Università di Lund (Svezia).

- 9 September 2010, Conference *"Understanding reaction outcomes in ionic liquids – Can we achieve solvent-controlled reactivity?"* Dr. Jason Harper, School of Chemistry, University of New South Wales, Sydney, Australia.

- 20 September 2010, Conference *"Activated Peptides: for Ligation and Large Cyclic Transition States"* Prof. Alan Katritzky, University of Florida - Gainesville (FL) – USA.

- 24 February 2010, Seminar *"Magnetically-Enhanced Chemical, Biological and Environmental Processing Using Functionalized Magnetic Nanoparticles and High Gradient Magnetic Separations"* Prof. T. Alan Hatton, of Chemical Engineering Department, MIT.

UNIVERSITÀ DEGLI STUDI DI PALERMO

DIPARTIMENTO DI BENI CULTURALI, STORICO-ARCHEOLOGICI,

TUTOR
MARIO ROSSI

MAGISTRALE